FRACTIONAL APPROACH TO FLUID DYNAMICS

Ph.D. THESIS

KAVITA KHANDELWAL

(ID - 2011RMA7116)

DEPARTMENT OF MATHEMATICS

MALAVIYA NATIONAL INSTITUTE OF TECHNOLOGY

JAIPUR – 302017

May, 2016

FRACTIONAL APPROACH TO FLUID DYNAMICS

Submitted by:

KAVITA KHANDELWAL

(ID - 2011RMA7116)

Under the Supervision of

Dr. VATSALA MATHUR

(Associate Professor & Head)

Submitted in the partial fulfillment of the requirements for the degree of

Doctor of Philosophy

DEPARTMENT OF MATHEMATICS

MALAVIYA NATIONAL INSTITUTE OF TECHNOLOGY

JAIPUR – 302017

May, 2016

Malaviya National Institute of Technology, Jaipur

Department of Mathematics

CERTIFICATE

This is to certify that the thesis entitled **'FRACTIONAL APPROACH TO FLUID DYNAMICS'** is written by **Ms. Kavita Khandelwal**, who has carried out this work under my supervision, is her original piece of research work.

To the best of my knowledge and belief, such Thesis has not been submitted so far by any person to this or any other Institute.

Dr. Vatsala Mathur

Head,

Department of Mathematics

Malaviya National Institute of Technology, Jaipur

May, 2016

Malaviya National Institute of Technology

Jaipur -302017 (INDIA)

CANDIDATE'S DECLARATION

I hereby declare that the Ph.D. thesis entitled **'FRACTIONAL APPROACH TO FLUID DYNAMICS'** is my own work conducted under the supervision of Dr. Vatsala Mathur, Head, Department of Mathematics, Malaviya National Institute of Technology, Jaipur (Rajasthan), India.

I firmly declare that the presented work does not contain any part of any work that has been submitted for the award of any degree either in this University or in any other University/ Deemed University without proper citation.

Kavita Khandelwal

ACKNOWLEDGEMENT

I expressed my profound sense of gratitude, indebtedness and deep respect to Dr. Vatsala Mathur, Head, Department of Mathematics, Malaviya National Institute of Technology, Jaipur, who inspired me to take up the present study. Her valuable guidance, expert advice, constructive criticism, useful suggestions and constant encouragement at every step, enabled me to complete the study.

I express my sincere thanks to Prof. I.K. Bhat, Malaviya National institute of Technology, Jaipur, for providing necessary assistance from time to time.

I also gratefully acknowledge my deep sense of reverence to Prof. K.C. Jain and all faculty members of the Department of Mathematics, Malaviya National institute of Technology, Jaipur and Dr. Sanjeev Tyagi, Lecturer, Department of Mathematics, Govt. College, Jaipur, for their affectionate and proper encouragement in developing my research attitude.

I also owe a debt of gratitude to Mr. Akshay Kumar Gupta, Sr. Staff Engineer Qualcomm, Bangalore, who provided me all assistance and guidance at every stage.

I very sincerely acknowledge my thanks to all my friends, Parents, who directly encouraged and assisted me in more than one way, in completing my work. I would like to make a special mention of Mr. Manish Kumar Gupta, Sr. Analyst, Capital One, Bangalore, who provided valuable suggestions.

Kavita Khandelwal

ABSTRACT

The main intent of this thesis is to establish some new results for non-Newtonian fluids. Such results refer to different motions of fluids such as fractional Maxwell fluid, fractional Oldroyd-B fluid. The study is presented, having divided into seven chapters.

- **First chapter** 'Introduction' presents brief summary about fluids, constitutive equations, equation of continuity, equation of motion, fractional calculus and some integral transforms.
- **In chapter 2**, we study the flow of fractional Maxwell fluid in an annular pipe. More exactly, by means of the sequential fractional derivatives Laplace and finite Hankel transforms we establish the solutions corresponding to the motion of fractional Maxwell fluid between two oscillating infinite coaxial circular cylinders.
- **Chapter 3** provides exact solutions for the velocity field and shear stress corresponding to the unsteady flow of an incompressible fractional Maxwell fluid in annular region between two infinitely long coaxial circular cylinders. At time $t=0^+$, the inner cylinder applies a time dependent torsional shear to the fluid and outer cylinder is moving at a constant velocity.
- **In chapter 4**, it is studied the flow of fractional Maxwell fluid in pipe-like domains by the inner cylinder is pulled with a time-dependent shear stress and the outer cylinder is moving at a constant velocity. The solution is obtained using Laplace and Hankel transform methods and the results are presented in terms of generalized G and R functions.
- **Chapter 5** provides exact solution for the velocity field of flow for Oldroyd-B fluid in annular region between two infinitely long coaxial cylinders. This solution is obtained using finite Hankel and Laplace transform methods and the result is presented in terms of the generalized-G functions. Finally, the influence of different values of parameters, constants and fractional coefficients on the velocity field is also analyzed using graphical illustration. This chapter is divided into three parts. In part A, the motion is produced by constant pressure gradient, inner cylinder is pulled with constant shear and outer cylinder is moving with time dependent velocity. In part B, the motion is created by a constant pressure gradient & the inner cylinder start moving along

its axis of symmetry with the constant velocity. In part C, the motion is created by inner cylinder is pulled with constant shear and outer cylinder is moving with time dependent velocity.

- **Chapter 6** deals with the study of helical flow of fractional Oldroyd-B fluid in a circular cylinder. Both components of the velocity and shear stresses have been found in terms of generalized G function. Further, the solutions for ordinary Oldroyd-B fluid, fractional Maxwell fluid, ordinary Maxwell fluid and Newtonian fluid are easily obtained by imposing appropriate limits to the exact solution.
- **Chapter 7** contains exact solution for the velocity field and shear stress of rotational flow for fractional Oldroyd-B fluid filled between two coaxial circular cylinders by the inner cylinder begins to rotate about its axis with a time dependent shear stress while outer cylinder is moving at a constant velocity.

TABLE OF CONTENTS

LIST OF FIGURES

Chapter 1. Introduction

1.1 Fluids

Materials have always been an integral part of human life. They are so important that they have been used to designate part of human civilization period e.g. Stone Age, Bronze Age, Iron Age etc.

All materials show deformation under the action of external forces. If the deformation in a material, under the action of shearing forces, increases continuously without limit, the material is called fluid. Fridtjov [1] says “A fluid is a material that continuously deforms when it is subjected to anisotropic states of stress”. Thus, a fluid may be defined as a material that deforms continuously under the action of shearing forces.

Generally, fluids are classified as liquids or gases. A liquid has intermolecular forces which hold it together. It possesses volume but does not have a definite shape. When it is poured into a container, it fills the container upto the volume of the liquid, regardless of the shape of the container. Liquids are slightly compressible, however, for most of the practical purposes it is sufficient to consider liquids as incompressible fluids. On the other hand, a gas consists of molecules which collide with each other tending to disperse it while in motion. Hence, a gas has no volume or shape. The intermolecular forces are extremely small in gases. A gas fills any container into which it is placed and is therefore known as a (highly) compressible fluid.

Based on the flow properties, fluids can be classified into Ideal, Real, Newtonian and non-Newtonian Fluids. An Ideal Fluid has no viscosity (or no friction) and it is incompressible in nature. Practically, there are no ideal fluid that exists. Real fluids have some viscosity and they are compressible in nature. Examples of such fluids are Kerosene, Petrol, Castor oil, etc. The fluids, which obey Newton’s law of viscosity $(\tau = \mu \frac{dv}{dy})$, are described as Newtonian fluids. In Newtonian fluids, the relationship between shear stress and the strain rate is linear. Examples of such fluids are water, air etc. For Newtonian fluids, viscosity entirely dependents on the temperature and pressure of the fluid. The fluids, which do not obey Newton’s law of viscosity, are described as non-Newtonian fluids. For non-Newtonian fluids, the relationship between shear stress and the strain rate is non-linear and can even be time dependent. Thus, a constant coefficient of viscosity cannot be determined. Example of such fluids are blood, saliva, semen, synovial fluid, butter, cheese, jam, ketchup, soup, mayonnaise, magma, lava, gums, slurries, emulsions, etc. While Newtonian fluid simplifies the mathematical modeling, in industries, most fluid properties differ from this model. Hence, it is important to study the behavior of Non-Newtonian fluids.

Fluids play a very important role in many aspects of our life. We drink them, breath them and it runs through our bodies. Fluids control the weather and also have many applications in the industries. The study of motion of fluids is a complex phenomenon. The Navier-Stokes equations are the most famous form of equations which are widely studied and applied in fluid mechanics. These are non-linear partial differential equations that are applicable in almost every real situation. Therefore, there are a limited number of exact solutions under certain conditions such that many terms in the equations of motion either disappear automatically or may be neglected. The resulting equations thus reduce to a form that can be easily solved.

Thus, classical Navier-Stokes equations are used to describe the behavior of Newtonian fluids. However, due to the non-linear viscoelastic behavior, the ordinary Navier-Stokes equations are inadequate to describe rheological complex fluids such as plastic and polymer solutions. This has led to development of models for non-Newtonian fluids. These models include rate type [2], differential type [3] and integral type. Among them, rate type model is the most popular. Differential type model does not describe the influence of relaxation and retardation times and also cannot describe the flow of some polymers.

The non-Newtonian fluids play an important role in technological applications. A large number of industrial materials fall under this category. Fluids such as solutions and liquid polymers, soap and cellulose solutions, biological fluids, various colloids and paints, certain oils and asphalts belongs to this category. These fluids are very frequently encountered in many different fields such as food industries, chemical engineering, petroleum industry, biomedicine etc. and also are relevant to many other industrial processes. Hence, study of flow of non-Newtonian fluids has become a subject of great importance. In comparison to Newtonian fluids, the analysis of the motion of such fluids is much more difficult because of non-linear relationship between stress and the rate of strain.

It has been a challenge for mathematicians and physicists to analyze the flow characteristics and the properties of non-Newtonian fluids due to complicated partial differential equations arising in the mathematical formulation of the flows. Typical non-Newtonian characteristics include shear thinning, viscoelasticity, viscoplasticity and shear thickening behavior. Classical Navier-Stokes equations, which are sufficient to describe the flows of fluids with less atomic mass, fail to explain the behavior of such rheological complex fluids. Therefore, some mathematical models have been proposed to describe the characteristics of these complex fluids. Due to their wide applications in the industry, mathematicians are very much interested in the study of non-Newtonian fluids. These applications include the plastic manufacture, performance of lubricants, clay suspensions, drilling muds, paints, processing of food and moment of biological fluids which contain higher molecular weight components. When a constant shear stress is applied, Viscosity for Thixotropic fluids decreases with time, while it increases for Rheopectic fluids. Many paints are classified as thixotropic fluids. Similarly, few fluids return to their original shape after the applied stress is released, such fluids are called viscoelastic fluids.

The oscillating flow of the viscoelastic fluid in cylindrical pipes has been applied in many industrial areas such as oil exploitation, chemical industry, food industry and bioengineering. This type of analysis is of particular interest in bioengineering since blood in veins is forced by a periodic pressure gradient. Similarly, there are many applications in the petroleum and chemical industries which involve the dynamic response of the fluid to the frequency of the periodic pressure gradient.

So far numerous number of papers have been dedicated to study motions of Newtonian and Non-Newtonian fluids. The study of the motion of a fluid in the vicinity of a rotating or sliding cylinder is of great interest for engineering & industry.

For Newtonian fluids, the velocity distribution for a fluid contained in a circular cylinder was studied by G.K. Batchelor [4]. For non-Newtonian fluids, the first exact solution corresponding to motions of second grade fluids in a cylindrical domain seem to be those of Ting [5]. Similarly, Srivastava [6] and Waters & King [7] proposed first exact solution for Maxwell and Oldroyd-B fluids respectively. The first exact solution for motion of non-Newtonian fluids that applies a constant shear stress to the fluid are those of Bandelli and Rajagopal [8] and Bandelli et al. [9] for second-grade fluids. Recently, a lot of papers have been published regarding such fluid motions. Exact solutions for the velocity field and the shear stress corresponding to the unsteady flow of a generalized Oldroyd-B fluid due to an infinite circular cylinder subject to a longitudinal time-dependent shear stress have been obtained by Qammar et al. [10]. Tong et al. [11] published their work on unsteady unidirectional transient flows of Oldroyd-B fluid in an annular pipe. They used fractional calculus approach to build a generalized Jeffreys model. Muhammad Athar et al. [12] published exact solutions for a fractional Maxwell fluid for unsteady axial Couette flow due to an accelerated shear. Amir Mahmood et al. [13] presented their work on exact solutions for unsteady flow of generalized second grade fluids in cylindrical domains. Fang et al. [14] published their work on the Rayleigh–Stokes problem for a heated generalized second grade fluid using fractional derivative model. M. Kamran et al. [15] obtained expressions for the velocity field and shear stress corresponding to the motion of a fractional second grade fluid as limiting cases of general solutions corresponding to the fractional Oldroyd-B fluid. Recently, other similar solutions have been obtained in [16-26].

During 1886, Stokes [27] published an exact solution for the rotational oscillations of an infinite rod immersed in a linearly viscous fluid. Casarella and Laura [28] established an exact solution for oscillating rod with longitudinal and torsional motion. Exact solutions for the flow of a second grade fluid induced by the longitudinal and torsional oscillations of a rod have been obtained by Rajagopal [29]. Rajagopal and Bhatnagar [30] studied two simple but elegant solutions for the flows of an Oldroyd-B fluid induced by the longitudinal and torsional oscillations of an infinite long rod. Hayat et al. [31] studied the influences of Hall current on the flow of a Burgers' fluid in a pipe. Many important studies of non-Newtonian fluids for oscillating flows inside a cylindrical region have been done by various authors [32-40]. Fetecau and Corina Fetecau [41] proposed the most general solutions corresponding to the helical flow of a second grade fluid. Some exact solutions for the helical flow of a generalized Oldroyd-B fluid in a circular cylinder have been obtained by Fetecau et al. [42]. Wood [43] obtained exact solutions for helical flows of Oldroyd-B fluids in cylindrical domains. Qi and Jin [44] studied some helical flows of Oldroyd-B fluids in two infinite coaxial circular cylinders. Fetecau et al. [45-47], Jamil et al. [48-51] and Shah [52] studied some helical flows of Oldroyd-B and Maxwell fluids within an infinite circular cylinder or between two infinite coaxial circular cylinders.

In order to describe rheological properties of various classes of materials in detail, the rheological constitutive equations with fractional derivatives have been introduced for a long time. These have been discussed in the papers published time to time by various authors, to name a few, Bagley [53], Friedrich [54], Makris and Constantinou [55], Glockle and Nonnenmacher [56], Mainardi [57], Rossikhin and Shitikova [58, 59], Mainardi and Gorenflo [60].

Fractional calculus has been widely used to describe viscoelastic behavior of fluids [61-63]. The starting point of the fractional derivative model of viscoelastic fluid is usually a classical differential equation. This is being modified by replacing the time derivative of an integer order by the so-called Caputo fractional calculus operators [64]. Hence, many exact solutions for non-Newtonian fluids with fractional derivatives have been established [65-69] due to the importance of viscoelasticity.

Exact solutions play a key role not only because they are solutions of some fundamental flows but also because they are used as an accuracy checks for experimental, numerical or empirical and asymptotic methods. Even though computer techniques make it feasible to integrate complete equation of motion, the accuracy of the results can only be established by comparison with an exact solution.

1.2 Constitutive Equations

Rheological properties of materials can be specified by their constitutive equations. A constitutive equation can be defined as a relation between two physical quantities that is specific to a material and approximates the response of that material to external forces. Fridtjov [1] described constitutive equation as “A relation between stress and different measures of deformations, as strains, rates of deformation and rates of rotation”. In other words, we can say a relation between entities that describe a physical process is called constitutive equation.

Generally, constitutive equations define the ideal materials that have mathematical models to describe the behavior of some classes of real materials. In other words, we can say the constitutive equations represent macro-mechanical models for the real materials. The constitutive equations corresponding to different materials must satisfy some general principles. Examples of such principles are symmetry principle and the objectivity principle [70]. The constitutive equations for the non-Newtonian fluids lead to a problem in which the order of the differential equations exceeds the number of available conditions. In three dimension, the simplest constitutive equation form is a Newtonian one. The constitutive equations of some fluids are given below as [71]

1. Newtonian fluid

$$T = -pI + S, \quad where \quad \mathrm{S} = \mu \mathrm{A} \tag{1.2.1}$$

where A is the first Rivlin-Ericksen tensor.

2. Maxwell fluid

$$T = -pI + S\,,\; S + \lambda \frac{\delta S}{\delta t} = \mu A, \tag{1.2.2}$$

3. Oldroyd-B fluid

$$T = -pI + S\,, S + \lambda \frac{\delta S}{\delta t} = \mu\left(A + \lambda_r \frac{\delta A}{\delta t}\right), \tag{1.2.3}$$

where T is the Cauchy stress tensor, S is the extra-stress tensor and $\frac{\delta S}{\delta t}$ is the upper convective derivative defined as

$$\frac{\delta S}{\delta t} = \dot{S} - LS - SL^T\,, \tag{1.2.4}$$

where the dot denotes the material time differentiation.

p is the pressure, I is the identity tensor, λ and λ_r are relaxation and retardation times, $A = L + L^T$ is the first Rivlin-Ericksen tensor with L the velocity gradient, μ is the dynamic viscosity and the superscript T indicates the transpose operation.

1.3 Equation of Continuity

The continuity equation is based on the law of conservation of mass. The law of conservation of mass states that the mass is neither created nor destroyed inside a control volume region. Thus the rate of increase of the mass in the closed volume is equal to the mass of the fluid entering per unit time through the surface enclosing the volume. The equation of continuity in vector notation is given by

$$\frac{\partial \rho}{\partial t} + div(\rho \vec{V}) = 0\,, \tag{1.3.1}$$

where ρ is the density, t is the time and $\vec{V}$ is the velocity vector.

For steady compressible fluid flow, the equation of continuity reduces to

$$div(\rho\vec{V})=0. \tag{1.3.2}$$

For incompressible fluid flow, the equation of continuity reduces to

$$div(\vec{V})=0. \tag{1.3.3}$$

1.4 Equation of Motion

The equations of motion are derived from Newton's second law of motion which states that the rate of change of linear momentum is equal to the total force acting on the flowing fluid in the arbitrary volume. In vector notation, the equations of motion are given by

$$\rho\frac{D\vec{V}}{Dt}=\rho\vec{F}-\nabla p+\mu\nabla^2\vec{V} \tag{1.4.1}$$

where $\frac{D}{Dt}=\frac{\partial}{\partial t}+(\vec{V}.\nabla)$ is the material derivative, ρ is the density of fluid, $\vec{F}$ is the body force per unit volume, μ is the coefficient of viscosity, t is time, ∇ is the gradient operator and $\vec{V}$ is the velocity vector. Equations of motion are also known as Navier-Stokes equations.

1.5 Fractional Calculus

The branch of Mathematics in which we study differentiation and integration to an arbitrary order is popularly known as fractional calculus. Many famous mathematicians such as Leibnitz, Euler, Laplace, Fourier, Abel, Liouville, Riemann, Weyl, Kober have contributed a lot to the development of fractional calculus. The first use of fractional operations was done by Abel in the solution of tautochrone problem. Since then, the subject of fractional calculus has gained importance during the last three decades. Its applications in various fields of science and engineering, such as fluid flow, rheology, hydraulics of dams, diffusion problems, electrical networks, probability, electrochemistry, transport theory, scattering theory, electromagnetic theory, statistics, visco-elasticity have been extremely powerful in solving complex mathematical problems. Fractional derivatives are used to provide an excellent mechanism to describe the hereditary properties and memory of different materials and processes. Fractional calculus is applicable in deriving the solution of certain integral equations involving special functions of mathematical physics. Fractional calculus is very convenient for describing properties of real materials, i.e. polymers. Few problems related to elasticity were formulated and solved by M. Caputo with his own definition of fractional differentiation. Considerable research has been going on in this field and published through books, research papers, workshops, symposiums and international conferences in the last 35 years.

The mathematical aspects of the fractional calculus have been widely discussed by Caputo [72], Oldham and Spanier [73], McBride and Roach [74], Gorenflo and Vessela [75], Samko et al. [76], Miller and Ross [77], Kiryakova [78], Nishimoto [79], Podlubny [64] etc.

Fractional calculus can be defined as the theory of derivatives and integrals of an arbitrary order (called fractional derivatives and fractional integrals), which unifies and generalizes the notion of integer-order differentiation and n-fold integration. The infinite sequence of n-fold integrals and n-fold derivatives is given by

$$\ldots, \quad \int_a^t d\tau_2 \int_a^{\tau_2} f(\tau_1)d\tau_1, \quad \int_a^t f(\tau_1)d\tau_1, \quad f(t), \quad \frac{df(t)}{dt}, \quad \frac{d^2 f(t)}{d^2 t}, \quad \ldots$$

The derivative of arbitrary real order α can be considered as an interpolation of this sequence of operators. We will use it for the notation suggested and used by Davis [80]

$${}_a D_t^{\alpha} f(t)$$

Fractional derivative is the short name for derivatives of arbitrary order of fractional order. The subscripts *a* and *t* denote the two limits related to the operation of fractional differentiation. Following Ross [81], we will call them the terminals of fractional differentiation. The fractional integrals mean integrals of arbitrary order and correspond to negative values of α . We will denote the fractional integral of order $\beta > 0$ by

$$ {}_aD_t^{-\beta} f(t) $$

The Theory of fractional calculus is mainly based upon the study of the well-known fractional integral operators and fractional derivative operators. In which some integral operators such as Riemann Liouville and Weyl and fractional derivatives such as Riemann Liouville and Caputo given below as

1. Riemann Liouville fractional integral operator [77]

$$ {}_aD_x^{-\upsilon}\left[f(x)\right] = \frac{1}{\Gamma(\upsilon)}\int_a^x (x-t)^{\upsilon-1} f(t)dt, \qquad \mathrm{Re}(\upsilon) > 0, x > a \qquad (1.5.1) $$

2. Weyl fractional integral operator [77]

$$ {}_xW_\infty^{-\upsilon}\left[f(x)\right] = \frac{1}{\Gamma(\upsilon)}\int_x^\infty (t-x)^{\upsilon-1} f(t)dt, \qquad \mathrm{Re}(\upsilon) > 0,\ x > 0 \qquad (1.5.2) $$

3. Riemann Liouville fractional derivative operator [77]

$$ {}_aD_x^{\upsilon}\left[f(x)\right] = D^n[D^{-(n-\upsilon)} f(x)], \qquad n-1 \le \upsilon < n,\ \upsilon > 0 \qquad (1.5.3) $$

4. Caputo fractional derivative operator [64]

$$ {}_a^CD_t^{\beta} f(t) = \frac{1}{\Gamma(n-\beta)}\int_a^t \frac{f^n(\tau)}{(t-\tau)^{\beta+1-n}}d\tau, \qquad n-1 < \beta < n \qquad (1.5.4) $$

Several generalizations of Riemann Lioville fractional integrals have been introduced and widely studied by a number of eminent mathematicians notably Eardely, Kober and several other. Due to important role played by Riemann-Lioville and Weyl integral operators in different branches of science, engineering and mathematical physics, a number of generalizations of fractional integral operators have been introduced from time to time by many research workers notably Kober [82], Erdélyi

[83,84], Manocha [85,86], Saxena [87], Kalla and Saxena [88], Kalla [89], Saigo [90], Raina and Kiryakova [91], Srivastava and Goyal [92], Sneddon [93], Kalla and Kiryakova [94, 95], Srivastava et al. [96], Gupta and Jain [97], Goyal and Tariq [98], Gupta and Soni [99] etc.

A systemic analysis of various fractional integral operators studied from time to time has been given by Srivastava and Saxena [100].

Fractional derivatives have been used by many famous mathematicians such as Caputo [101], Smit and Vries [102], Mainardi [103], Luchko and Srivastava [104], Hadid and Luchko [105], Giona et al. [106], Friedrich [54, 107], Fenander [108], Enelund and Josefson [109], El-Sayed [110, 111], Beyer and Kempfle [112], Bagley and Torvik [113].

1.6 Some Integral Transforms

The integral transform of a function *f(x)* defined on a given interval (a, b) is denoted by $T\{f(x);p\}=F(p)$, defined by the integral equation, as follows

$$T\{f(x);p\}=\int_a^b K(x,p)f(x)dx, \tag{1.6.1}$$

where *K(x, p)* is called the kernel of the transform, *p* is a parameter (real or complex) independent of *x* and the operator *T* is called integral transform operator. The properties of integral transforms vary widely but all integral transforms have common linearity properties as follows

$$T(f+g)=T(f)+T(g), \tag{1.6.2}$$

$$\mathrm{T}(cf)=cT(f) \quad \text{for constants c.} \tag{1.6.3}$$

Some important and well-known integral transforms are Laplace, Mellin, Fourier, Hankel, Hilbert and Legendre transforms. These transforms are defined by choosing different kernels *K(x, p)* and different values for *a* and *b* involved in Eq. (1.6.1). Therefore, it is observed from the above that an integral transformation is a unique mathematical operation through which a real or complex-valued function f is transformed into another function $F = Tf$.

The integral transform is important because it transforms a complicated mathematical problem into a simpler one, which can be easily solved. Integral transforms are very useful to solve different type of problems in mathematics, especially in dealing with differential equations subject to particular boundary conditions. In the study of initial or boundary value problems involving differential equations, the differential operators are replaced by much simpler algebraic operations involving F which can easily be solved. Then the required solution can be obtained by the inverse transformation.

Integral transforms is very efficient and powerful tool to solve different types of problems in mathematics involving differential equations. Many different integral transforms are used for this purpose. In the following section, we introduce few integral transforms and their inverses that have been used in present work.

1.6.1 Laplace Transform

The Laplace transform of a function *f(t)* defined on $0 < t < \infty$ is denoted by $L\{f(t);s\} = F(s)$, defined by

$$L\{f(t);s\} = F(s) = \int_0^\infty e^{-st} f(t)dt, \qquad \mathrm{Re(s)} > 0, \tag{1.6.4}$$

where e^{-st} is the kernel of the Laplace transform, the parameter s is a real or complex number and the operator L is Laplace transform operator.

The inverse Laplace transform is defined as

$$f(t) = L^{-1}\{F(s);t\} \tag{1.6.5}$$

where L^{-1} is known as the inverse Laplace transformation operator.

All functions of *f(t)* are not Laplace transformable. The Laplace transformation for a function *f(t)* is possible if it should satisfy the Dirichlet conditions (a set of sufficient but not necessary conditions). These conditions are given below

1. The function *f(t)* must be sectionally or piecewise continuous; that is, it must be single valued but can have a finite number of finite isolated discontinuities for $t > 0$.

2. The function *f(t)* must be of exponential order; that is, *f(t)* must remain less than $Me^{a_0 t}$ as t approaches ∞, where M is a positive constant and a_0 is a real positive number.

The Laplace transformation is not possible for the functions such as *tan (t)*, *cot (t)* and e^{t^2}. The convolution theorem is an important result of Laplace transform, as defined by

If $L\{f(t)\}=F(s)$ and $L\{g(t)\}=G(s)$, then

$$L^{-1}\{F(s)G(s)\}=\int_0^x f(u)g(t-u)du = f * g. \tag{1.6.6}$$

Laplace transforms are used to solve different types of problems in mathematics such as partial differential equations, initial and boundary value problems, integral equations, difference equations and many other fields.

1.6.2 Finite Hankel Transform

The finite Hankel transform of order n of a function *f(r)* defined in $0 \le r \le R$, is defined by

$$H_n\{f(r)\}=\overline{f_n}(r_i)=\int_0^R rJ_n(rr_i)\,f(r)dr, \tag{1.6.7}$$

where r_i are the positive roots of the transcendental equation $J_n(Rr_i)=0$ and $J_n(.)$ is the Bessel function of first kind of order n.

The inverse finite Hankel transform is defined by

$$H_n^{-1}\{\overline{f_n}(r_i)\}=f(r)=\frac{2}{R^2}\sum_{i=1}^{\infty}\overline{f_n}(r_i)\frac{J_n(rr_i)}{[J_{n+1}(Rr_i)]^2}, \tag{1.6.8}$$

The finite Hankel transforms defined in Eq. (1.6.7) used for the solution of problems in which only one cylinder is used.

Hankel transform is used in the study of functions which depend only on the distance from the origin. This transform involves the Bessel functions as the kernel appearing in axisymmetric problems formulated in cylindrical polar coordinates.

The partial differential equations with adequate initial and boundary conditions can be solved by several methods. However, the integral transforms technique is a systematic, efficient and powerful tool. The finite Hankel transform is very useful when we are dealing with problems that show circular symmetry. The finite Hankel transforms and Laplace transform are used to solve partial differential equations involving fractional calculus.

Chapter 2. Flow of fractional Maxwell fluid in oscillating pipe-like domains

The paper submitted on the work described in this chapter:

Mathur V. and Khandelwal K., Flow of fractional Maxwell fluid in pipe-like domains, International Journal of Applied and Computational Mathematics, 1-18. DOI: 10.1007/s40819-016-0139-x(Springer)

2.1 Introduction

The oscillating flow of the viscoelastic fluid in cylindrical domain has applications in many industrial areas. This chapter presents an analysis for oscillating flows of fractional Maxwell fluid in the annular region between two infinite concentric circular cylinders. The fluid motion is created as both cylinders begin to oscillate around their common axis. The exact solutions are established using the sequential fractional derivatives Laplace transform and finite Hankel transform in terms of generalized G and R functions. Also, we obtain the solutions for ordinary Maxwell fluid and Newtonian fluid as special cases of the generalized solutions. Moreover, the effects of various parameters on the velocity field and shear stress are analyzed by graphical illustration. Finally, a comparison is drawn between motions of fractional Maxwell fluid, ordinary Maxwell fluid and Newtonian fluid.

2.2 Governing equations

The constitutive equations of an incompressible Maxwell fluid are given by [71, 114]

$$T = -pI + S, \quad S + \lambda\left(\dot{S} - LS - SL^T\right) = \mu A, \tag{2.2.1}$$

where T is the Cauchy stress tensor, $-pI$ denotes the indeterminate spherical stress, S is the extra-stress tensor, λ is relaxation time, $A = L + L^T$ with L the velocity gradient, the superscript T indicates the transpose operation and the dot denotes the material time differentiation.

For the problem under consideration, we use a velocity field of the form and extra stress S as in the form of

$$V = V(r,t) = w(r,t)e_\theta, \qquad \mathrm{S} = \mathrm{S}(r,t), \tag{2.2.2}$$

where e_θ is the unit vector in the θ direction of the cylindrical coordinates.

At time $t=0$, the fluid is at rest in an annular region between two infinite coaxial circular cylinders. At time $t=0^+$, both cylinders begin to oscillate. For these flows, the constraint of incompressibility is automatically satisfied. Initially the fluid is at rest, hence

$$V(r,0) = 0, \qquad S(\mathrm{r},0) = 0. \tag{2.2.3}$$

The governing equations corresponding to incompressible Maxwell fluid in the absence of body forces and a pressure gradient in the θ direction are given by [115]

$$\left(1+\lambda D_t^{\beta}\right)\frac{\partial w(r,t)}{\partial t} = \upsilon\left(\frac{\partial^2}{\partial r^2}+\frac{1}{r}\frac{\partial}{\partial r}-\frac{1}{r^2}\right)w(r,t), \tag{2.2.4}$$

$$\left(1+\lambda D_t^{\beta}\right)\tau(r,t) = \mu\left(\frac{\partial}{\partial r}-\frac{1}{r}\right)w(r,t), \tag{2.2.5}$$

where $\tau(r,t) = S_{r\theta}(r,t)$ is the non-trivial shear stress, $\upsilon = \dfrac{\mu}{\rho}$ is the kinematic viscosity, ρ is the constant density of the fluid and the Caputo fractional derivative of order β as defined by [64]

$$D_t^{\beta} f(t) = \begin{cases} \dfrac{1}{\Gamma(1-\beta)}\dfrac{d}{dt}\displaystyle\int_0^t \dfrac{f(\tau)}{(t-\tau)^{\beta}}d\tau, & 0<\beta<1; \\ \dfrac{d}{dt} f(t), & \beta = 1, \end{cases} \tag{2.2.6}$$

where $\Gamma(.)$ is the Gamma function. This model can be reduced to ordinary Maxwell model when $\beta \to 1$ and to Newtonian model when $\beta \to 1$ and $\lambda \to 0$.

To solve this problem we use Laplace and finite Hankel transforms.

2.3 Mathematical formulation and solution of the problem

Let us consider an incompressible fractional Maxwell fluid at rest in an annular region between two coaxial circular cylinders of radii R_1 and $R_2 (> R_1)$. At time $t=0^+$, both cylinders begin to oscillate around their common axis (r = 0) with the velocities

$V_1 \sin(\omega_1 t)$ and $V_2 \sin(\omega_2 t)$. Due to the shear, the fluid between the cylinders is gradually moved and its velocity is of the form Eq. (2.2.2)$_1$. The governing equations are given by Eqs. (2.2.4) and (2.2.5), while the appropriate initial and boundary conditions are

$$w(r,0) = 0, \qquad \tau(\mathrm{r},0) = 0, \tag{2.3.1}$$

and

$$w(R_1,t) = V_1 \sin(\omega_1 t), \qquad w(R_2,t) = V_2 \sin(\omega_2 t), \qquad \mathrm{t} \geq 0, \tag{2.3.2}$$

where ω_1 and ω_2 are the frequencies of the velocity of the cylinder and V_1, V_2 are constant amplitudes.

2.3.1 Calculation of the velocity field

Applying Laplace transform to Eq. (2.2.4) and using the initial conditions as given in Eq. (2.3.1), we obtain

$$\left(q + \lambda q^{\beta+1}\right)\overline{w}(r,q) = \upsilon\left(\frac{\partial^2}{\partial r^2} + \frac{1}{r}\frac{\partial}{\partial r} - \frac{1}{r^2}\right)\overline{w}(r,q). \tag{2.3.3}$$

Applying Laplace transform to Eq. (2.3.2), we obtain

$$\overline{w}(R_1,q) = \frac{V_1\omega_1}{q^2 + \omega_1^2}, \qquad \overline{w}(R_2,q) = \frac{V_2\omega_2}{q^2 + \omega_2^2}. \tag{2.3.4}$$

The Hankel transform method with respect to r is used and defined as follows

$$\overline{w}_H(r_n,q) = \int_{R_1}^{R_2} r\overline{w}(r,q)B(r,r_n)dr, \tag{2.3.5}$$

where

$$B(r,r_n) = J_1(rr_n)Y_1(R_2 r_n) - J_1(R_2 r_n)Y_1(rr_n), \tag{2.3.6}$$

r_n being the positive roots of the transcendental equation $B(R_1,r) = 0$. The inverse Hankel transform as defined by [116], is given below

$$\bar{w}(r,q)=\frac{\pi^2}{2}\sum_{n=1}^{\infty}\frac{r_n^2J_1^2(R_1r_n)B(r,r_n)}{J_1^2(R_1r_n)-J_1^2(R_2r_n)}\bar{w}_H(r_n,q). \tag{2.3.7}$$

Multiplying both sides of Eq. (2.3.3) by *rB(r, r_n)*, then integrating with respect to *r* from R_1 to R_2 and taking into account the conditions Eq. (2.3.4) along with the following relation

$$J_{\upsilon+1}(x)Y_{\upsilon}(x)-J_{\upsilon}(x)Y_{\upsilon+1}(x)=\frac{2}{\pi x} \tag{2.3.8}$$

and the equality

$$\int_{R_1}^{R_2} r\left(\frac{\partial^2}{\partial r^2}+\frac{1}{r}\frac{\partial}{\partial r}-\frac{1}{r^2}\right)\bar{w}(r,q)B(r,r_n)dr$$
$$= -r_n^2\,\bar{w}_H(r_n,q)+\frac{2}{\pi}\left[\frac{V_2\omega_2}{q^2+\omega_2^2}-\frac{V_1\omega_1}{q^2+\omega_1^2}\frac{J_1(R_2r_n)}{J_1(R_1r_n)}\right], \tag{2.3.9}$$

we obtain

$$\bar{w}_H(r_n,q)=\frac{2\upsilon}{\pi(q+\lambda q^{\beta+1}+\upsilon r_n^2)}\left[\frac{V_2\omega_2}{q^2+\omega_2^2}-\frac{V_1\omega_1}{q^2+\omega_1^2}\frac{J_1(R_2r_n)}{J_1(R_1r_n)}\right]. \tag{2.3.10}$$

Rewriting Eq. (2.3.10) into a suitable equivalent form, we obtain below

$$\bar{w}_H(r_n,q)=\frac{2V_2\omega_2}{\pi r_n^2}\left[\frac{1}{(q^2+\omega_2^2)}-\frac{q(\lambda q^{\beta}+1)}{(q^2+\omega_2^2)(q+\lambda q^{\beta+1}+\upsilon r_n^2)}\right]$$
$$-\frac{2V_1\omega_1}{\pi r_n^2}\frac{J_1(R_2r_n)}{J_1(R_1r_n)}\left[\frac{1}{(q^2+\omega_1^2)}-\frac{q(\lambda q^{\beta}+1)}{(q^2+\omega_1^2)(q+\lambda q^{\beta+1}+\upsilon r_n^2)}\right]. \tag{2.3.11}$$

Applying inverse Hankel transform to Eq. (2.3.11) and taking into account the following result

$$a_n=\int_{R_1}^{R_2} r\left\{\frac{AR_1(R_2^2-r^2)+BR_2(r^2-R_1^2)}{(R_2^2-R_1^2)r}\right\}B(r,r_n)dr=\frac{2B}{\pi r_n^2}-\frac{2A}{\pi r_n^2}\frac{J_1(R_2r_n)}{J_1(R_1r_n)}, \tag{2.3.12}$$

we obtain

$$\overline{w}(r,q)=\frac{V_1R_1\left(R_2^2-r^2\right)\dfrac{\omega_1}{\left(q^2+\omega_1^2\right)}+V_2R_2\left(r^2-R_1^2\right)\dfrac{\omega_2}{\left(q^2+\omega_2^2\right)}}{\left(R_2^2-R_1^2\right)r}$$
$$-\pi\sum_{n=1}^{\infty}\frac{J_1^2(R_1r_n)B(r,r_n)}{J_1^2(R_1r_n)-J_1^2(R_2r_n)}\frac{\left(\lambda q^{\beta+1}+q\right)}{(q+\lambda q^{\beta+1}+\upsilon r_n^2)}\left[\frac{V_2\omega_2}{\left(q^2+\omega_2^2\right)}-\frac{J_1(R_2r_n)}{J_1(R_1r_n)}\frac{V_1\omega_1}{\left(q^2+\omega_1^2\right)}\right]. \tag{2.3.13}$$

Applying Inverse-Laplace transform to Eq. (2.3.13) and then using the expansion

$$\frac{1}{q+\lambda q^{\beta+1}+\upsilon r_n^2}=\frac{1}{\lambda}\sum_{k=0}^{\infty}\left(\frac{-\upsilon r_n^2}{\lambda}\right)^k\frac{q^{-k-1}}{(q^{\beta}+\lambda^{-1})^{k+1}}, \tag{2.3.14}$$

and taking into account the following result [117]

$$G_{a,b,c}(d,t)=L^{-1}\left\{\frac{q^b}{(q^a-d)^c}\right\}$$
$$=\sum_{j=0}^{\infty}\frac{\mathrm{d}^j\Gamma(c+j)}{\Gamma(c)\Gamma(j+1)}\frac{t^{(c+j)a-b-1}}{\Gamma[(c+j)a-b]};$$

$$\mathrm{Re}(ac-b)>0,\quad \mathrm{Re}(\mathrm{q})>0,\quad \left|\frac{\mathrm{d}}{\mathrm{q}^{\mathrm{a}}}\right|<1, \tag{2.3.15}$$

we obtain

$$w(r,t)=\frac{V_1R_1\left(R_2^2-r^2\right)\sin(\omega_1t)+V_2R_2\left(r^2-R_1^2\right)\sin(\omega_2t)}{\left(R_2^2-R_1^2\right)r}$$
$$-\frac{\pi}{\lambda}\sum_{n=1}^{\infty}\frac{J_1^2(R_1r_n)B(r,r_n)}{J_1^2(R_1r_n)-J_1^2(R_2r_n)}\sum_{j=0}^{\infty}\sum_{k=0}^{\infty}\left(\frac{-\upsilon r_n^2}{\lambda}\right)^k\left\{\lambda G_{\beta,\beta-k-2j-2,k+1}(-\lambda^{-1},t)+G_{\beta,-k-2j-2,k+1}(-\lambda^{-1},t)\right\}$$
$$\times\left\{V_2\omega_2\left(-\omega_2^2\right)^j-V_1\omega_1\left(-\omega_1^2\right)^j\frac{J_1(R_2r_n)}{J_1(R_1r_n)}\right\}. \tag{2.3.16}$$

2.3.2 Calculation of the shear stress

Applying Laplace transform to Eq. (2.2.5), we obtain

$$\overline{\tau}(r,q)=\mu\frac{1}{(1+\lambda q^{\beta})}\left(\frac{\partial}{\partial r}-\frac{1}{r}\right)\overline{w}(r,q). \tag{2.3.17}$$

Substitute Eq. (2.3.13) into Eq. (2.3.17), we obtain

$$\bar{\tau}(r,q)=\frac{2\mu R_1R_2}{\left(R_2^2-R_1^2\right)r^2}\left\{\frac{V_2\omega_2R_1}{\left(q^2+\omega_2^2\right)\left(1+\lambda q^\beta\right)}-\frac{V_1\omega_1R_2}{\left(q^2+\omega_1^2\right)\left(1+\lambda q^\beta\right)}\right\}$$
$$+\pi\mu\sum_{n=1}^{\infty}\frac{J_1^2(R_1r_n)\left(\frac{2}{r}B(r,r_n)-r_n\bar{B}(r,r_n)\right)}{J_1^2(R_1r_n)-J_1^2(R_2r_n)}\frac{q}{(q+\lambda q^{\beta+1}+\upsilon r_n^2)}\left\{\frac{V_2\omega_2}{\left(q^2+\omega_2^2\right)}-\frac{J_1(R_2r_n)}{J_1(R_1r_n)}\frac{V_1\omega_1}{\left(q^2+\omega_1^2\right)}\right\},\quad(2.3.18)$$

where

$$\bar{B}(r,r_n)=J_0(rr_n)Y_1(R_2r_n)-J_1(R_2r_n)Y_0(rr_n).\qquad(2.3.19)$$

Applying inverse Laplace transform to Eq. (2.3.18), then using Eq. (2.3.15) and taking into account the following result [117]

$$R_{a,b}(d,t)=L^{-1}\left\{\frac{q^b}{q^a-d}\right\}=\sum_{n=0}^{\infty}\frac{d^n t^{(n+1)a-b-1}}{\Gamma[(n+1)a-b]};$$
$$\mathrm{Re}(a-b)>0,\quad \mathrm{Re}(q)>0,\quad \left|\frac{\mathrm{d}}{\mathrm{q}^{\mathrm{a}}}\right|<1,\qquad(2.3.20)$$

we obtain

$$\tau(r,t)=\frac{2\mu R_1R_2}{\lambda\left(R_2^2-R_1^2\right)r^2}\sum_{j=0}^{\infty}R_{\beta,-2j-2}(-\lambda^{-1},t)\left\{V_2\omega_2R_1\left(-\omega_2^2\right)^j-V_1\omega_1R_2\left(-\omega_1^2\right)^j\right\}$$
$$+\frac{\pi\mu}{\lambda}\sum_{n=1}^{\infty}\frac{J_1^2(R_1r_n)\left(\frac{2}{r}B(r,r_n)-r_n\bar{B}(r,r_n)\right)}{J_1^2(R_1r_n)-J_1^2(R_2r_n)}\sum_{j=0}^{\infty}\sum_{k=0}^{\infty}\left(\frac{-\upsilon r_n^2}{\lambda}\right)^kG_{\beta,-2j-k-2,k+1}(-\lambda^{-1},t)$$
$$\times\left\{V_2\omega_2\left(-\omega_2^2\right)^j-V_1\omega_1\left(-\omega_1^2\right)^j\frac{J_1(R_2r_n)}{J_1(R_1r_n)}\right\}.\qquad(2.3.21)$$

2.4 Limiting Cases

2.4.1 Ordinary Maxwell Fluid

Applying $\beta\to 1$ into Eqs. (2.3.16) and (2.3.21), we obtain the velocity field

$$w_M(r,t)=\frac{V_1R_1\left(R_2^2-r^2\right)\sin(\omega_1 t)+V_2R_2\left(r^2-R_1^2\right)\sin(\omega_2 t)}{\left(R_2^2-R_1^2\right)r}$$
$$-\frac{\pi}{\lambda}\sum_{n=1}^{\infty}\frac{J_1^2(R_1r_n)B(r,r_n)}{J_1^2(R_1r_n)-J_1^2(R_2r_n)}\sum_{j=0}^{\infty}\sum_{k=0}^{\infty}\left(\frac{-\upsilon r_n^2}{\lambda}\right)^k\left\{\lambda G_{1,-k-2j-1,k+1}(-\lambda^{-1},t)+G_{1,-k-2j-2,k+1}(-\lambda^{-1},t)\right\}$$
$$\times\left\{V_2\omega_2\left(-\omega_2^2\right)^j-V_1\omega_1\left(-\omega_1^2\right)^j\frac{J_1(R_2r_n)}{J_1(R_1r_n)}\right\}, \tag{2.4.1}$$

and its associated shear stress corresponding to ordinary Maxwell fluid performing the same motion

$$\tau_M(r,t)=\frac{2\mu R_1R_2}{\lambda\left(R_2^2-R_1^2\right)r^2}\sum_{j=0}^{\infty}R_{1,-2j-2}(-\lambda^{-1},t)\left\{V_2\omega_2R_1\left(-\omega_2^2\right)^j-V_1\omega_1R_2\left(-\omega_1^2\right)^j\right\}$$
$$+\frac{\pi\mu}{\lambda}\sum_{n=1}^{\infty}\frac{J_1^2(R_1r_n)\left(\frac{2}{r}B(r,r_n)-r_n\overline{B}(r,r_n)\right)}{J_1^2(R_1r_n)-J_1^2(R_2r_n)}\sum_{j=0}^{\infty}\sum_{k=0}^{\infty}\left(\frac{-\upsilon r_n^2}{\lambda}\right)^k G_{1,-2j-k-2,k+1}(-\lambda^{-1},t)$$
$$\times\left\{V_2\omega_2\left(-\omega_2^2\right)^j-V_1\omega_1\left(-\omega_1^2\right)^j\frac{J_1(R_2r_n)}{J_1(R_1r_n)}\right\}. \tag{2.4.2}$$

2.4.2 Newtonian Fluid

Applying $\lambda\to 0$ into Eqs. (2.4.1) and (2.4.2) and taking into account the following results [22]

$$\lim_{\lambda\to 0}\frac{1}{\lambda^k}G_{1,b,k}(-\lambda^{-1},t)=\frac{t^{-b-1}}{\Gamma(-b)},\quad \mathrm{b}<0, \tag{2.4.3}$$

$$\lim_{\lambda\to 0}\frac{1}{\lambda}R_{1,b}(-\lambda^{-1},t)=\frac{t^{-b-1}}{\Gamma(-b)},\quad \mathrm{b}<0, \tag{2.4.4}$$

we obtain the corresponding solutions for the Newtonian fluid, as follows

$$w_N(r,t)=\frac{V_1R_1\left(R_2^2-r^2\right)\sin(\omega_1 t)+V_2R_2\left(r^2-R_1^2\right)\sin(\omega_2 t)}{\left(R_2^2-R_1^2\right)r}$$
$$-\pi\sum_{n=1}^{\infty}\frac{J_1^2(R_1r_n)B(r,r_n)}{J_1^2(R_1r_n)-J_1^2(R_2r_n)}\sum_{j=0}^{\infty}\sum_{k=0}^{\infty}\left(-\upsilon r_n^2\right)^k\frac{t^{k+2j+1}}{\Gamma(k+2j+2)}$$
$$\times\left\{V_2\omega_2\left(-\omega_2^2\right)^j-V_1\omega_1\left(-\omega_1^2\right)^j\frac{J_1(R_2r_n)}{J_1(R_1r_n)}\right\}, \tag{2.4.5}$$

and

$$\tau_N(r,t)=\frac{2\mu R_1R_2}{\left(R_2^2-R_1^2\right)r^2}\sum_{j=0}^{\infty}\frac{t^{2j+1}}{\Gamma(2j+2)}\left\{V_2\omega_2R_1\left(-\omega_2^2\right)^j-V_1\omega_1R_2\left(-\omega_1^2\right)^j\right\}$$
$$+\pi\mu\sum_{n=1}^{\infty}\frac{J_1^2(R_1r_n)\left(\frac{2}{r}B(r,r_n)-r_n\overline{B}(r,r_n)\right)}{J_1^2(R_1r_n)-J_1^2(R_2r_n)}\sum_{j=0}^{\infty}\sum_{k=0}^{\infty}\left(-\upsilon r_n^2\right)^k\frac{t^{k+2j+1}}{\Gamma(k+2j+2)}$$
$$\times\left\{V_2\omega_2\left(-\omega_2^2\right)^j-V_1\omega_1\left(-\omega_1^2\right)^j\frac{J_1(R_2r_n)}{J_1(R_1r_n)}\right\}. \tag{2.4.6}$$

2.5 Conclusions and Numerical results

In this chapter, we obtained the expressions for the velocity field and shear stress. We obtained these expressions for an incompressible fractional Maxwell fluid in the annular region. The fluid motion is created as both cylinders begin to oscillate around their common axis with different angular frequencies ω_1 and ω_2 of their velocities. The results have been determined using sequential fractional derivatives Laplace and finite Hankel transform methods. These results are also presented in a series form in terms of the generalized G and R functions. Similar solutions are obtained for ordinary Maxwell and Newtonian fluids as limiting cases of the solution for fractional Maxwell fluid.

Importantly, we can obtain the velocity field and the shear stress, when one of the cylinder is at rest, by making V_1 = 0, V_2 = V and $\omega_2=\omega$ (when inner cylinder is at rest) or V_1 = V, V_2 = 0, and $\omega_1=\omega$ (when outer cylinder is at rest). For instance, the velocity field for the flow of fractional Maxwell fluid, when inner cylinder is at rest and outer cylinder is oscillating, is given by below equation

$$w(r,t)=\frac{VR_2\left(r^2-R_1^2\right)\sin(\omega t)}{\left(R_2^2-R_1^2\right)r}-\frac{\pi}{\lambda}\sum_{n=1}^{\infty}\frac{J_1^2(R_1r_n)B(r,r_n)}{J_1^2(R_1r_n)-J_1^2(R_2r_n)}\sum_{j=0}^{\infty}\sum_{k=0}^{\infty}V\omega\left(-\omega^2\right)^j\left(\frac{-\upsilon r_n^2}{\lambda}\right)^k$$
$$\times\left\{\lambda G_{\beta,\beta-k-2j-2,k+1}(-\lambda^{-1},t)+G_{\beta,-k-2j-2,k+1}(-\lambda^{-1},t)\right\}. \tag{2.5.1}$$

Similarly, the velocity field for the flow of fractional Maxwell fluid, when outer cylinder is at rest and inner cylinder is oscillating, is given by below equation

$$w(r,t)=\frac{VR_1\left(R_2^2-r^2\right)\sin(\omega t)}{\left(R_2^2-R_1^2\right)r}$$
$$+\frac{\pi}{\lambda}\sum_{n=1}^{\infty}\frac{J_1(R_1r_n)J_1(R_2r_n)B(r,r_n)}{J_1^2(R_1r_n)-J_1^2(R_2r_n)}\sum_{j=0}^{\infty}\sum_{k=0}^{\infty}V\omega\left(-\omega^2\right)^j\left(\frac{-\upsilon r_n^2}{\lambda}\right)^k$$
$$\times\ \left\{\lambda G_{\beta,\beta-k-2j-2,k+1}(-\lambda^{-1},t)+G_{\beta,-k-2j-2,k+1}(-\lambda^{-1},t)\right\}. \tag{2.5.2}$$

Similarly, we can obtain shear stress solution by appropriate substitutions.

In order to demonstrate impact of physical parameters, the obtained results are presented in the form of diagrams for the velocity $w(r,t)$ and the shear stress $\tau(r,t)$. They are given by Eqs. (2.3.16) and (2.3.21) and have been drawn against r for different values of the time t and other relevant parameters as shown in diagrams. It can be observed from the figures that the velocity component w is decreasing function of r. The influence of the time t on fluid motion is shown in Figure 2.1. The influence of the frequency of oscillations ω_1 and ω_2 on fluid motion is shown in figures 2.2 and 2.3. Both parameters have opposite effect on the fluid motion. Figures 2.4 and 2.5 are showing the effect of different values of $V_1$and V_2 on the fluid motion. Figures 2.6(a) and 2.6(b) are showing the effect of different values of kinematic viscosity on the fluid motion. It indicates that the velocity is decreasing and the shear stress is increasing function of υ. The dependency of the relaxation time on the fluid motion is shown in the figure 2.7. It indicates that the velocity and the shear stress are increasing function of λ. Figure 2.8 is showing the effect of different values of fractional parameter β on the fluid motion. It can be observed that the velocity is increasing while the shear stress is decreasing function of β. Figure 2.9 exhibits a comparative diagram of the velocity $w(r,t)$ and the shear stress $\tau(r,t)$ corresponding to the motions of fractional Maxwell fluid, ordinary Maxwell fluid and Newtonian fluid in a circular cylinder, for same values of the common material constants and time t. The velocity in the neighborhood of inner cylinders is swiftest for Newtonian fluid while it is slowest for the Fractional Maxwell fluid. Similarly, shear stress on the whole flow domains highest for Maxwell fluid while it is slowest for the Newtonian fluid. In all of the figures 2.1-2.9, the units of the material constants are in SI units and the root r_n has been approximated by $\dfrac{(2n-1)\pi}{2(R_2-R_1)}$.

Figure 2.1

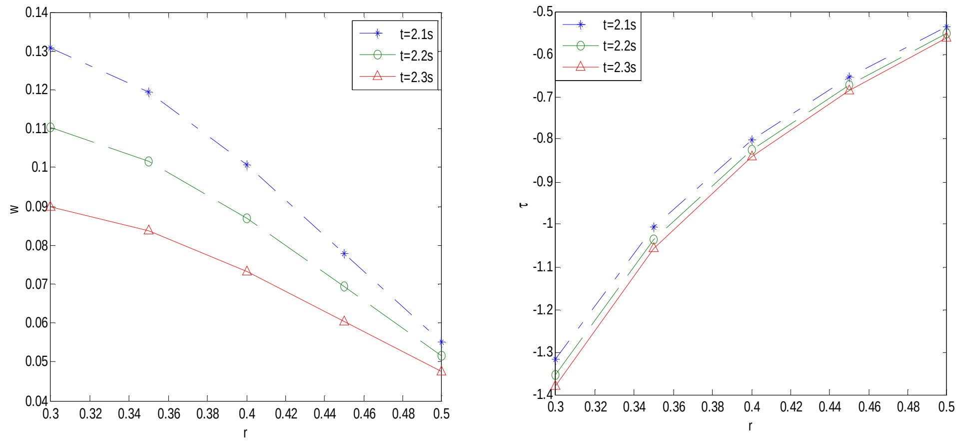

2.1(a) 2.1(b)

Fig. 2.1 Profiles of the velocity w(r, t) and shear stress τ(r, t) given by Eqs. (2.3.16) and (2.3.21) for $R_1 = 0.3$, $R_2 = 0.5$, $\omega_1 = 1$, $\omega_2 = 1$, $V_1 = 1$, $V_2 = 1$, $\upsilon = 0.5566$, $\mu = 1.01$, $\lambda = 4$, $\beta = 0.8$ and different values of t.

Figure 2.2

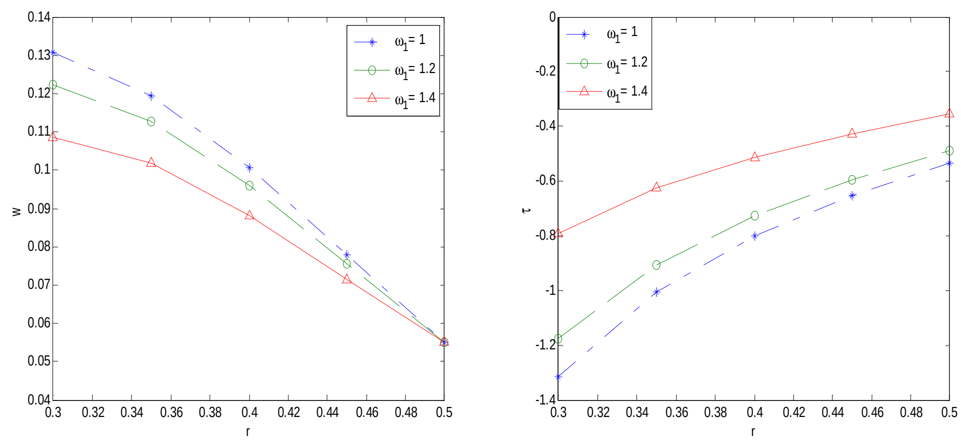

2.2(a) 2.2(b)

Fig. 2.2 Profiles of the velocity w(r, t) and shear stress τ(r, t) given by Eqs. (2.3.16) and (2.3.21) for $R_1 = 0.3$, $R_2 = 0.5$, $t = 2.1$, $\omega_2 = 1$, $V_1 = 1$, $V_2 = 1$, $\upsilon = 0.5566$, $\mu = 1.01$, $\lambda = 4$, $\beta = 0.8$ and different values of ω_1.

Figure 2.3

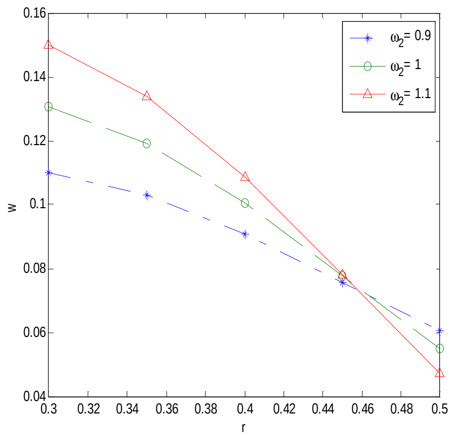

2.3(a)

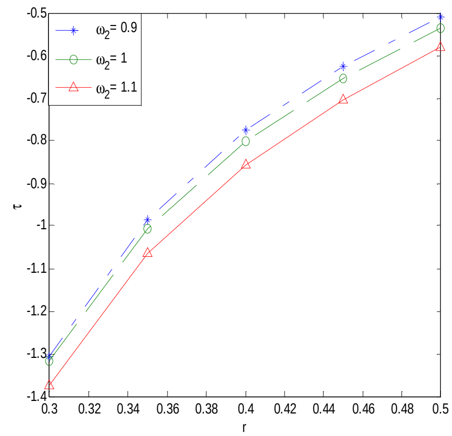

2.3(b)

Fig. 2.3 Profiles of the velocity w(r, t) and shear stress $\tau(\mathrm{r,t})$ given by Eqs. (2.3.16) and (2.3.21) for $R_1 = 0.3$, $R_2 = 0.5$, $t = 2.1$, $\omega_1 = 1$, $\mathrm{V}_1 = 1$, $\mathrm{V}_2 = 1$, $\upsilon = 0.5566$, $\mu = 1.01$, $\lambda = 4$, $\beta = 0.8$ and different values of ω_2.

Figure 2.4

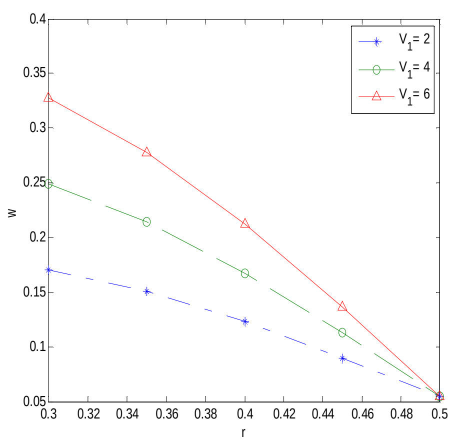

2.4(a)

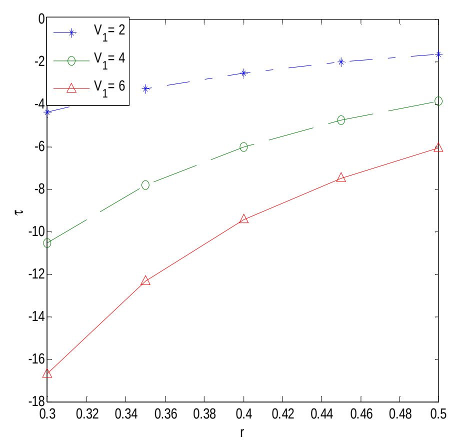

2.4(b)

Fig. 2.4 Profiles of the velocity w(r, t) and shear stress $\tau(\mathrm{r,t})$ given by Eqs. (2.3.16) and (2.3.21) for $R_1 = 0.3$, $R_2 = 0.5$, $\mathrm{t} = 2.1$, $\omega_1 = 1$, $\omega_2 = 1$, $\mathrm{V}_2 = 1$, $\upsilon = 0.5566$, $\mu = 1.01$, $\lambda = 4$, $\beta = 0.8$ and different values of V_1.

Figure 2.5

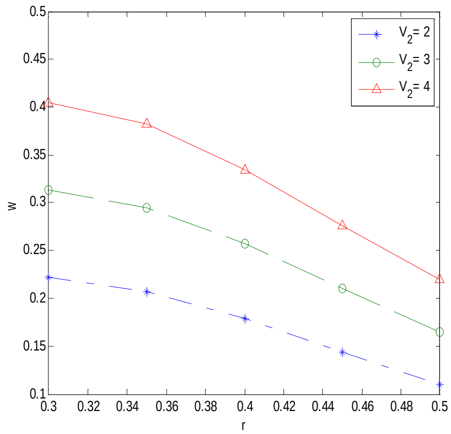

2.5(a)

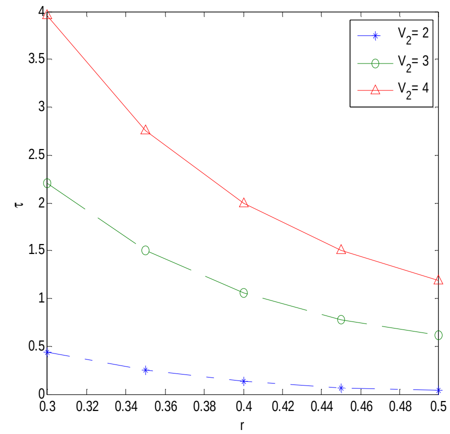

2.5(b)

Fig. 2.5 Profiles of the velocity w(r, t) and shear stress τ(r, t) given by Eqs. (2.3.16) and (2.3.21) for $R_1 = 0.3$, $R_2 = 0.5$, $t = 2.1$, $\omega_1 = 1$, $\omega_2 = 1$, $V_1 = 1$, $\upsilon = 0.5566$, $\mu = 1.01$, $\lambda = 4$, $\beta = 0.8$ and different values of V_2.

Figure 2.6

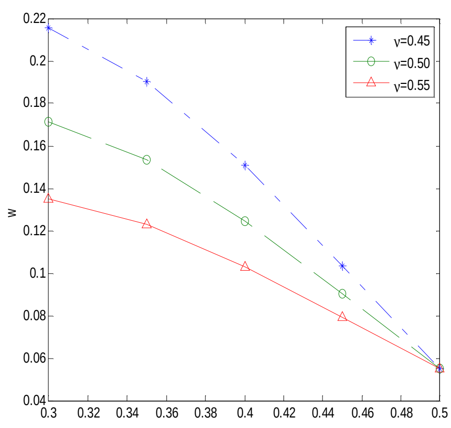

2.6(a)

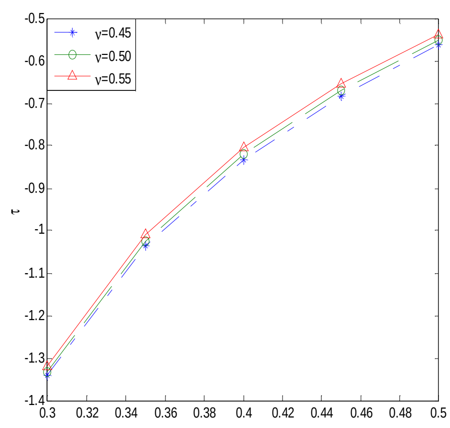

2.6(b)

Fig. 2.6 Profiles of the velocity w(r, t) and shear stress τ(r, t) given by Eqs. (2.3.16) and (2.3.21) for $R_1 = 0.3$, $R_2 = 0.5$, $t = 2.1$, $\omega_1 = 1$, $\omega_2 = 1$, $V_1 = 1$, $V_2 = 1$, $\mu = 1.01$, $\lambda = 4$, $\beta = 0.8$ and different values of υ.

Figure 2.7

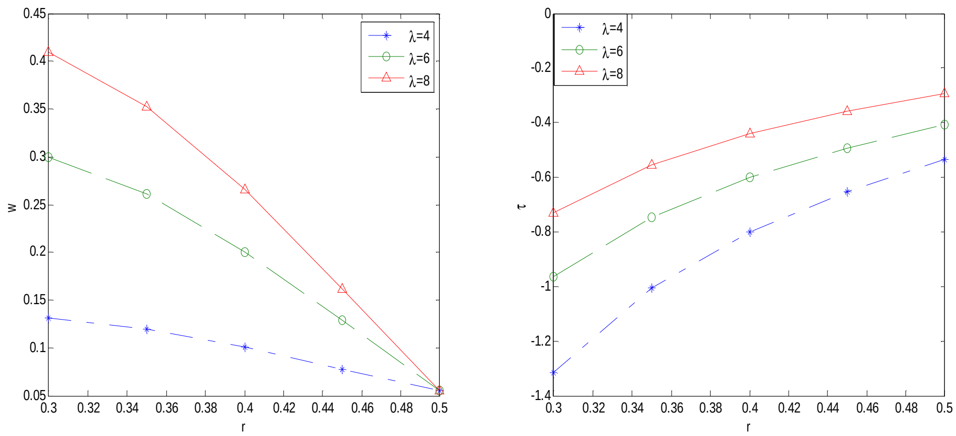

2.7(a) 2.7(b)

Fig. 2.7 Profiles of the velocity $w(r,t)$ and shear stress $\tau(r,t)$ given by Eqs. (2.3.16) and (2.3.21) for $R_1 = 0.3$, $R_2 = 0.5$, $t = 2.1$, $\omega_1 = 1$, $\omega_2 = 1$, $V_1 = 1$, $V_2 = 1$, $\upsilon = 0.5566$, $\mu = 1.01$, $\beta = 0.8$ and different values of λ.

Figure 2.8

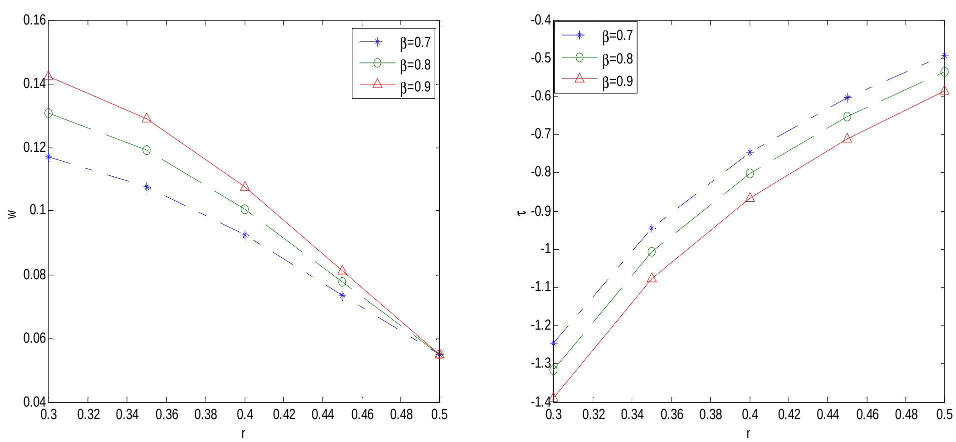

2.8(a) 2.8(b)

Fig. 2.8 Profiles of the velocity $w(r,t)$ and shear stress $\tau(r,t)$ given by Eqs. (2.3.16) and (2.3.21) for $R_1 = 0.3$, $R_2 = 0.5$, $t = 2.1$, $\omega_1 = 1$, $\omega_2 = 1$, $V_1 = 1$, $V_2 = 1$, $\upsilon = 0.5566$, $\mu = 1.01$, $\lambda = 4$ and different values of β.

Figure 2.9

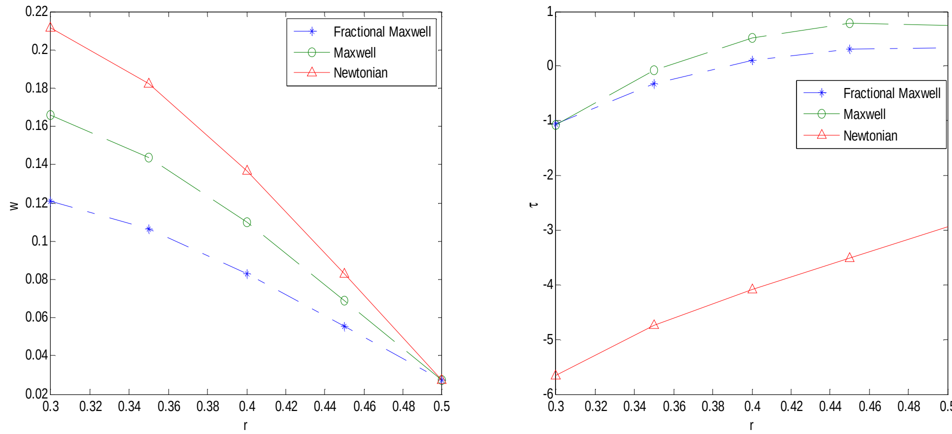

2. 9(a) 2.9(b)

Fig. 2.9 Profiles of the velocity $w(r, t)$ and shear stress $\tau(r, t)$ corresponding to the fractional Maxwell, ordinary Maxwell and Newtonian fluids, for $R_1 = 0.3$, $R_2 = 0.5$, $t = 2.7$, $\omega_1 = 1$, $\omega_2 = 1$, $V_1 = 1$, $V_2 = 1$, $\upsilon = 0.0155$, $\mu = 1.2$, $\lambda = 2$ and $\beta = 0.7$.

Chapter 3. Exact solutions for an unsteady flow of viscoelastic fluid in cylindrical domains using the fractional Maxwell model

---

The paper published on the work described in this chapter:

Khandelwal K. and Mathur V., Exact solutions for an unsteady flow of viscoelastic fluid in cylindrical domains using the fractional Maxwell model, International Journal of Applied and Computational Mathematics (Springer) 1, 143-156, (2015).

3.1 Introduction

The constitutive equations of an incompressible Maxwell fluid, as it is given by Eq. (2.2.1), are

$$T=-pI+S, \quad S+\lambda\left(\dot{S}-LS-SL^{T}\right)=\mu A, \tag{3.1.1}$$

where T, $-pI$, S, λ, A, L, μ, the superscript T and $\dot{S}$ have the same significance as before. The motion of a fluid in the annular region of sliding or rotating cylinders is of great interest for industry and academic workers. This chapter deals with the unsteady flow of an incompressible fractional Maxwell fluid filled in the annular region between two infinite coaxial circular cylinders. The motion of the fluid is due to the inner cylinder that applies a time dependent torsional shear to the fluid and outer cylinder which is moving at a constant velocity. The velocity field and shear stress are determined by the Laplace and finite Hankel transforms. The obtained solutions are presented in terms of the generalized G and R functions. Solutions for ordinary Maxwell fluid and Newtonian fluid are also obtained by imposing appropriate limits. Finally, the influence of different values of parameters, constants and fractional coefficient, as well as a comparison between the velocity field and shear stress are also analyzed using graphical illustration.

3.2 Governing equations

Let us consider an incompressible fractional Maxwell fluid with velocity V and extra stress S as in the form of

$$V=V(r,t)=w(r,t)e_{\theta}, \qquad \mathrm{S}=\mathrm{S}(r,t), \tag{3.2.1}$$

where e_{θ} is the unit vector in the θ direction of the cylindrical coordinates.

At time $t=0$, the fluid is at rest in an annular region between two infinite coaxial circular cylinders. At time $t=0^{+}$, the inner cylinder applies a time dependent torsional shear to the fluid and outer cylinder is moving at a constant velocity. For these flows, the constraint of incompressibility is automatically satisfied. Initially the fluid is at rest, hence

$$V(r,0) = 0, \qquad S(r,0) = 0. \tag{3.2.2}$$

For such flows the constraint of incompressibility is automatically satisfied, while the governing equations [17] are

$$\left(1 + \lambda D_t^{\alpha}\right)\frac{\partial w(r,t)}{\partial t} = \upsilon\left(\frac{\partial^2}{\partial r^2} + \frac{1}{r}\frac{\partial}{\partial r} - \frac{1}{r^2}\right)w(r,t), \qquad t > 0, \tag{3.2.3}$$

$$\left(1 + \lambda D_t^{\alpha}\right)\tau(r,t) = \mu\left(\frac{\partial}{\partial r} - \frac{1}{r}\right)w(r,t), \qquad t > 0, \tag{3.2.4}$$

where $\tau(r,t) = S_{r\theta}(r,t)$ is the non-trivial shear stress, λ is relaxation time, μ is the dynamic viscosity, ρ is the constant density of the fluid, $\upsilon = \dfrac{\mu}{\rho}$ is the kinematic viscosity and D_t^{α} is the Caputo fractional derivative of order α as defined by [64]

$$D_t^{\alpha} f(t) = \begin{cases} \dfrac{1}{\Gamma(1-\alpha)}\dfrac{d}{dt}\displaystyle\int_0^t \frac{f(\tau)}{(t-\tau)^{\alpha}}d\tau, & 0 < \alpha < 1; \\ \dfrac{d}{dt}f(t), & \alpha = 1, \end{cases} \tag{3.2.5}$$

where $\Gamma(.)$ is the Gamma function.

For $\alpha \to 1$ when $D_t^{\alpha} f(t) \to df(t)/dt$, Eqs. (3.2.3) and (3.2.4) are reduced to the governing equations for an ordinary Maxwell fluid.

3.3 Flow through the annular region

Let us consider an incompressible fractional Maxwell fluid at rest in the annular region between two infinite coaxial circular cylinders. Also, consider that radius of inner and outer cylinders are R_1 and $R_2(> R_1)$ respectively. At time $t=0^+$, the outer cylinder moving at a constant velocity and the inner cylinder begins to rotate about its axis with a time dependent torque per unit length $2\pi R_1 \tau(R_1,t)$ [17], where

$$\tau(R_1,t)=\frac{f_1}{\lambda}R_{\alpha,-1}\left(-\frac{1}{\lambda},t\right);\qquad 0<\alpha<1, \tag{3.3.1}$$

where f_1 is a constant and generalized R functions are defined by [117]

$$R_{a,b}(d,t)=L^{-1}\left\{\frac{q^b}{q^a-d}\right\}=\sum_{n=0}^{\infty}\frac{d^n t^{(n+1)a-b-1}}{\Gamma[(n+1)a-b]};$$
$$\mathrm{Re}(a-b)>0,\quad \mathrm{Re}(q)>0,\quad \left|\frac{\mathrm{d}}{\mathrm{q}^{\mathrm{a}}}\right|<1. \tag{3.3.2}$$

The governing equations are given by Eqs. (3.2.3) and (3.2.4), while appropriate initial and boundary conditions are

$$w(r,0)=0,\qquad \tau(\mathrm{r},0)=0, \tag{3.3.3}$$

and

$$\left(1+\lambda D_t^{\alpha}\right)\tau(r,t)\Big|_{r=R_1}=\mu\left(\frac{\partial}{\partial r}-\frac{1}{r}\right)w(r,t)\Big|_{r=R_1}=f_1,$$
$$w(R_2,t)=f_2,\quad \mathrm{t}>0, \tag{3.3.4}$$

where f_2 is the constant velocity of outer cylinder. Eq. (3.3.1) is the solution of Eq. (3.3.4). To solve this problem we use Laplace and Hankel transform methods.

3.3.1 Calculation of the velocity field

Applying Laplace transform of Eq. (3.2.3) and using the initial conditions as given in Eq. (3.3.3), we obtain

$$\left(q+\lambda q^{\alpha+1}\right)\overline{w}(r,q)=\upsilon\left(\frac{\partial^2}{\partial r^2}+\frac{1}{r}\frac{\partial}{\partial r}-\frac{1}{r^2}\right)\overline{w}(r,q), \tag{3.3.5}$$

where $\overline{w}(r,q)=\int_0^{\infty}e^{-qt}w(r,t)dt$ is the Laplace transform of function $w(r,t)$ and q is the transform parameter.

Applying Laplace transform of Eq. (3.3.4), we obtain

$$\left(\frac{\partial}{\partial r}-\frac{1}{r}\right)\overline{w}(r,q)\Big|_{r=R_1}=\frac{f_1}{\mu q};$$
$$\overline{w}(R_2,q)=\frac{f_2}{q}. \tag{3.3.6}$$

The Hankel transform method with respect to r is used and defined as follows

$$\overline{w}_H(r_n,q)=\int_{R_1}^{R_2} r\overline{w}(r,q)B(r,r_n)dr, \tag{3.3.7}$$

where

$$B(r,r_n)=J_1(rr_n)Y_2(R_1r_n)-J_2(R_1r_n)Y_1(rr_n), \tag{3.3.8}$$

r_n being the positive roots of the transcendental equation $B(R_2,r)=0$. The inverse Hankel transform as defined [17], is given below

$$\overline{w}(r,q)=\frac{\pi^2}{2}\sum_{n=1}^{\infty}\frac{r_n^2J_1^2(R_2r_n)B(r,r_n)}{J_2^2(R_1r_n)-J_1^2(R_2r_n)}\overline{w}_H(r_n,q). \tag{3.3.9}$$

Multiplying both sides of Eq. (3.3.5) by $rB(r, r_n)$, then integrating with respect to r from R_1 to R_2 and taking into account the conditions Eq. (3.3.6) and the equality

$$\begin{aligned}&\int_{R_1}^{R_2} r\left(\frac{\partial^2}{\partial r^2}+\frac{1}{r}\frac{\partial}{\partial r}-\frac{1}{r^2}\right)\overline{w}(r,q)B(r,r_n)dr\\
&=-r_n^2\overline{w}_H(r_n,q)+\frac{2}{\pi r_n}\left(\frac{\partial}{\partial r}-\frac{1}{r}\right)\overline{w}(r,q)\Big|_{r=R_1}+R_2r_n\overline{w}(R_2,q)[Y_2(R_1r_n)J_2(R_2r_n)-J_2(R_1r_n)Y_2(R_2r_n)]\\
&=-r_n^2\overline{w}_H(r_n,q)+\frac{2}{\pi r_n}\frac{f_1}{\mu q}+\frac{R_2r_nf_2}{q}[Y_2(R_1r_n)J_2(R_2r_n)-J_2(R_1r_n)Y_2(R_2r_n)],\end{aligned} \tag{3.3.10}$$

we obtain

$$\begin{aligned}&\overline{w}_H(r_n,q)\\
&=\frac{2f_1\upsilon}{\pi\mu r_n}\frac{1}{q(q+\lambda q^{\alpha+1}+\upsilon r_n^2)}\\
&\quad+\upsilon R_2r_nf_2[Y_2(R_1r_n)J_2(R_2r_n)-J_2(R_1r_n)Y_2(R_2r_n)]\frac{1}{q(q+\lambda q^{\alpha+1}+\upsilon r_n^2)}.\end{aligned} \tag{3.3.11}$$

Rewriting Eq. (3.3.11) into a suitable equivalent form, we obtain below

$$\overline{w}_H(r_n,q)$$
$$=\frac{2f_1}{\pi\mu r_n^3}\frac{1}{q}-\frac{2f_1(1+\lambda q^\alpha)}{\pi\mu r_n^3(q+\lambda q^{\alpha+1}+\upsilon r_n^2)}$$
$$+\frac{f_2R_2}{r_n}[Y_2(R_1r_n)J_2(R_2r_n)-J_2(R_1r_n)Y_2(R_2r_n)]\left[\frac{1}{q}-\frac{(1+\lambda q^\alpha)}{(q+\lambda q^{\alpha+1}+\upsilon r_n^2)}\right]. \quad (3.3.12)$$

Applying inverse Hankel transform to Eq. (3.3.12) and taking into account the following result

$$\int_{R_1}^{R_2}\left(r^2-R_2^2\right)B(r,r_n)dr=\frac{4}{\pi r_n^3}\left(\frac{R_2}{R_1}\right)^2, \quad (3.3.13)$$

we obtain

$$\overline{w}(r,q)$$
$$=\frac{f_1}{2\mu}\left(\frac{R_1}{R_2}\right)^2\left(r-\frac{R_2^2}{r}\right)\frac{1}{q}-\frac{\pi f_1}{\mu}\sum_{n=1}^{\infty}\frac{J_1^2(R_2r_n)B(r,r_n)}{r_n[J_2^2(R_1r_n)-J_1^2(R_2r_n)]}\frac{(1+\lambda q^\alpha)}{(q+\lambda q^{\alpha+1}+\upsilon r_n^2)}$$
$$+\frac{\pi^2}{2}R_2f_2\sum_{n=1}^{\infty}\frac{r_nJ_1^2(R_2r_n)B(r,r_n)}{[J_2^2(R_1r_n)-J_1^2(R_2r_n)]}[Y_2(R_1r_n)J_2(R_2r_n)-J_2(R_1r_n)Y_2(R_2r_n)]$$
$$\times\left[\frac{1}{q}-\frac{(1+\lambda q^\alpha)}{(q+\lambda q^{\alpha+1}+\upsilon r_n^2)}\right]. \quad (3.3.14)$$

Applying Inverse-Laplace transform of Eq. (3.3.14) and taking into account the following result [117]

$$G_{a,b,c}(d,t)=L^{-1}\left\{\frac{q^b}{(q^a-d)^c}\right\}$$
$$=\sum_{\mathrm{j}=0}^{\infty}\frac{\mathrm{d}^{\mathrm{j}}\Gamma(c+j)}{\Gamma(c)\Gamma(j+1)}\frac{t^{(c+j)a-b-1}}{\Pi[(c+j)a-b]};$$

$$\mathrm{Re}(ac-b)>0,\quad \mathrm{Re(q)}>0,\quad \left|\frac{\mathrm{d}}{\mathrm{q^a}}\right|<1, \quad (3.3.15)$$

we obtain

$$
\begin{aligned}
&w(r,t)\\
&=\frac{f_1}{2\mu}\left(\frac{R_1}{R_2}\right)^2\left(r-\frac{R_2^2}{r}\right)-\frac{\pi f_1}{\mu\lambda}\sum_{n=1}^{\infty}\frac{J_1^2(R_2r_n)B(r,r_n)}{r_n[J_2^2(R_1r_n)-J_1^2(R_2r_n)]}\sum_{k=0}^{\infty}\left(\frac{-\upsilon r_n^2}{\lambda}\right)^k\\
&\quad\times\left[G_{\alpha,-k-1,k+1}(-\lambda^{-1},t)+\lambda G_{\alpha,\alpha-k-1,k+1}(-\lambda^{-1},t)\right]\\
&\quad+\frac{\pi^2}{2}R_2 f_2\sum_{n=1}^{\infty}\frac{r_nJ_1^2(R_2r_n)B(r,r_n)}{[J_2^2(R_1r_n)-J_1^2(R_2r_n)]}[Y_2(R_1r_n)J_2(R_2r_n)-J_2(R_1r_n)Y_2(R_2r_n)]\\
&\quad\times\left[1-\frac{1}{\lambda}\sum_{k=0}^{\infty}\left(\frac{-\upsilon r_n^2}{\lambda}\right)^k\left\{G_{\alpha,-k-1,k+1}(-\lambda^{-1},t)+\lambda G_{\alpha,\alpha-k-1,k+1}(-\lambda^{-1},t)\right\}\right].
\end{aligned}
\tag{3.3.16}
$$

3.3.2 Calculation of the shear stress

Applying Laplace transform to Eq. (3.2.4), we obtain

$$\bar{\tau}(r,q)=\mu\frac{1}{(1+\lambda q^{\alpha})}\left(\frac{\partial}{\partial r}-\frac{1}{r}\right)\bar{w}(r,q). \tag{3.3.17}$$

Substitute Eq. (3.3.14) in Eq. (3.3.17), we obtain

$$
\begin{aligned}
\bar{\tau}(r,q)&=f_1\left(\frac{R_1}{r}\right)^2\frac{1}{q(1+\lambda q^{\alpha})}+\pi f_1\sum_{n=1}^{\infty}\frac{J_1^2(R_2r_n)\bar{B}(r,r_n)}{[J_2^2(R_1r_n)-J_1^2(R_2r_n)]}\frac{1}{(q+\lambda q^{\alpha+1}+\upsilon r_n^2)}\\
&\quad-\frac{\pi^2}{2}\mu R_2 f_2\sum_{n=1}^{\infty}\frac{r_n^2J_1^2(R_2r_n)\bar{B}(r,r_n)}{[J_2^2(R_1r_n)-J_1^2(R_2r_n)]}[Y_2(R_1r_n)J_2(R_2r_n)-J_2(R_1r_n)Y_2(R_2r_n)]\\
&\quad\times\left[\frac{1}{q(1+\lambda q^{\alpha})}-\frac{1}{(q+\lambda q^{\alpha+1}+\upsilon r_n^2)}\right],
\end{aligned}
\tag{3.3.18}
$$

where

$$\bar{B}(r,r_n)=J_2(rr_n)Y_2(R_1r_n)-J_2(R_1r_n)Y_2(rr_n). \tag{3.3.19}$$

Applying inverse Laplace transform to Eq. (3.3.18) and using Eq. (3.3.15), we obtain

$$\tau(r,t) = f_1\left(\frac{R_1}{r}\right)^2 \frac{1}{\lambda} R_{\alpha,-1}(-\lambda^{-1},t)$$
$$+\frac{\pi f_1}{\lambda}\sum_{n=1}^{\infty}\frac{J_1^2(R_2 r_n)\overline{B}(r,r_n)}{[J_2^2(R_1 r_n)-J_1^2(R_2 r_n)]}\sum_{k=0}^{\infty}\left(\frac{-\upsilon r_n^2}{\lambda}\right)^k G_{\alpha,-k-1,k+1}(-\lambda^{-1},t)$$
$$-\frac{\pi^2}{2}\frac{\mu R_2 f_2}{\lambda}\sum_{n=1}^{\infty}\frac{r_n^2 J_1^2(R_2 r_n)\overline{B}(r,r_n)}{[J_2^2(R_1 r_n)-J_1^2(R_2 r_n)]}[Y_2(R_1 r_n)J_2(R_2 r_n)-J_2(R_1 r_n)Y_2(R_2 r_n)]$$
$$\times\left[R_{\alpha,-1}(-\lambda^{-1},t)-\sum_{k=0}^{\infty}\left(\frac{-\upsilon r_n^2}{\lambda}\right)^k G_{\alpha,-k-1,k+1}(-\lambda^{-1},t)\right]. \tag{3.3.20}$$

3.4 Limiting Cases

3.4.1 Ordinary Maxwell Fluid

Applying $\alpha \to 1$ into Eqs. (3.3.16) and (3.3.20), we obtain the velocity field

$$w_M(r,t)$$
$$=\frac{f_1}{2\mu}\left(\frac{R_1}{R_2}\right)^2\left(r-\frac{R_2^2}{r}\right)-\frac{\pi f_1}{\mu\lambda}\sum_{n=1}^{\infty}\frac{J_1^2(R_2 r_n)B(r,r_n)}{r_n[J_2^2(R_1 r_n)-J_1^2(R_2 r_n)]}\sum_{k=0}^{\infty}\left(\frac{-\upsilon r_n^2}{\lambda}\right)^k$$
$$\times\left[G_{1,-k-1,k+1}(-\lambda^{-1},t)+\lambda G_{1,-k,k+1}(-\lambda^{-1},t)\right]$$
$$+\frac{\pi^2}{2}R_2 f_2\sum_{n=1}^{\infty}\frac{r_n J_1^2(R_2 r_n)B(r,r_n)}{[J_2^2(R_1 r_n)-J_1^2(R_2 r_n)]}[Y_2(R_1 r_n)J_2(R_2 r_n)-J_2(R_1 r_n)Y_2(R_2 r_n)]$$
$$\times\left[1-\frac{1}{\lambda}\sum_{k=0}^{\infty}\left(\frac{-\upsilon r_n^2}{\lambda}\right)^k\left\{G_{1,-k-1,k+1}(-\lambda^{-1},t)+\lambda G_{1,-k,k+1}(-\lambda^{-1},t)\right\}\right], \tag{3.4.1}$$

and its associated shear stress corresponding to ordinary Maxwell fluid performing the same motion

$$\tau_M(r,t) = f_1\left(\frac{R_1}{r}\right)^2\left(1-e^{-t/\lambda}\right)$$
$$+\frac{\pi f_1}{\lambda}\sum_{n=1}^{\infty}\frac{J_1^2(R_2 r_n)\overline{B}(r,r_n)}{[J_2^2(R_1 r_n)-J_1^2(R_2 r_n)]}\sum_{k=0}^{\infty}\left(\frac{-\upsilon r_n^2}{\lambda}\right)^k G_{1,-k-1,k+1}(-\lambda^{-1},t)$$
$$-\frac{\pi^2}{2}\frac{\mu R_2 f_2}{\lambda}\sum_{n=1}^{\infty}\frac{r_n^2 J_1^2(R_2 r_n)\overline{B}(r,r_n)}{[J_2^2(R_1 r_n)-J_1^2(R_2 r_n)]}[Y_2(R_1 r_n)J_2(R_2 r_n)-J_2(R_1 r_n)Y_2(R_2 r_n)]$$
$$\times\left[\lambda\left(1-e^{-t/\lambda}\right)-\sum_{k=0}^{\infty}\left(\frac{-\upsilon r_n^2}{\lambda}\right)^k G_{1,-k-1,k+1}(-\lambda^{-1},t)\right]. \tag{3.4.2}$$

3.4.2 Newtonian Fluid

Applying $\lambda \to 0$ into Eqs. (3.4.1) and (3.4.2) and taking into account the following result [22]

$$\lim_{\lambda\to 0}\frac{1}{\lambda^m}G_{1,b,m}(-\lambda^{-1},t)=\frac{t^{-b-1}}{\Gamma(-b)}, \quad \mathrm{b}<0,$$

we obtain the corresponding solutions for the Newtonian fluid, as follows

$$w_N(r,t)=\frac{f_1}{2\mu}\left(\frac{R_1}{R_2}\right)^2\left(r-\frac{R_2^2}{r}\right)-\frac{\pi f_1}{\mu}\sum_{n=1}^{\infty}\frac{J_1^2(R_2r_n)B(r,r_n)}{r_n[J_2^2(R_1r_n)-J_1^2(R_2r_n)]}e^{-\upsilon r_n^2 t}$$
$$+\frac{\pi^2}{2}R_2 f_2\sum_{n=1}^{\infty}\frac{r_nJ_1^2(R_2r_n)B(r,r_n)}{[J_2^2(R_1r_n)-J_1^2(R_2r_n)]}[Y_2(R_1r_n)J_2(R_2r_n)-J_2(R_1r_n)Y_2(R_2r_n)]\left(1-e^{-\upsilon r_n^2 t}\right), \tag{3.4.3}$$

and

$$\tau_N(r,t)=f_1\left(\frac{R_1}{r}\right)^2+\pi f_1\sum_{n=1}^{\infty}\frac{J_1^2(R_2r_n)\overline{B}(r,r_n)}{[J_2^2(R_1r_n)-J_1^2(R_2r_n)]}e^{-\upsilon r_n^2 t}$$
$$-\frac{\pi^2}{2}\mu R_2 f_2\sum_{n=1}^{\infty}\frac{r_n^2J_1^2(R_2r_n)\overline{B}(r,r_n)}{[J_2^2(R_1r_n)-J_1^2(R_2r_n)]}[Y_2(R_1r_n)J_2(R_2r_n)-J_2(R_1r_n)Y_2(R_2r_n)]\left(1-e^{-\upsilon r_n^2 t}\right). \tag{3.4.4}$$

3.5 Conclusions and Numerical results

The purpose of this chapter is to establish exact solutions for the velocity field and shear stress corresponding to the unsteady flow of an incompressible fractional Maxwell fluid flow in the annular region. Where, the motion is produced by the inner cylinder that applies a time dependent torsional shear to the fluid and outer cylinder which is moving at a constant velocity. The solution is obtained by finite Hankel and Laplace transform methods and the result is presented under series form in terms of the generalized G and R functions. The similar solutions for ordinary Maxwell and Newtonian fluids are also obtained as limiting cases of the solution for fractional Maxwell fluid. The velocity field and shear stress are also analyzed using graphical illustration for various parameters, constants and fractional coefficients and a comparison between models of the velocity field and shear stress are also analyzed using graphical illustration.

As shown in below diagrams, the velocity $w(r,t)$ and the shear stress $\tau(r,t)$ given by Eq. (3.3.16) and Eq. (3.3.20) have been drawn against r for different values of the time t, f_1, f_2 and other relevant parameters. It can be clearly seen from the figures that the velocity component w is decreasing function of r and the shear stress component τ is increasing function of r. The motion of the fluid is relatively higher and shear stress lower in the neighborhood of the inner cylinder for given boundary conditions and $f_1<0$, $f_2<0$. Figures 3.1(a) and 3.1(b) are showing the effect of different values of time on the fluid motion. It can be seen that the velocity and the shear stress are the decreasing function of time t. The influence of relaxation time λ and fractional parameter α on the fluid motion is shown in figures 3.2 and 3.3. Both parameters have opposite effect on the fluid motion. The velocity and the shear stress are increasing function of λ and decreasing function of α. Figures 3.4(a) and 3.4(b) are showing the effect of different values of dynamic viscosity on the fluid motion. The results indicate that the velocity and the shear stress are increasing function of dynamic viscosity. Figures 3.5 and 3.6 are showing the behavior of f_1 and f_2 on the fluid motion for their different values. Figure 3.7 is showing a comparison diagram of the velocity $w(r,t)$ and the shear stress $\tau(r,t)$ among three models (Fractional Maxwell fluid, ordinary Maxwell fluid and Newtonian fluid) for same values of the common material constants and time t. The velocity in the neighborhood of inner cylinders is swiftest for fractional Maxwell fluid while it is slowest for the ordinary Maxwell fluid. Similarly, shear stress on the whole flow domains highest for fractional Maxwell fluid while it is slowest for the Newtonian fluid.

In all of the figures 3.1-3.7, the units of the material constants are in SI units and the root r_n has been approximated by $\dfrac{(2n-1)\pi}{2(R_2-R_1)}$.

Figure 3.1

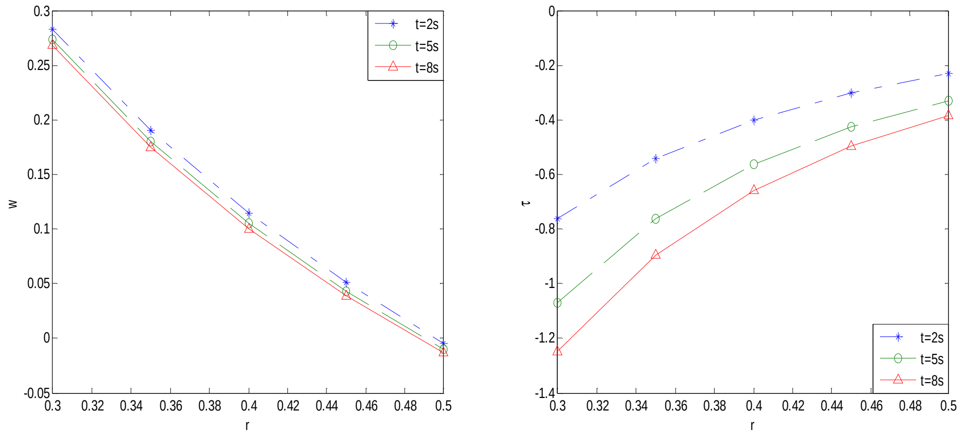

3.1(a) 3.1(b)

Fig.3.1 Profiles of the velocity w(r, t) and shear stress τ(r, t) given by Eqs. (3.3.16) and (3.3.20) for $R_1 = 0.3$, $R_2 = 0.5$, $f_1 = -3$, $f_2 = -2$, $\upsilon = 0.015$, $\mu = 1.01$, $\lambda = 5$, $\alpha = 0.5$ and different values of t.

Figure 3.2

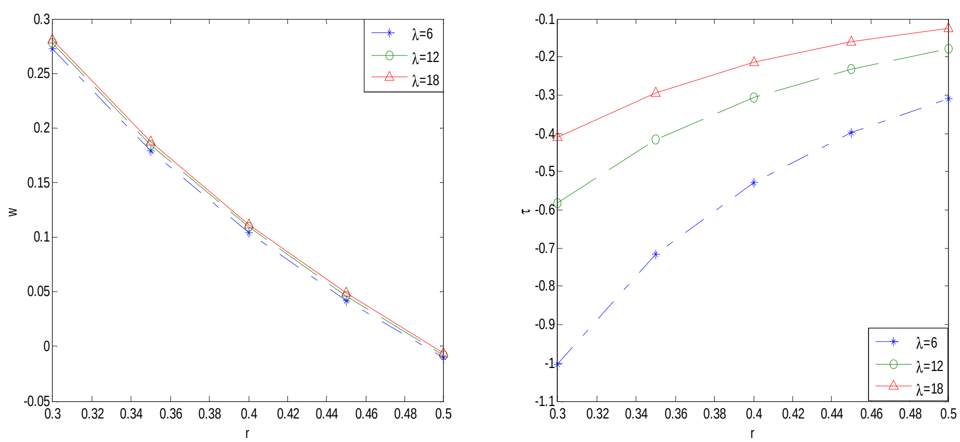

3.2(a) 3.2(b)

Fig. 3.2 Profiles of the velocity w(r, t) and shear stress τ(r, t) given by Eqs. (3.3.16) and (3.3.20) for $R_1 = 0.3$, $R_2 = 0.5$, $f_1 = -3$, $f_2 = -2$, t = 6s, $\upsilon = 0.015$, $\mu = 1.01$, $\alpha = 0.5$ and different values of λ.

Figure 3.3

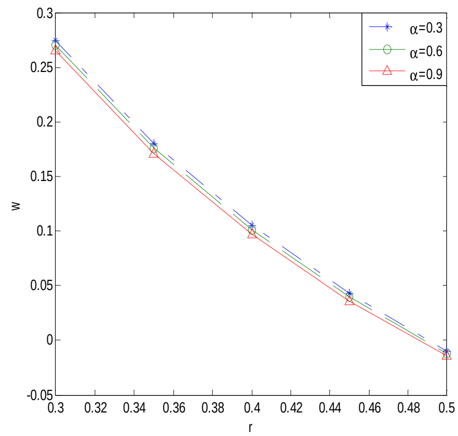

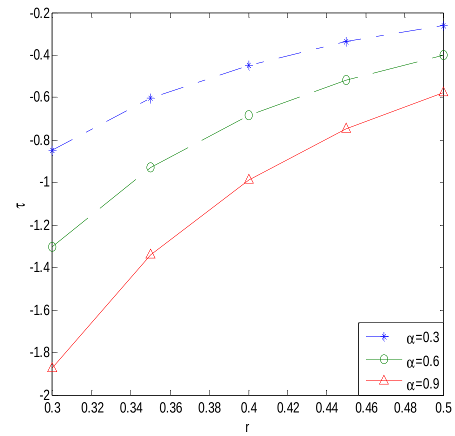

3.3(a) 3.3(b)

Fig. 3.3 Profiles of the velocity $w(r,t)$ and shear stress $\tau(r,t)$ given by Eqs. (3.3.16) and (3.3.20) for $R_1 = 0.3, R_2 = 0.5, f_1 = -3, f_2 = -2, t = 6s, \upsilon = 0.015, \mu = 1.01, \lambda = 5$ and different values of α.

Figure 3.4

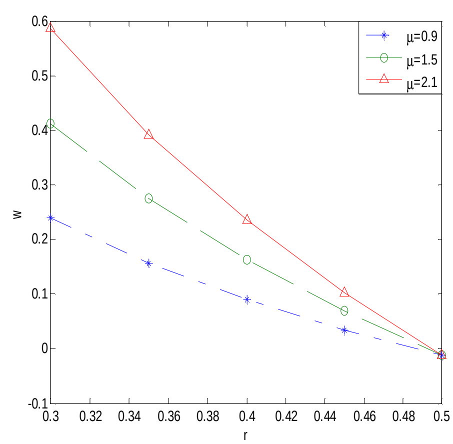

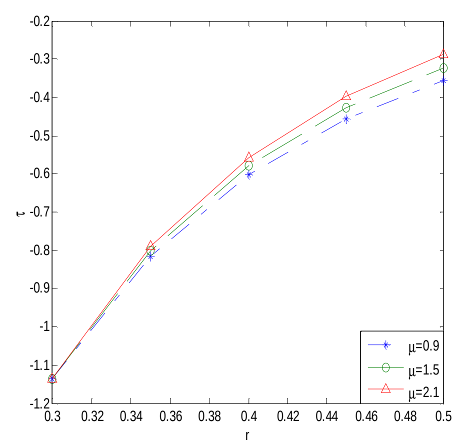

3.4(a) 3.4(b)

Fig. 3.4 Profiles of the velocity $w(r,t)$ and shear stress $\tau(r,t)$ given by Eqs. (3.3.16) and (3.3.20) for $R_1 = 0.3, R_2 = 0.5, f_1 = -3, f_2 = -2, t = 6s, \upsilon = 0.015, \lambda = 5, \alpha = 0.5$ and different values of μ.

Figure 3.5

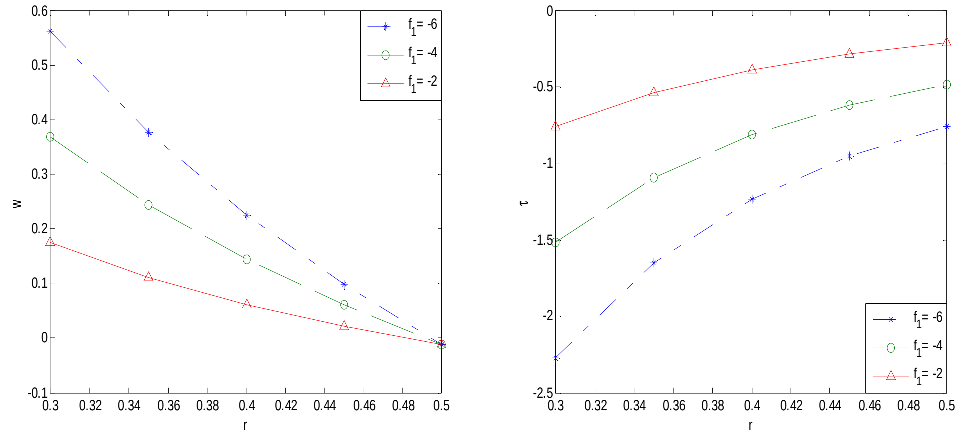

3.5(a) 3.5(b)

Fig. 3.5 Profiles of the velocity w(r, t) and shear stress $\tau(\mathrm{r},\mathrm{t})$ given by Eqs. (3.3.16) and (3.3.20) for $R_1 = 0.3, R_2 = 0.5,\ f_2 = -2,\ \mathrm{t} = 6\mathrm{s}, \upsilon = 0.015, \mu = 1.01, \lambda = 5, \alpha = 0.5$ and different values of f_1.

Figure 3.6

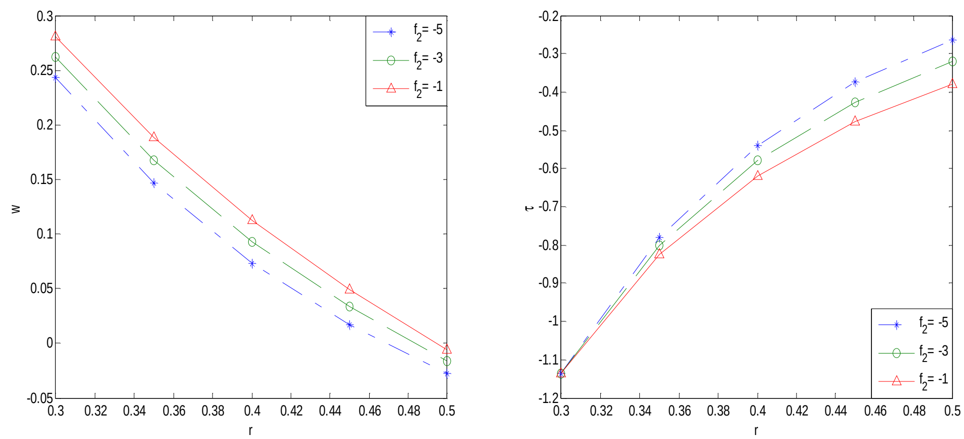

3.6(a) 3.6(b)

Fig. 3.6 Profiles of the velocity w(r, t) and shear stress $\tau(\mathrm{r},\mathrm{t})$ given by Eqs. (3.3.16) and (3.3.20) for $R_1 = 0.3, R_2 = 0.5,\ f_1 = -3, \mathrm{t} = 6\mathrm{s}, \upsilon = 0.015,\ \mu = 1.01,\ \lambda = 5, \alpha = 0.5$ and different values of f_2.

Figure 3.7

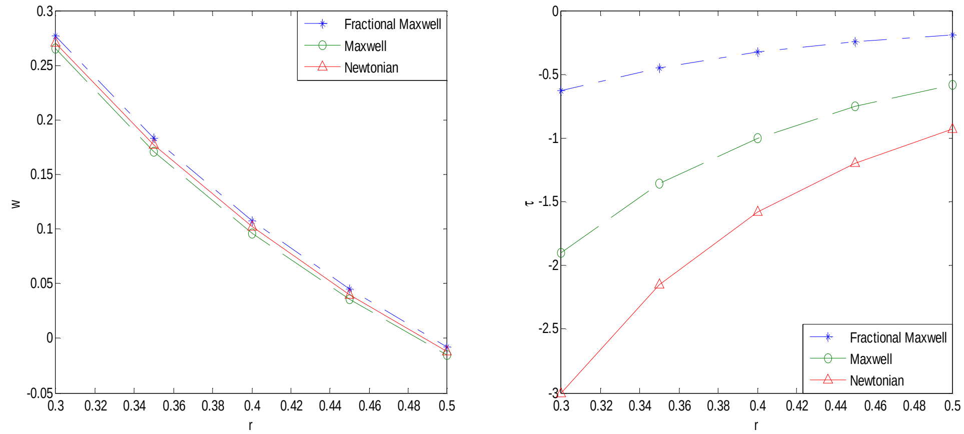

3.7(a) 3.7(b)

Fig. 3.7 Profiles of the velocity w(r, t) and shear stress τ(r, t) corresponding to the fractional Maxwell, ordinary Maxwell and Newtonian fluids, for $R_1 = 0.3$, $R_2 = 0.5$, $f_1 = -3$, $f_2 = -2$, t = 6 s, $\upsilon = 0.015$, $\mu = 1.01$, $\lambda = 6$ and $\alpha = 0.2$.

Chapter 4. Exact solutions for the flow of fractional Maxwell fluid in pipe-like domains

The paper published on the work described in this chapter:

Mathur V. and Khandelwal K., Flow of fractional Maxwell fluid in pipe-like domains, Advances in Applied Mathematics and Mechanics, 8, 1-11 (2016). DOI: 10.4208/aamm.2014.m588 (SCI Publication).

4.1 Introduction

This chapter presents an analysis of unsteady flow of incompressible fractional Maxwell fluid filled in the annular region between two infinite coaxial circular cylinders. The fluid motion is created by the inner cylinder that applies a longitudinal time-dependent shear stress and the outer cylinder that is moving at a constant velocity. The velocity field and shear stress are determined using the Laplace and finite Hankel transforms. Obtained solutions are presented in terms of the generalized G and R functions. The solutions for ordinary Maxwell and Newtonian fluids are also obtained as limiting cases of $\alpha \to 1$ and $\alpha \to 1, \lambda \to 0$ respectively. The influence of different parameters on the velocity field and shear stress are also presented using graphical illustration. Finally, a comparison is drawn between motions of fractional Maxwell fluid, ordinary Maxwell fluid and Newtonian fluid.

4.2 Governing equations

Consider an incompressible fractional Maxwell fluid that has a velocity V and extra shear stress S of the form [69]

$$V = V(r,t) = v(r,t)e_z, \qquad S = S(r,t), \tag{4.2.1}$$

where e_z is the unit vector in the z direction of the cylindrical coordinates. For such flows, the constraint of incompressibility is automatically satisfied, while the governing equations are [69]

$$\left(1 + \lambda D_t^{\alpha}\right)\frac{\partial \mathrm{v}(\mathrm{r},\mathrm{t})}{\partial \mathrm{t}} = \upsilon\left(\frac{\partial^2}{\partial \mathrm{r}^2} + \frac{1}{r}\frac{\partial}{\partial r}\right)\mathrm{v}(\mathrm{r},\mathrm{t}), \tag{4.2.2}$$

$$\left(1 + \lambda D_t^{\alpha}\right)\tau(r,t) = \mu\frac{\partial v(r,t)}{\partial r}, \tag{4.2.3}$$

where $\tau(r,t) = S_{rz}(r,t)$ is the non-trivial shear stress, λ is relaxation time, μ is the dynamic viscosity, $\upsilon = \dfrac{\mu}{\rho}$ is the kinematic viscosity, ρ is the constant density of the fluid and D_t^{β} is the Caputo fractional derivative of order β as defined by [64]

$$D_t^{\beta} f(t) = \begin{cases} \dfrac{1}{\Gamma(1-\beta)} \dfrac{d}{dt} \displaystyle\int_0^t \dfrac{f(\tau)}{(t-\tau)^{\beta}} d\tau, & 0 < \beta < 1; \\ \dfrac{d}{dt} f(t), & \beta = 1, \end{cases} \tag{4.2.4}$$

where $\Gamma(.)$ is the Gamma function. For $\beta \to 1$, Eqs. (4.2.2) and (4.2.3) are reduced to the governing equations for an ordinary Maxwell fluid.

4.3 Flow through the annular region between coaxial circular cylinders

Let us consider an incompressible fractional Maxwell fluid at rest in infinite coaxial circular cylinders of radii R_1 and $R_2 (> R_1)$. At time $t=0^+$, the inner cylinder is pulled with a time-dependent shear stress and the outer cylinder is moving at a constant velocity. At time $t=0^+$, a time dependent longitudinal shear stress can be defined by [12]

$$\tau(R_1, t) = \frac{f_1 \Gamma(a+1)}{\lambda} R_{\alpha,-a-1}\left(-\lambda^{-1}, t\right), \qquad 0 < \alpha < 1, \qquad a \geq 0, \tag{4.3.1}$$

where f_1 is a real constant and generalized $R_{a,b}(d,t)$ function is defined by [117]

$$R_{a,b}(d,t) = L^{-1}\left\{\frac{q^b}{q^a - d}\right\} = \sum_{n=0}^{\infty} \frac{d^n t^{(n+1)a-b-1}}{\Gamma[(n+1)a-b]};$$
$$\mathrm{Re}(a-b) > 0, \quad \mathrm{Re}(q) > 0, \quad \left|\frac{\mathrm{d}}{\mathrm{q^a}}\right| < 1. \tag{4.3.2}$$

The governing equations given by Eqs. (4.2.2) and (4.2.3) with appropriate initial and boundary conditions are

$$v(r,0) = 0, \qquad \tau(\mathrm{r},0) = 0, \tag{4.3.3}$$

and

$$\left(1 + \lambda D_t^{\alpha}\right)\tau(r,t)\Big|_{r=R_1} = \mu \frac{\partial v(r,t)}{\partial r}\Big|_{r=R_1} = f_1 t^a, \qquad t > 0, \qquad a \geq 0$$
$$v(R_2, t) = f_2, \qquad \mathrm{t} > 0, \tag{4.3.4}$$

where f_2 is the constant velocity of outer cylinder. Eq. (4.3.1) is the solution of first equation of Eq. (4.3.4). To solve this problem, we use Laplace and finite Hankel transforms.

4.3.1 Calculation of the velocity field

Applying Laplace transform to Eq. (4.2.2) and using the initial conditions as given in Eq. (4.3.3), we obtain

$$\left(q+\lambda q^{\alpha+1}\right)\bar{v}(r,q)=\upsilon\left(\frac{\partial^2}{\partial r^2}+\frac{1}{r}\frac{\partial}{\partial r}\right)\bar{v}(r,q), \tag{4.3.5}$$

applying Laplace transform to Eq. (4.3.4), we obtain

$$\frac{\partial\bar{v}(r,q)}{\partial r}\Big|_{r=R_1}=\frac{f_1\Gamma(a+1)}{\mu q^{a+1}}, \qquad \bar{v}(R_2,q)=\frac{f_2}{q}. \tag{4.3.6}$$

The Hankel transform method with respect to r is used and defined by [116]

$$\bar{v}_H(r_n,q)=\int_{R_1}^{R_2} r\bar{v}(r,q)B(r,r_n)dr, \tag{4.3.7}$$

where

$$B(r,r_n)=J_0(rr_n)Y_1(R_1r_n)-J_1(R_1r_n)Y_0(rr_n), \tag{4.3.8}$$

and r_n being the positive roots of the transcendental equation $B(R_2,r)=0$. The inverse Hankel transform is given by [116]

$$\bar{v}(r,q)=\frac{\pi^2}{2}\sum_{n=1}^{\infty}\frac{r_n^2J_0^2(R_2r_n)B(r,r_n)}{J_1^2(R_1r_n)-J_0^2(R_2r_n)}\bar{v}_H(r_n,q). \tag{4.3.9}$$

Multiplying both sides of Eq. (4.3.5) by $rB(r, r_n)$ and integrating with respect to r from R_1 to R_2, taking into account the Eq. (4.3.6) and the equality

$$\int_{R_1}^{R_2} r\left(\frac{\partial^2}{\partial r^2}+\frac{1}{r}\frac{\partial}{\partial r}\right)\bar{v}(r,q)B(r,r_n)dr$$

$$=-r_n^2\bar{v}_H(r_n,q)+\frac{2}{\pi r_n}\frac{\partial\bar{v}(R_1,q)}{\partial r}+\frac{2}{\pi}\frac{J_1(R_1r_n)}{J_0(R_2r_n)}\bar{v}(R_2,q)$$

$$=-r_n^2\bar{v}_H(r_n,q)+\frac{2}{\pi r_n}\frac{f_1\Gamma(a+1)}{\mu q^{a+1}}-\frac{2}{\pi}\frac{J_0'(R_1r_n)}{J_0(R_2r_n)}\frac{f_2}{q}. \quad (4.3.10)$$

we obtain

$$\bar{v}_H(r_n,q)$$
$$=\frac{2\upsilon f_1\Gamma(a+1)}{\pi\mu r_n}\frac{1}{q^{a+1}(q+\lambda q^{\alpha+1}+\upsilon r_n^2)}-\frac{2\upsilon f_2}{\pi}\frac{J_0'(R_1r_n)}{J_0(R_2r_n)}\frac{1}{q(q+\lambda q^{\alpha+1}+\upsilon r_n^2)}. \quad (4.3.11)$$

Rewriting Eq. (4.3.11) into a suitable equivalent form, we obtain

$$\bar{v}_H(r_n,q)$$
$$=\frac{2f_1\Gamma(a+1)}{\pi\mu r_n^3}\frac{1}{q^{a+1}}-\frac{2f_1\Gamma(a+1)}{\pi\mu r_n^3}\frac{(1+\lambda q^{\alpha})}{q^a(q+\lambda q^{\alpha+1}+\upsilon r_n^2)}$$
$$-\frac{2f_2}{\pi r_n^2}\frac{J_0'(R_1r_n)}{J_0(R_2r_n)}\frac{1}{q}+\frac{2f_2}{\pi r_n^2}\frac{J_0'(R_1r_n)}{J_0(R_2r_n)}\frac{(1+\lambda q^{\alpha})}{(q+\lambda q^{\alpha+1}+\upsilon r_n^2)}. \quad (4.3.12)$$

Applying inverse Hankel transform to Eq. (4.3.12) and taking into account the following result

$$\int_{R_1}^{R_2} r\ln\left(\frac{r}{R_2}\right)B(r,r_n)dr=\frac{2}{\pi R_1r_n^3}, \quad (4.3.13)$$

we obtain

$$\bar{v}(r,q)$$
$$=\frac{f_1R_1\Gamma(a+1)}{\mu}\ln\left(\frac{r}{R_2}\right)\frac{1}{q^{a+1}}+\frac{\pi^2}{2}\sum_{n=1}^{\infty}\frac{r_n^2J_0^2(R_2r_n)B(r,r_n)}{[J_1^2(R_1r_n)-J_0^2(R_2r_n)]}\left[-\frac{2f_1\Gamma(a+1)}{\pi\mu r_n^3}\frac{(1+\lambda q^{\alpha})}{q^a(q+\lambda q^{\alpha+1}+\upsilon r_n^2)}\right.$$
$$\left.-\frac{2f_2}{\pi r_n^2}\frac{J_0'(R_1r_n)}{J_0(R_2r_n)}\frac{1}{q}+\frac{2f_2}{\pi r_n^2}\frac{J_0'(R_1r_n)}{J_0(R_2r_n)}\frac{(1+\lambda q^{\alpha})}{(q+\lambda q^{\alpha+1}+\upsilon r_n^2)}\right]. \quad (4.3.14)$$

Applying Inverse-Laplace transform to Eq. (4.3.14) and taking into account the following results

$$\frac{1}{q+\lambda q^{\alpha+1}+\upsilon r_n^2}=\frac{1}{\lambda}\sum_{k=0}^{\infty}\left(\frac{-\upsilon r_n^2}{\lambda}\right)^k\frac{q^{-k-1}}{(q^{\alpha}+\lambda^{-1})^{k+1}}, \tag{4.3.15}$$

$$\begin{aligned}G_{a,b,c}(d,t)&=L^{-1}\left\{\frac{q^b}{(q^a-d)^c}\right\}\\&=\sum_{j=0}^{\infty}\frac{\mathrm{d}^j\Gamma(c+j)}{\Gamma(c)\Gamma(j+1)}\frac{t^{(c+j)a-b-1}}{\Gamma[(c+j)a-b]};\end{aligned}$$

$$\mathrm{Re}(ac-b)>0,\qquad \mathrm{Re(q)}>0,\quad \left|\frac{\mathrm{d}}{\mathrm{q^a}}\right|<1, \tag{4.3.16}$$

we obtain

$$\begin{aligned}v(r,t)=&\frac{R_1}{\mu}\ln\left(\frac{r}{R_2}\right)f_1t^a+\pi\sum_{n=1}^{\infty}\frac{J_0^2(R_2r_n)B(r,r_n)}{[J_1^2(R_1r_n)-J_0^2(R_2r_n)]}\left[-\frac{f_1\Gamma(a+1)}{\mu r_n}\frac{1}{\lambda}\sum_{k=0}^{\infty}\left(\frac{-\upsilon r_n^2}{\lambda}\right)^k\right.\\&\times\left\{G_{\alpha,-a-k-1,k+1}(-\lambda^{-1},t)+\lambda G_{\alpha,\alpha-a-k-1,k+1}(-\lambda^{-1},t)\right\}-f_2\frac{J_0'(R_1r_n)}{J_0(R_2r_n)}\\&\left.+\frac{f_2}{\lambda}\frac{J_0'(R_1r_n)}{J_0(R_2r_n)}\sum_{k=0}^{\infty}\left(\frac{-\upsilon r_n^2}{\lambda}\right)^k\left\{G_{\alpha,-k-1,k+1}(-\lambda^{-1},t)+\lambda G_{\alpha,\alpha-k-1,k+1}(-\lambda^{-1},t)\right\}\right].\end{aligned} \tag{4.3.17}$$

4.3.2 Calculation of the shear stress

Applying Laplace transform to Eq. (4.2.3), we obtain

$$\bar{\tau}(r,q)=\mu\frac{1}{(1+\lambda q^{\alpha})}\frac{\partial\bar{v}(r,q)}{\partial r}. \tag{4.3.18}$$

Substitute Eq. (4.3.14) in Eq. (4.3.18), we obtain

$$\begin{aligned}\bar{\tau}(r,q)=&\frac{f_1R_1}{r}\frac{\Gamma(a+1)}{q^{a+1}(1+\lambda q^{\alpha})}-\pi\sum_{n=1}^{\infty}\frac{r_nJ_0^2(R_2r_n)\bar{B}(r,r_n)}{[J_1^2(R_1r_n)-J_0^2(R_2r_n)]}\left[-\frac{f_1\Gamma(a+1)}{r_n}\frac{1}{q^a(q+\lambda q^{\alpha+1}+\upsilon r_n^2)}\right.\\&\left.-f_2\mu\frac{J_0'(R_1r_n)}{J_0(R_2r_n)}\frac{1}{q(1+\lambda q^{\alpha})}+f_2\mu\frac{J_0'(R_1r_n)}{J_0(R_2r_n)}\frac{1}{(q+\lambda q^{\alpha+1}+\upsilon r_n^2)}\right],\end{aligned} \tag{4.3.19}$$

where

$$\bar{B}(r,r_n) = J_1(rr_n)Y_1(R_1r_n) - J_1(R_1r_n)Y_1(rr_n). \tag{4.3.20}$$

Applying inverse Laplace transform to Eq. (4.3.19) and using Eqs. (4.3.15) and (4.3.16), we obtain

$$\tau(r,t) = \frac{f_1R_1\Gamma(a+1)}{\lambda r}R_{\alpha,-a-1}(-\lambda^{-1},t) - \pi\sum_{n=1}^{\infty}\frac{r_nJ_0^2(R_2r_n)\bar{B}(r,r_n)}{[J_1^2(R_1r_n)-J_0^2(R_2r_n)]}\left[-\frac{f_1\Gamma(a+1)}{\lambda r_n}\right.$$
$$\times\sum_{k=0}^{\infty}\left(\frac{-\upsilon r_n^2}{\lambda}\right)^k G_{\alpha,-a-k-1,k+1}(-\lambda^{-1},t) - \frac{f_2\mu}{\lambda}\frac{J_0'(R_1r_n)}{J_0(R_2r_n)}R_{\alpha,-1}(-\lambda^{-1},t)$$
$$\left.+\frac{f_2\mu}{\lambda}\frac{J_0'(R_1r_n)}{J_0(R_2r_n)}\sum_{k=0}^{\infty}\left(\frac{-\upsilon r_n^2}{\lambda}\right)^k G_{\alpha,-k-1,k+1}(-\lambda^{-1},t)\right]. \tag{4.3.21}$$

4.4 Limiting Cases

4.4.1 Ordinary Maxwell Fluid

Applying $\alpha \to 1$ into Eqs. (4.3.17) and (4.3.21), we obtain the velocity field

$$v_M(r,t) = \frac{R_1}{\mu}\ln\left(\frac{r}{R_2}\right)f_1t^a + \pi\sum_{n=1}^{\infty}\frac{J_0^2(R_2r_n)B(r,r_n)}{[J_1^2(R_1r_n)-J_0^2(R_2r_n)]}\left[-\frac{f_1\Gamma(a+1)}{\mu r_n}\frac{1}{\lambda}\sum_{k=0}^{\infty}\left(\frac{-\upsilon r_n^2}{\lambda}\right)^k\right.$$
$$\times\left\{G_{1,-a-k-1,k+1}(-\lambda^{-1},t) + \lambda G_{1,-a-k,k+1}(-\lambda^{-1},t)\right\} - f_2\frac{J_0'(R_1r_n)}{J_0(R_2r_n)}$$
$$\left.+\frac{f_2}{\lambda}\frac{J_0'(R_1r_n)}{J_0(R_2r_n)}\sum_{k=0}^{\infty}\left(\frac{-\upsilon r_n^2}{\lambda}\right)^k\left\{G_{1,-k-1,k+1}(-\lambda^{-1},t) + \lambda G_{1,-k,k+1}(-\lambda^{-1},t)\right\}\right], \tag{4.4.1}$$

and the associated shear stress

$$\tau_M(r,t)=\frac{f_1R_1\Gamma(a+1)}{\lambda r}R_{1,-a-1}(-\lambda^{-1},t)-\pi\sum_{n=1}^{\infty}\frac{r_nJ_0^2(R_2r_n)\overline{B}(r,r_n)}{[J_1^2(R_1r_n)-J_0^2(R_2r_n)]}\Bigg[-\frac{f_1\Gamma(a+1)}{\lambda r_n}$$
$$\times\sum_{k=0}^{\infty}\left(\frac{-\upsilon r_n^2}{\lambda}\right)^k G_{1,-a-k-1,k+1}(-\lambda^{-1},t)-\frac{f_2\mu}{\lambda}\frac{J_0^{'}(R_1r_n)}{J_0(R_2r_n)}R_{1,-1}(-\lambda^{-1},t)$$
$$+\frac{f_2\mu}{\lambda}\frac{J_0^{'}(R_1r_n)}{J_0(R_2r_n)}\sum_{k=0}^{\infty}\left(\frac{-\upsilon r_n^2}{\lambda}\right)^k G_{1,-k-1,k+1}(-\lambda^{-1},t)\Bigg]. \tag{4.4.2}$$

4.4.2 Newtonian Fluid

Applying $\lambda\to 0$ into Eqs. (4.4.1) and (4.4.2) and taking into account the following results [22]

$$\lim_{\lambda\to 0}\frac{1}{\lambda^m}G_{1,b,m}(-\lambda^{-1},t)=\frac{t^{-b-1}}{\Gamma(-b)},\quad \mathrm{b}<0, \tag{4.4.3}$$

and

$$\lim_{\lambda\to 0}\frac{1}{\lambda}R_{1,b}(-\lambda^{-1},t)=\frac{t^{-b-1}}{\Gamma(-b)},\quad \mathrm{b}<0, \tag{4.4.4}$$

we obtain the corresponding solutions for the Newtonian fluid, as follows

$$v_N(r,t)=\frac{R_1}{\mu}\ln\left(\frac{r}{R_2}\right)f_1t^a+\pi\sum_{n=1}^{\infty}\frac{J_0^2(R_2r_n)B(r,r_n)}{[J_1^2(R_1r_n)-J_0^2(R_2r_n)]}\Bigg[-\frac{f_1\Gamma(a+1)}{\mu r_n}\sum_{k=0}^{\infty}\left(-\upsilon r_n^2\right)^k\frac{t^{a+k}}{\Gamma(a+k+1)}$$
$$-f_2\frac{J_0^{'}(R_1r_n)}{J_0(R_2r_n)}+f_2\frac{J_0^{'}(R_1r_n)}{J_0(R_2r_n)}\sum_{k=0}^{\infty}\left(-\upsilon r_n^2\right)^k\frac{t^k}{\Gamma(k+1)}\Bigg], \tag{4.4.5}$$

$$\tau_N(r,t)=\frac{f_1R_1}{r}t^a-\pi\sum_{n=1}^{\infty}\frac{r_nJ_0^2(R_2r_n)\overline{B}(r,r_n)}{[J_1^2(R_1r_n)-J_0^2(R_2r_n)]}\Bigg[-\frac{f_1\Gamma(a+1)}{r_n}\sum_{k=0}^{\infty}\left(-\upsilon r_n^2\right)^k\frac{t^{a+k}}{\Gamma(a+k+1)}$$
$$-f_2\mu\frac{J_0^{'}(R_1r_n)}{J_0(R_2r_n)}+f_2\mu\frac{J_0^{'}(R_1r_n)}{J_0(R_2r_n)}\sum_{k=0}^{\infty}\left(-\upsilon r_n^2\right)^k\frac{t^k}{\Gamma(k+1)}\Bigg]. \tag{4.4.6}$$

4.5 Conclusions and Numerical results

The intent of this chapter is to establish the exact solution for the velocity field and shear stress corresponding to the unsteady flow of an incompressible fractional

Maxwell fluid filled between two infinite coaxial circular cylinders. We obtain this solution using Laplace and finite Hankel transform methods. The fluid motion is produced by the inner cylinder that is pulled with a time-dependent shear stress and the outer cylinder that is moving at a constant velocity. The results are presented in the form of series of the generalized G and R functions. Similar solutions are obtained for ordinary Maxwell and Newtonian fluids as limiting cases of solution derived for fractional Maxwell fluid. The velocity field and shear stress are also analyzed using graphical illustration for various parameters. The motions of fractional Maxwell fluid, ordinary Maxwell and Newtonian fluids are also analyzed graphically.

As shown in below diagrams, the velocity $v(r,t)$ and the shear stress $\tau(r,t)$ given by Eq. (4.3.17) and Eq. (4.3.21) have been drawn against *r* for different values of the time t and other relevant parameters. It can be clearly seen from the figures that the velocity component *v* is decreasing and the shear stress component τ is increasing function of *r*. The fluid velocity is relatively higher and shear stress is lower in the neighborhood of the inner cylinder for given boundary conditions. Figures 4.1(a) and 4.1(b) are showing the fluid motion at different times. It can be seen that the velocity is increasing and the shear stress is the decreasing function of time *t*. The influence of kinematic viscosity $\upsilon$and relaxation time λ on the fluid motion is shown in figures 4.2 and 4.3. Both parameters have opposite effect on the fluid motion. Figure 4.4 is showing a comparison diagram of the velocity $v(r,t)$ and the shear stress $\tau(r,t)$ among three models (Fractional Maxwell fluid, ordinary Maxwell fluid and Newtonian fluid) for the same values of common material constants and time t. The velocity in the neighborhood of inner cylinders is swiftest for Newtonian fluid while it is slowest for the fractional Maxwell fluid. Similarly, shear stress is highest for fractional Maxwell fluid while it is slowest for the Newtonian fluid.In all of the figures 4.1-4.4, the units of the material constants are in SI units andthe root r_n has been approximated by $\dfrac{(2n-1)\pi}{2(R_2-R_1)}$.

Figure 4.1

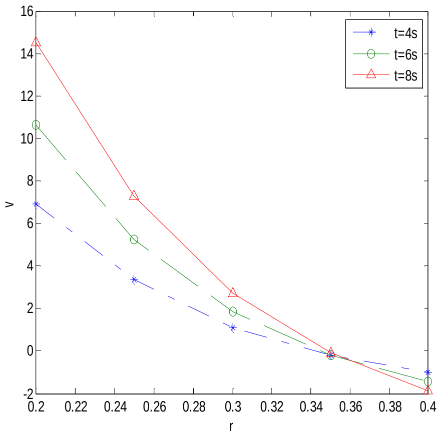

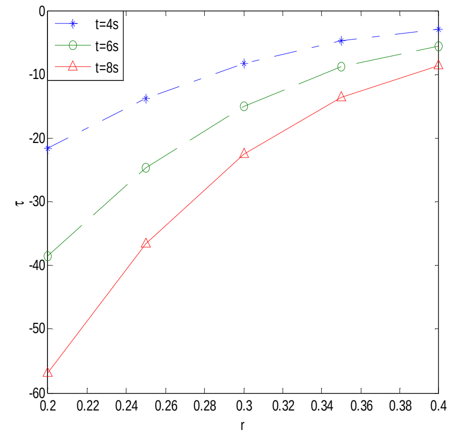

4.1(a) 4.1(b)

Fig.4.1 Profiles of the velocity v(r,t) and shear stress τ(r,t) given by Eqs.(4.3.17) and (4.3.21) for $R_1 = 0.2$, $R_2 = 0.4$, $f_1 = -10$, $f_2 = 4$, $\upsilon = 0.00052$, $\mu = 0.45$, $\lambda = 2$, $\alpha = 0.9$ and different values of t.

Figure 4.2

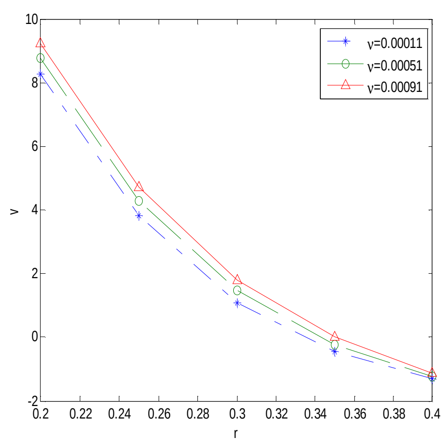

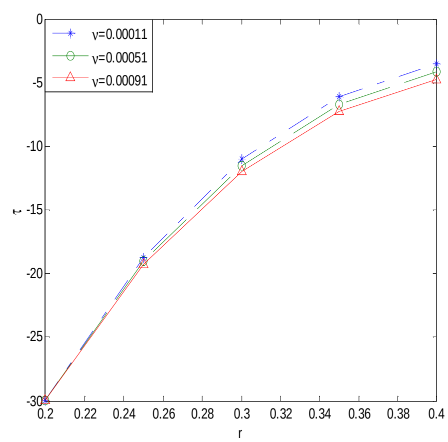

4.2(a) 4.2(b)

Fig. 4.2 Profiles of the velocity v(r, t) and shear stress τ(r, t) given by Eqs. (4.3.17) and (4.3.21) for $R_1 = 0.2$, $R_2 = 0.4$, $f_1 = -10$, $f_2 = 4$, t = 5s, $\mu = 0.45$, $\lambda = 2$, $\alpha = 0.9$ and different values of υ.

Figure 4.3

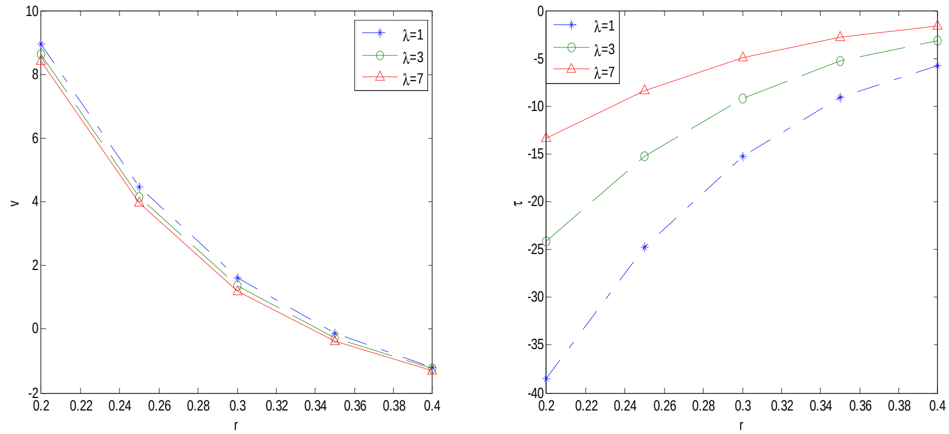

4.3(a) 4.3(b)

Fig.4.3 Profiles of the velocity $v(r,t)$ and shear stress $\tau(r,t)$ given by Eqs.(4.3.17) and (4.3.21) for $R_1 = 0.2$, $R_2 = 0.4$, $f_1 = -10$, $f_2 = 4$, $t = 5s$, $\upsilon = 0.00052$, $\mu = 0.45$, $\alpha = 0.9$ and different values of λ.

Figure 4.4

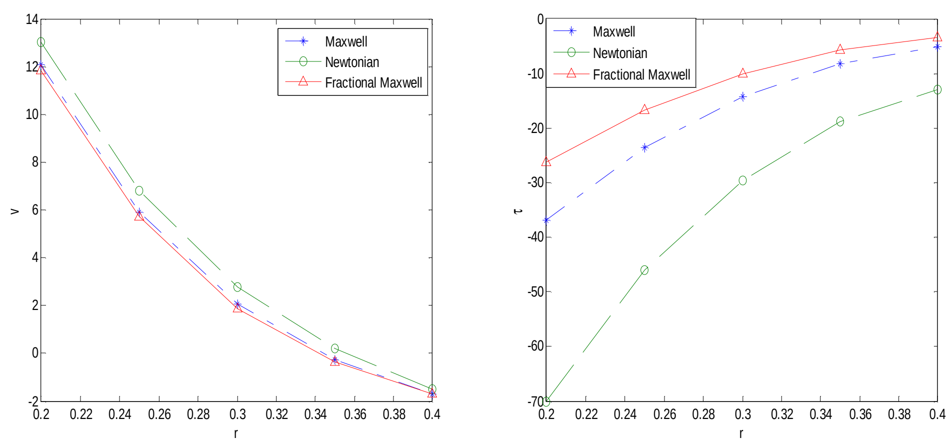

4.4(a) 4.4(b)

Fig.4.4 Profiles of the velocity $v(r,t)$ and shear stress $\tau(r,t)$ corresponding to the fractional Maxwell fluid, ordinary Maxwell fluid, Newtonian fluid, for $R_1 = 0.2$, $R_2 = 0.4$, $f_1 = -10$, $f_2 = 4$, $t = 7\,s$, $\upsilon = 0.00055$, $\mu = 0.46$, $\lambda = 4$, $\alpha = 0.6$

Chapter 5. Exact solutions for the flow of Oldroyd-B fluid between two infinitely long coaxial cylinders

The paper published on the work described in this chapter:

1. Khandelwal K. and Mathur V., Unsteady unidirectional flow of Oldroyd-B fluid between two infinitely long coaxial cylinders, International Journal of Mathematical Sciences & Applications 4, 1-10, (2014).
2. Mathur V. and Khandelwal K., Exact solution for the flow of Oldroyd-B fluid between coaxial cylinders, International Journal of Engineering Research & Technology 3, 949-954, (2014).
3. Mathur V. and Khandelwal K., Exact solution for the flow of Oldroyd-B fluid due to constant shear and time dependent velocity, IOSR Journal of Mathematics 10, 38-45, (2014).

5.1 Introduction

This chapter deals with flows of Oldroyd-B fluid between two infinitely long coaxial cylinders. Initially, the fluid is at rest. We use Hankel and Laplace transforms to reach the exact solution. The obtained solution is presented in terms of generalized G functions.

This chapter is divided into three parts. In part-A, the motion is produced by a constant pressure gradient. The inner cylinder is pulled with constant shear and outer cylinder is moving with time dependent velocity. In part-B, the motion is produced by a constant pressure gradient & the inner cylinder start moving along its axis of symmetry with the constant velocity. In part-C, the motion is produced by the inner cylinder pulled with a constant shear and outer cylinder moving with time dependent velocity.

Fetecau [21] obtained analytical solutions for non-Newtonian fluid flowing in cylindrical structures and used constitutive relation given as

$$(1+\lambda\partial_t)\tau = \mu(1+\lambda_r\partial_t)\partial_r v(r,t), \qquad (5.1.1)$$

where v is the velocity, λ and λ_r are relaxation and retardation times, τ is tangential tension and μ is the dynamic viscosity.

Using fractional calculus approach, the constitutive relation of the generalized Oldroyd-B fluid in Eq. (5.1.1) can be written as

$$(1+\lambda D_t^{\alpha})\tau = \mu(1+\lambda_r D_t^{\beta})\partial_r v(r,t), \qquad (5.1.2)$$

where D_t^{α} and D_t^{β} are fractional operators and are defined as [64]

$$D_t^{\alpha} f(t) = \begin{cases} \dfrac{1}{\Gamma(1-\alpha)}\dfrac{d}{dt}\displaystyle\int_0^t \dfrac{f(\tau)}{(t-\tau)^{\alpha}}d\tau, & 0<\alpha<1; \\ \dfrac{d}{dt} f(t), & \alpha = 1, \end{cases} \qquad (5.1.3)$$

where $\Gamma(.)$ is the Gamma function. When $\alpha=\beta=1$, Eq. (5.1.2) simplified as Eq. (5.1.1).

5.2 Governing equations

Let us consider the unsteady flow of an incompressible Oldroyd-B fluid in coaxial cylinders. The following assumptions are considered during this mathematical study. The flows are assumed to be axi-symmmetric. The fluid velocity at the direction of the pipe radius is assumed to be zero. The axial velocity is assumed to be only relevant to the cylinder radius.

The equation of axial flow motion is written as [11]

$$\rho\frac{\partial v}{\partial t}=\frac{\partial \tau}{\partial r}+\frac{1}{r}\tau-\frac{\partial p}{\partial z}, \qquad (5.2.1)$$

where ρ is the constant density of the fluid.

Substitute Eq. (5.1.2) into Eq. (5.2.1), we get

$$\left(1+\lambda D_t^{\alpha}\right)\frac{\partial v}{\partial t}=A+\lambda A\frac{t^{-\alpha}}{\Gamma(1-\alpha)}+\upsilon\left(1+\lambda_r D_t^{\beta}\right)\left(\partial_r^2+\frac{1}{r}\partial_r\right)v(r,t), \qquad (5.2.2)$$

where $\upsilon=\dfrac{\mu}{\rho}$ is the kinematical viscosity and $-A\rho=\dfrac{\partial p}{\partial z}$ is the constant pressure gradient that acts on the liquid in the z-direction.

Part A

5.3 Flow through the annular region

Let us consider a constant pressure gradient applied at time $t=0^+$ to an Oldroyd-B fluid contained in the annular region between two infinitely long coaxial cylinders of radii R_1 and $R_2(>R_1)$ .At time $t=0^+$, the inner cylinder is pulled with constant shear and outer cylinder is moving with time dependent velocity. We have to solve the next initial and boundary problem.

$$(1+\lambda D_t^{\alpha})\frac{\partial v}{\partial t}=A+\lambda A\frac{t^{-\alpha}}{\Gamma(1-\alpha)}+\upsilon(1+\lambda_r D_t^{\beta})\left(\partial_r^2+\frac{1}{r}\partial_r\right)v(r,t), \quad t>0. \quad (5.3.1)$$

The initial and boundary conditions are expressed by

$$v(r,0)=0, \qquad \partial_t v(r,0)=0, \qquad \mathrm{R}_1 \le r \le \mathrm{R}_2, \qquad (5.3.2)$$

$$\mu(1+\lambda_r D_t^{\beta})\partial_r v(r,t)|_{r=R_1}=f_1, \qquad v(R_2,t)=f_2 t^{p}, \quad \mathrm{t}>0, \qquad \mathrm{p}\ge 0, \qquad (5.3.3)$$

where f_1, f_2 are constants.

Making the change of unknown function

$$v(r,t)=V(r)+u(r,t), \qquad (5.3.4)$$

where

$$V(r)=\frac{A}{4\upsilon}(R_2^2-r^2)+\left(\frac{R_1 f_1}{\mu}+\frac{AR_1^2}{2\upsilon}\right)\ln(r/R_2). \qquad (5.3.5)$$

Substitute Eq. (5.3.4) in Eq. (5.3.1), we get

$$(1+\lambda D_t^{\alpha})\frac{\partial u(r,t)}{\partial t}=\upsilon(1+\lambda_r D_t^{\beta})\left(\partial_r^2+\frac{1}{r}\partial_r\right)u(r,t)+\lambda A\frac{t^{-\alpha}}{\Gamma(1-\alpha)}-\lambda_r A\frac{t^{-\beta}}{\Gamma(1-\beta)}. \quad (5.3.6)$$

Substitute Eq. (5.3.4) in Eqs. (5.3.2) & (5.3.3), we get

$$u(r,0)=-V(r), \qquad \partial_t u(r,0)=0, \qquad (5.3.7)$$

$$\mu(1+\lambda_r D_t^{\beta})\partial_r u(R_1,t)=-f_1\lambda_r\frac{t^{-\beta}}{\Gamma(1-\beta)}, \qquad u(R_2,t)=f_2 t^{p}, \ \mathrm{t}>0, \ \ \mathrm{p}\ge 0. \quad (5.3.8)$$

The Hankel Transform method with respect to r is used and is defined as follows [11]

$$\bar{u} = \int_{R_1}^{R_2} ru(r,s)\phi(s_n, r)dr. \tag{5.3.9}$$

The inverse Hankel Transform is

$$u(r,s) = \frac{\pi^2}{2}\sum_{n=1}^{\infty}\frac{s_n^2 J_0^2(R_2 s_n)\bar{u}(s_n, s)\phi(s_n, r)}{J_1^2(R_1 s_n) - J_0^2(R_2 s_n)}, \tag{5.3.10}$$

where $\phi(s_n, r) = J_1(R_1 s_n)Y_0(s_n r) - Y_1(R_1 s_n)J_0(s_n r)$, s_n is the positive root of $\phi(s_n, R_2) = 0.$

Applying the Hankel transform in Eq. (5.3.6), we obtain

$$\begin{aligned}(1+\lambda D_t^{\alpha})\frac{\partial \bar{u}(s_n,t)}{\partial t} &= -\upsilon s_n^2(1+\lambda_r D_t^{\beta})\bar{u}(s_n,t) + \frac{2\upsilon f_1 \lambda_r}{\pi s_n \mu}\frac{t^{-\beta}}{\Gamma(1-\beta)} - \frac{2\upsilon f_2 t^p}{\pi}\frac{J_1(R_1 s_n)}{J_0(R_2 s_n)} \\ &\quad - \frac{2\upsilon f_2 \lambda_r}{\pi}\frac{J_1(R_1 s_n)}{J_0(R_2 s_n)}\frac{\Gamma(p+1)}{\Gamma(p-\beta+1)}t^{p-\beta} + \lambda A\frac{t^{-\alpha}}{\Gamma(1-\alpha)}\frac{R_2}{s_n}g(s_n) \\ &\quad - \lambda_r A\frac{t^{-\beta}}{\Gamma(1-\beta)}\frac{R_2}{s_n}g(s_n),\end{aligned} \tag{5.3.11}$$

where $g(s_n) = [J_1(R_1 s_n)Y_1(R_2 s_n) - Y_1(R_1 s_n)J_1(R_2 s_n)].$

Applying the Hankel transform in Eq. (5.3.7), we obtain

$$\bar{u}(s_n, 0) = \frac{2}{\pi s_n^4}\left[\frac{A}{\upsilon}\frac{J_1(R_1 s_n)}{J_0(R_2 s_n)} + \frac{f_1 s_n}{\mu}\right], \quad \partial_t \bar{u}(s_n, 0) = 0. \tag{5.3.12}$$

Applying Laplace transform to Eq. (5.3.11) and using Eq. (5.3.12), we obtain

$$\bar{\bar{u}}(s_n,s)=\left[\frac{2}{\pi s_n^2}\left\{\frac{A}{\upsilon}\frac{J_1(R_1s_n)}{J_0(R_2s_n)}+\frac{f_1s_n}{\mu}\right\}\right]\frac{(1+\lambda s^{\alpha}+\upsilon s_n^2\lambda_r s^{\beta-1})}{s_n^2(s+\lambda s^{\alpha+1}+\upsilon s_n^2+\upsilon s_n^2\lambda_r s^{\beta})}$$
$$+\frac{\lambda AR_2g(s_n)}{s_n}\frac{1}{s^{1-\alpha}(s+\lambda s^{\alpha+1}+\upsilon s_n^2+\upsilon s_n^2\lambda_r s^{\beta})}$$
$$+\left\{\frac{2\upsilon f_1\lambda_r}{\pi\mu s_n}-\frac{\lambda_r AR_2g(s_n)}{s_n}\right\}\frac{1}{s^{1-\beta}(s+\lambda s^{\alpha+1}+\upsilon s_n^2+\upsilon s_n^2\lambda_r s^{\beta})}$$
$$-\frac{2\upsilon f_2\Gamma(p+1)}{\pi}\frac{J_1(R_1s_n)}{J_0(R_2s_n)}\frac{1}{s^{p+1}(s+\lambda s^{\alpha+1}+\upsilon s_n^2+\upsilon s_n^2\lambda_r s^{\beta})}$$
$$-\frac{2\upsilon\lambda_r f_2\Gamma(p+1)}{\pi}\frac{J_1(R_1s_n)}{J_0(R_2s_n)}\frac{1}{s^{p-\beta+1}(s+\lambda s^{\alpha+1}+\upsilon s_n^2+\upsilon s_n^2\lambda_r s^{\beta})}. \quad (5.3.13)$$

Applying Inverse-Laplace transform of Eq. (5.3.13) and taking into account the following result [117]

$$G_{a,b,c}(d,t)=L^{-1}\left\{\frac{q^b}{(q^a-d)^c}\right\}=\sum_{j=0}^{\infty}\frac{\mathrm{d}^j\Gamma(c+j)}{\Gamma(c)\Gamma(j+1)}\frac{t^{(c+j)a-b-1}}{\Gamma[(c+j)a-b]};$$
$$\mathrm{Re}(ac-b)>0,\ \left|\frac{\mathrm{d}}{\mathrm{q}^{\mathrm{a}}}\right|<1, \quad (5.3.14)$$

we obtain

$$\bar{u}(s_n,t)=\left[\frac{2}{\pi s_n^2}\left\{\frac{A}{\upsilon}\frac{J_1(R_1s_n)}{J_0(R_2s_n)}+\frac{f_1s_n}{\mu}\right\}\right]\left\{\frac{1}{s_n^2}-\frac{1}{s_n^2}\sum_{m=0}^{\infty}(-1)^m\left(\frac{\upsilon s_n^2}{\lambda}\right)^{m+1}\sum_{k=0}^{m}\binom{m}{k}\lambda_r^k G_{\alpha,\beta k-m-2,m+1}(-\lambda^{-1},t)\right\}$$
$$+\frac{\lambda AR_2g(s_n)}{\upsilon s_n^3}\sum_{m=0}^{\infty}(-1)^m\left(\frac{\upsilon s_n^2}{\lambda}\right)^{m+1}\sum_{k=0}^{m}\binom{m}{k}\lambda_r^k G_{\alpha,\beta k-m+\alpha-2,m+1}(-\lambda^{-1},t)$$
$$+\left\{\frac{2\upsilon f_1\lambda_r}{\pi\mu s_n}-\frac{\lambda_r AR_2g(s_n)}{s_n}\right\}\frac{1}{\upsilon s_n^2}\sum_{m=0}^{\infty}(-1)^m\left(\frac{\upsilon s_n^2}{\lambda}\right)^{m+1}\sum_{k=0}^{m}\binom{m}{k}\lambda_r^k G_{\alpha,\beta k-m+\beta-2,m+1}(-\lambda^{-1},t)$$
$$-\frac{2f_2\Gamma(p+1)}{\pi s_n^2}\frac{J_1(R_1s_n)}{J_0(R_2s_n)}\sum_{m=0}^{\infty}(-1)^m\left(\frac{\upsilon s_n^2}{\lambda}\right)^{m+1}\sum_{k=0}^{m}\binom{m}{k}\lambda_r^k G_{\alpha,\beta k-m-p-2,m+1}(-\lambda^{-1},t)$$
$$-\frac{2\lambda_r f_2\Gamma(p+1)}{\pi s_n^2}\frac{J_1(R_1s_n)}{J_0(R_2s_n)}\sum_{m=0}^{\infty}(-1)^m\left(\frac{\upsilon s_n^2}{\lambda}\right)^{m+1}\sum_{k=0}^{m}\binom{m}{k}\lambda_r^k G_{\alpha,\beta k-m-p+\beta-2,m+1}(-\lambda^{-1},t)\ . \quad (5.3.15)$$

The expression of the velocity field can be written as

$$v(r,t) = V(r) + \frac{\pi^2}{2}\sum_{n=1}^{\infty}\frac{J_0^2(R_2 s_n)\phi(s_n,r)}{J_1^2(R_1 s_n) - J_0^2(R_2 s_n)}\left[\left\{\frac{2}{\pi s_n^2}\left(\frac{A}{\upsilon}\frac{J_1(R_1 s_n)}{J_0(R_2 s_n)} + \frac{f_1 s_n}{\mu}\right)\right\}\right.$$

$$\times\left\{1 - \sum_{m=0}^{\infty}(-1)^m\left(\frac{\upsilon s_n^2}{\lambda}\right)^{m+1}\sum_{k=0}^{m}\binom{m}{k}\lambda_r^k G_{\alpha,\beta k-m-2,m+1}(-\lambda^{-1},t)\right\}$$

$$+\frac{\lambda A R_2 g(s_n)}{\upsilon s_n}\sum_{m=0}^{\infty}(-1)^m\left(\frac{\upsilon s_n^2}{\lambda}\right)^{m+1}\sum_{k=0}^{m}\binom{m}{k}\lambda_r^k G_{\alpha,\beta k-m+\alpha-2,m+1}(-\lambda^{-1},t)$$

$$+\frac{1}{\upsilon s_n}\left\{\frac{2\upsilon f_1\lambda_r}{\pi\mu} - \lambda_r A R_2 g(s_n)\right\}\sum_{m=0}^{\infty}(-1)^m\left(\frac{\upsilon s_n^2}{\lambda}\right)^{m+1}\sum_{k=0}^{m}\binom{m}{k}\lambda_r^k G_{\alpha,\beta k-m+\beta-2,m+1}(-\lambda^{-1},t)$$

$$-\frac{2 f_2\Gamma(p+1)}{\pi}\frac{J_1(R_1 s_n)}{J_0(R_2 s_n)}\sum_{m=0}^{\infty}(-1)^m\left(\frac{\upsilon s_n^2}{\lambda}\right)^{m+1}\sum_{k=0}^{m}\binom{m}{k}\lambda_r^k G_{\alpha,\beta k-m-p-2,m+1}(-\lambda^{-1},t)$$

$$\left.-\frac{2\lambda_r f_2\Gamma(p+1)}{\pi}\frac{J_1(R_1 s_n)}{J_0(R_2 s_n)}\sum_{m=0}^{\infty}(-1)^m\left(\frac{\upsilon s_n^2}{\lambda}\right)^{m+1}\sum_{k=0}^{m}\binom{m}{k}\lambda_r^k G_{\alpha,\beta k-m-p+\beta-2,m+1}(-\lambda^{-1},t)\right]. \tag{5.3.16}$$

5.4 Results

As shown in below diagrams, the velocity $v(r,t)$ given by Eq. (5.3.16) has been drawn against r for different values of the time t, constants and other relevant parameters. The velocity component v is decreasing function of r. The motion of the fluid is higher in the neighborhood of the inner cylinder for given boundary conditions and f_1>0, f_2>0. Figure 5.1 is showing the time dependency on the fluid motion. It can be clearly seen that the velocity is decreasing function of t. The influence of kinematic viscosity on the fluid motion is shown in figure 5.2. The velocity is increasing function of kinematic viscosity. Figures 5.3 and 5.4 show the influence of the relaxation and retardation times on the fluid motion. Both the two parameters have opposite effects on the fluid motion. The velocity is decreasing function of λ and increasing function of λ_r. The influence of fractional parameters α and β on the fluid motion is shown in figures 5.5 and 5.6. The velocity is decreasing function of α and increasing function of β. Figure 5.7 show the influence of dynamic viscosity on the fluid motion. The velocity is increasing function of μ. Figure 5.8 is showing the dependency of p on the fluid motion. It can be seen that the velocity increases, when p increases. Figures 5.9 and 5.10 show the influences of f_1 and f_2 on the fluid motion.

Figure 5.11 is showing the dependency of A on the fluid motion. It can also be seen that the velocity decreases, when A increases.

Figure 5.1

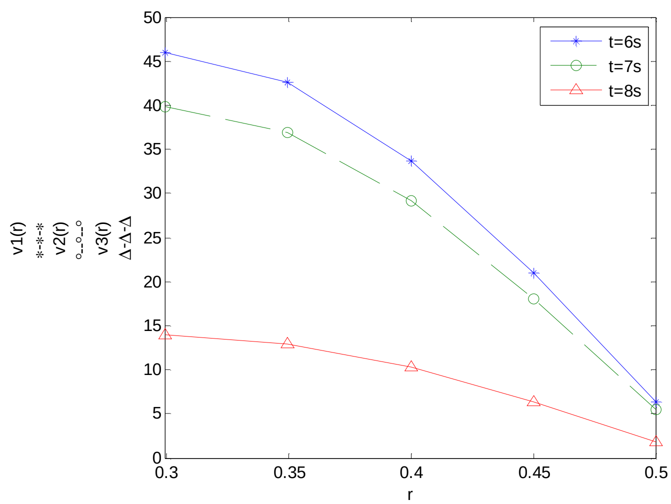

Fig. 5.1 Profiles of the velocity $v(r,t)$ given by Eq.(5.3.16) for $R_1 = 0.3, R_2 = 0.5,$ $f_1 = 4,\ f_2 = 3, \upsilon = 0.035, \lambda = 12,\ \lambda_r = 2.2,\ \alpha = 0.9,\ \beta = 0.6,\ \mathrm{p} = 2, \mathrm{A} = 3,\ \mu = 30$ and different values of t.

Figure 5.2

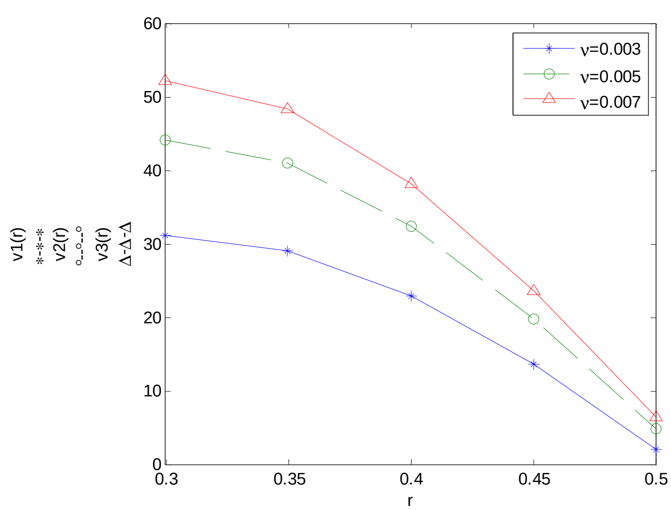

Fig. 5.2 Profiles of the velocity $v(r,t)$ given by Eq. (5.3.16) for $R_1 = 0.3,\ R_2 = 0.5,$ $f_1 = 4,\ f_2 = 3, \mathrm{t} = 6\mathrm{s},\ \lambda = 9,\ \lambda_r = 4,\ \alpha = 0.3,\ \beta = 0.3,\ \mathrm{p} = 2, \mathrm{A} = 3,\ \mu = 30$ and different values of υ.

Figure 5.3

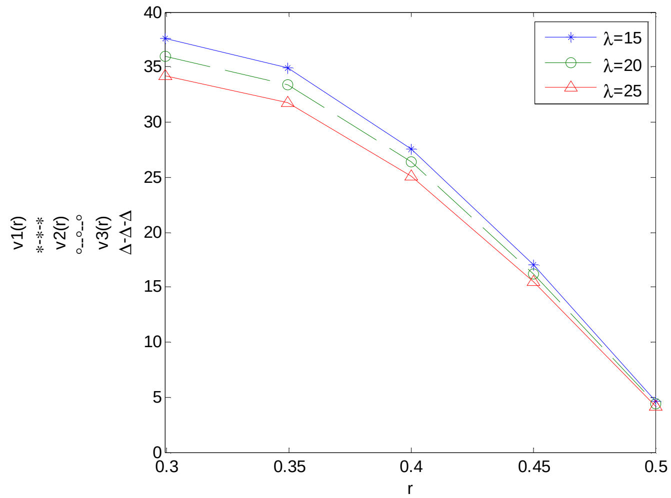

Fig. 5.3 Profiles of the velocity *v(r,t)* given by Eq. (5.3.16) for $R_1 = 0.3$, $R_2 = 0.5$, $f_1 = 4$, $f_2 = 3$, $\mathrm{t} = 5\mathrm{s}$, $\upsilon = 0.01$, $\lambda_{\mathrm{r}} = 7$, $\alpha = 0.3$, $\beta = 0.3$, $\mathrm{p} = 2$, $\mathrm{A} = 3$, $\mu = 30$ and different values of λ.

Figure 5.4

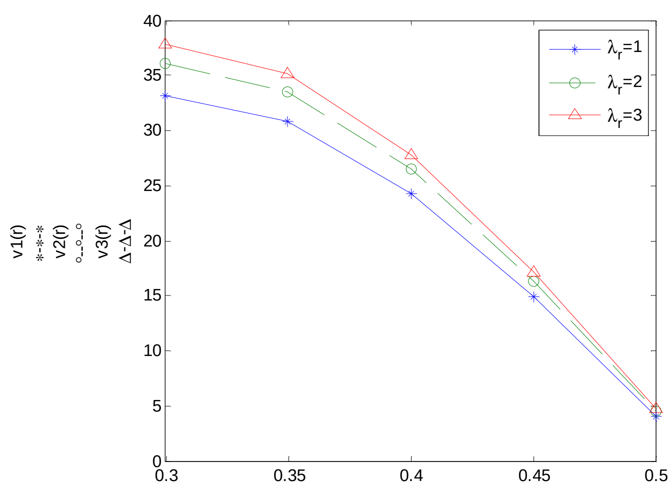

Fig. 5.4 Profiles of the velocity *v(r,t)* given by Eq. (5.3.16) for $R_1 = 0.3$, $R_2 = 0.5$, $f_1 = 4$, $f_2 = 3$, $\mathrm{t} = 5\mathrm{s}$, $\upsilon = 0.01$, $\lambda = 8$, $\alpha = 0.3$, $\beta = 0.9$, $\mathrm{p} = 2$, $\mathrm{A} = 3$, $\mu = 30$ and different values of λ_{r}.

Figure 5.5

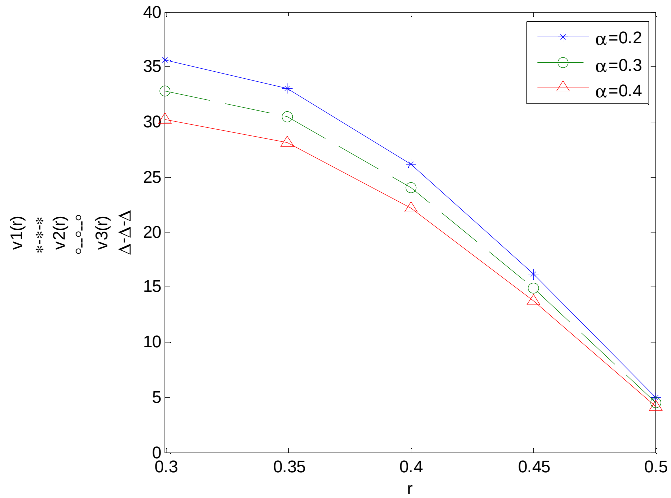

Fig. 5.5 Profiles of the velocity $v(r,t)$ given by Eq. (5.3.16) for $R_1 = 0.3$, $R_2 = 0.5$, $f_1 = 4$, $f_2 = 3$, $t = 6s$, $\upsilon = 0.04$, $\lambda = 25$, $\lambda_r = 5$, $\beta = 0.5$, $p = 2$, $A = 3$, $\mu = 30$ and different values of α.

Figure 5.6

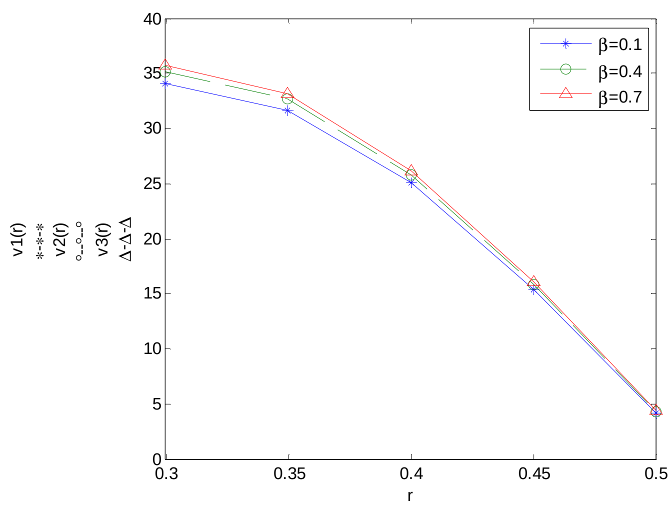

Fig. 5.6 Profiles of the velocity $v(r,t)$ given by Eq. (5.3.16) for $R_1 = 0.3$, $R_2 = 0.5$, $f_1 = 4$, $f_2 = 3$, $t = 5s$, $\upsilon = 0.01$, $\lambda = 8$, $\lambda_r = 1.5$, $\alpha = 1$, $p = 2$, $A = 3$, $\mu = 30$ and different values of β.

Figure 5.7

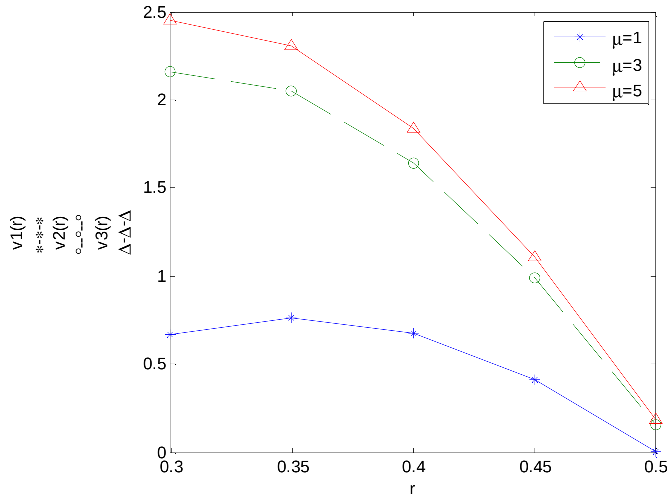

Fig. 5.7 Profiles of the velocity *v(r,t)* given by Eq.(5.3.16) for $R_1 = 0.3$, $R_2 = 0.5$, $f_1 = 4$, $f_2 = 3$, $t = 6s$, $\upsilon = 0.04$, $\lambda = 11$, $\lambda_r = 2.5$, $\alpha = 0.9$, $\beta = 0.6$, $\mathrm{p} = 2$, $\mathrm{A} = 3$ and different values of μ.

Figure 5.8

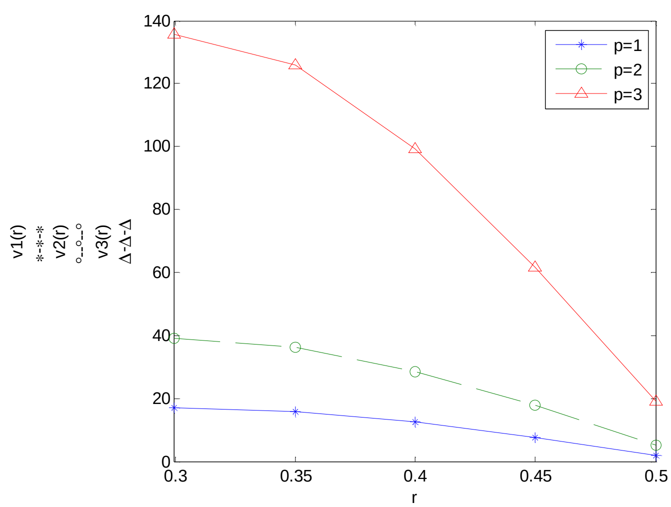

Fig. 5.8 Profiles of the velocity *v(r,t)* given by Eq.(5.3.16) for $R_1 = 0.3$, $R_2 = 0.5$, $f_1 = 4$, $f_2 = 3$, $\mathrm{t} = 5\mathrm{s}$, $\upsilon = 0.015$, $\lambda = 10$, $\lambda_r = 2$, $\alpha = 0.3$, $\beta = 0.9$, $\mathrm{A} = 3$, $\mu = 30$ and different values of p.

Figure 5.9

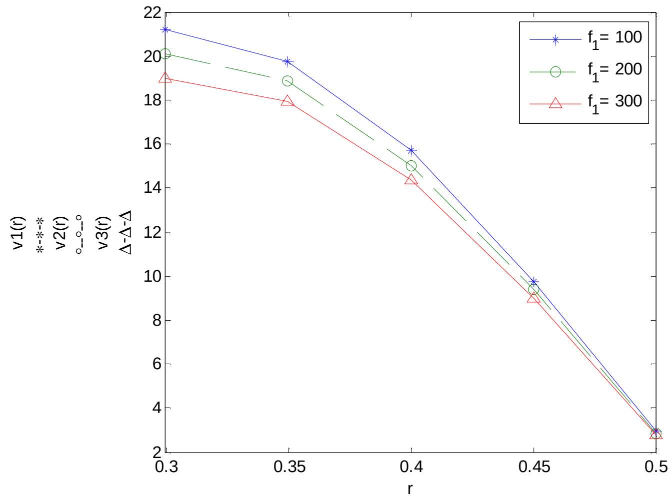

Fig. 5.9 Profiles of the velocity *v(r,t)* given by Eq.(5.3.16) for $R_1 = 0.3$, $R_2 = 0.5$, $f_2 = 3, t = 5s, \upsilon = 0.045, \lambda = 14, \lambda_r = 2.8, \alpha = 0.8, \beta = 0.5$, p = 2, A = 3, $\mu = 30$ and different values of f_1.

Figure 5.10

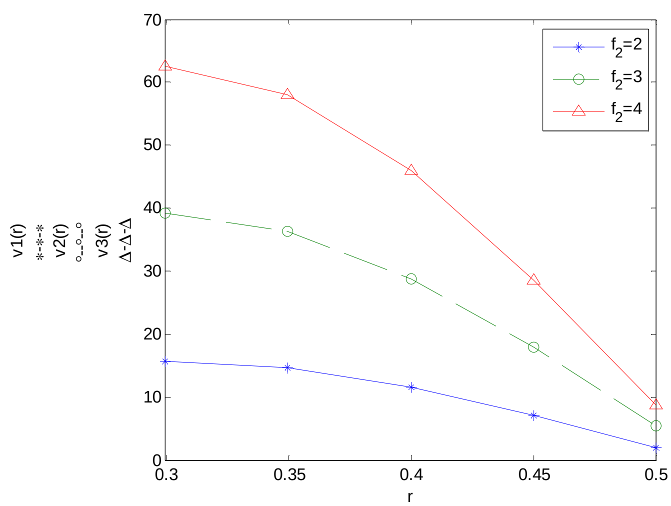

Fig. 5.10 Profiles of the velocity *v(r,t)* given by Eq.(5.3.16) for $R_1 = 0.3$, $R_2 = 0.5$, $f_1 = 4, t = 6s, \upsilon = 0.035, \lambda = 10, \lambda_r = 2, \alpha = 0.7, \beta = 0.4$, p = 2, A = 3, $\mu = 30$ and different values of f_2.

Figure 5.11

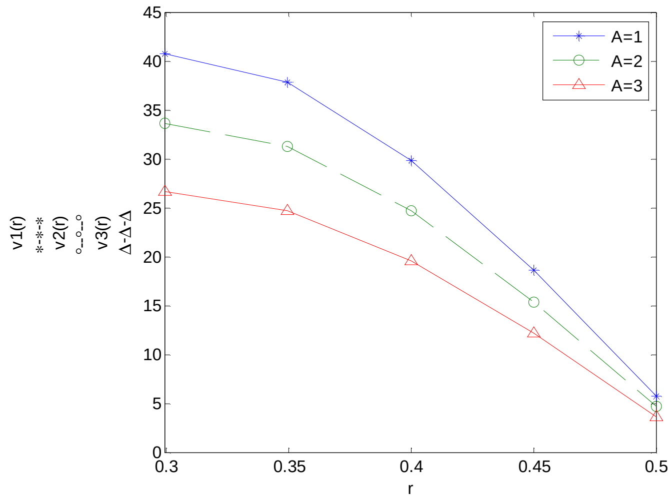

Fig. 5.11 Profiles of the velocity $v(r, t)$ given by Eq.(5.3.16) for $R_1 = 0.3$, $R_2 = 0.5$, $f_1 = 4$, $f_2 = 3$, $t = 5s$, $\upsilon = 0.041$, $\lambda = 13$, $\lambda_r = 2.7$, $\alpha = 0.8$, $\beta = 0.5$, $\mathrm{p} = 2$, $\mu = 30$ and different values of A.

Part B

5.5 Flow through the annular region

Let us consider an incompressible Oldroyd-B fluid in infinite coaxial circular cylinders. At time $t = 0$, fluid is assumed to be stationary. At time $t = 0^+$, a constant pressure gradient applied and the inner cylinder moves with constant velocity and the outer cylinder held fixed. Consider that the radius of inner and outer cylinders are R_1 and $R_2 (> R_1)$ respectively.

The initial and boundary conditions are

$$v(r,0) = 0, \quad \partial_t v(r,0) = 0, \quad \mathrm{R}_1 \le r \le \mathrm{R}_2, \tag{5.5.1}$$

$$v(R_1, t) = f, \quad v(R_2, t) = 0, \quad \mathrm{t} > 0, \tag{5.5.2}$$

where f is constant.

Making the change of unknown function

$$v(r,t) = V(r) + u(r,t), \tag{5.5.3}$$

where

$$V(r) = \frac{A}{4\upsilon}(R_2^2 - r^2) + \frac{A}{4\upsilon}\frac{(R_2^2 - R_1^2)}{\ln(R_2/R_1)}\ln(r/R_2). \tag{5.5.4}$$

Substitute Eq. (5.5.3) in Eq. (5.2.2), we obtain

$$(1+\lambda D_t^{\alpha})\frac{\partial u(r,t)}{\partial t} = \upsilon(1+\lambda_r D_t^{\beta})\left(\partial_r^2 + \frac{1}{r}\partial_r\right)u(r,t) + \lambda A\frac{t^{-\alpha}}{\Gamma(1-\alpha)} - \lambda_r A\frac{t^{-\beta}}{\Gamma(1-\beta)}. \tag{5.5.5}$$

Substitute Eq. (5.5.3) in Eqs. (5.5.1) & (5.5.2), we obtain

$$u(r,0) = -V(r), \quad \partial_t u(r,0) = 0, \tag{5.5.6}$$

$$u(R_1,t) = f, \quad u(R_2,t) = 0. \tag{5.5.7}$$

The Hankel Transform method with respect to r is used and is defined as follows [11]

$$\bar{u} = \int_{R_1}^{R_2} ru(r,s)\phi_1(s_n,r)dr. \tag{5.5.8}$$

The inverse Hankel Transform is

$$u(r,s) = \frac{\pi^2}{2}\sum_{n=1}^{\infty}\frac{s_n^2 J_0^2(R_2 s_n)\bar{u}(s_n,s)\phi_1(s_n,r)}{J_0^2(R_1 s_n) - J_0^2(R_2 s_n)}, \tag{5.5.9}$$

where $\phi_1(s_n,r) = Y_0(R_1 s_n)J_0(s_n r) - J_0(R_1 s_n)Y_0(s_n r)$, s_n is the positive root of $\phi_1(s_n,R_2) = 0$.

Applying the Hankel transform in Eq. (5.5.5), we obtain

$$\begin{aligned}(1+\lambda D_t^{\alpha})\frac{\partial\bar{u}(s_n,t)}{\partial t} &= -\upsilon s_n^2(1+\lambda_r D_t^{\beta})\bar{u}(s_n,t) - \frac{2\upsilon}{\pi}f - \frac{2\upsilon\lambda_r f}{\pi}\frac{1}{\Gamma(1-\beta)}t^{-\beta} \\ &+ \frac{2\lambda A g(s_n)t^{-\alpha}}{\pi s_n^2\Gamma(1-\alpha)} - \frac{2\lambda_r A g(s_n)t^{-\beta}}{\pi s_n^2\Gamma(1-\beta)},\end{aligned} \tag{5.5.10}$$

where

$$g(s_n)=\left[\frac{R_2\pi s_n}{2}\{Y_0(R_1s_n)J_1(R_2s_n)-J_0(R_1s_n)Y_1(R_2s_n)\}-1\right].$$

Applying the Hankel transform of Eq. (5.5.6), we obtain

$$\bar{u}(s_n,0)=-\frac{2A}{\pi s_n^4\upsilon}\left[\frac{J_0(R_1s_n)}{J_0(R_2s_n)}-1\right],\quad \partial_t\bar{u}(s_n,0)=0. \tag{5.5.11}$$

Applying Laplace transform of Eq. (5.5.10) and using Eq. (5.5.11), we obtain

$$\begin{aligned}\bar{\bar{u}}(s_n,s)=&\left[-\frac{2A}{\pi s_n^2\upsilon}\left\{\frac{J_0(R_1s_n)}{J_0(R_2s_n)}-1\right\}\right]\frac{(1+\lambda s^{\alpha}+\upsilon s_n^2\lambda_r s^{\beta-1})}{s_n^2(s+\lambda s^{\alpha+1}+\upsilon s_n^2+\upsilon s_n^2\lambda_r s^{\beta})}\\ &-\frac{2\upsilon f}{\pi}\frac{1}{s(s+\lambda s^{\alpha+1}+\upsilon s_n^2+\upsilon s_n^2\lambda_r s^{\beta})}-\frac{2\upsilon\lambda_r f}{\pi}\frac{1}{s^{1-\beta}(s+\lambda s^{\alpha+1}+\upsilon s_n^2+\upsilon s_n^2\lambda_r s^{\beta})}\\ &+\frac{2\lambda Ag(s_n)}{\pi s_n^2}\frac{1}{s^{1-\alpha}(s+\lambda s^{\alpha+1}+\upsilon s_n^2+\upsilon s_n^2\lambda_r s^{\beta})}\\ &-\frac{2\lambda_r Ag(s_n)}{\pi s_n^2}\frac{1}{s^{1-\beta}(s+\lambda s^{\alpha+1}+\upsilon s_n^2+\upsilon s_n^2\lambda_r s^{\beta})}\ .\end{aligned} \tag{5.5.12}$$

Applying Inverse-Laplace transform of Eq. (5.5.12) and taking into account the following result, as it is given by Eq. (5.3.14), is

$$G_{a,b,c}(d,t)=L^{-1}\left\{\frac{q^b}{(q^a-d)^c}\right\}$$

$$=\sum_{j=0}^{\infty}\frac{d^j\Gamma(c+j)}{\Gamma(c)\Gamma(j+1)}\frac{t^{(c+j)a-b-1}}{\Gamma[(c+j)a-b]};$$

$$\mathrm{Re}(ac-b)>0,\ \left|\frac{d}{q^a}\right|<1, \tag{5.5.13}$$

we obtain

$$\bar{u}(s_n,t)=\left[-\frac{2A}{\pi s_n^2\upsilon}\left\{\frac{J_0(R_1s_n)}{J_0(R_2s_n)}-1\right\}\right]\left\{\frac{1}{s_n^2}-\frac{1}{s_n^2}\sum_{m=0}^{\infty}(-1)^m\left(\frac{\upsilon s_n^2}{\lambda}\right)^{m+1}\sum_{k=0}^{m}\binom{m}{k}\lambda_r^k G_{\alpha,\beta k-m-2,m+1}(-\lambda^{-1},t)\right\}$$
$$-\frac{2}{\pi}f\frac{1}{s_n^2}\sum_{m=0}^{\infty}(-1)^m\left(\frac{\upsilon s_n^2}{\lambda}\right)^{m+1}\sum_{k=0}^{m}\binom{m}{k}\lambda_r^k G_{\alpha,\beta k-m-2,m+1}(-\lambda^{-1},t)$$
$$-\frac{2}{\pi}\lambda_r f\frac{1}{s_n^2}\sum_{m=0}^{\infty}(-1)^m\left(\frac{\upsilon s_n^2}{\lambda}\right)^{m+1}\sum_{k=0}^{m}\binom{m}{k}\lambda_r^k G_{\alpha,\beta k-m+\beta-2,m+1}(-\lambda^{-1},t)$$
$$+\frac{2\lambda Ag(s_n)}{\pi s_n^2}\frac{1}{\upsilon s_n^2}\sum_{m=0}^{\infty}(-1)^m\left(\frac{\upsilon s_n^2}{\lambda}\right)^{m+1}\sum_{k=0}^{m}\binom{m}{k}\lambda_r^k G_{\alpha,\beta k-m+\alpha-2,m+1}(-\lambda^{-1},t)$$
$$-\frac{2\lambda_r Ag(s_n)}{\pi s_n^2}\frac{1}{\upsilon s_n^2}\sum_{m=0}^{\infty}(-1)^m\left(\frac{\upsilon s_n^2}{\lambda}\right)^{m+1}\sum_{k=0}^{m}\binom{m}{k}\lambda_r^k G_{\alpha,\beta k-m+\beta-2,m+1}(-\lambda^{-1},t)\ . \qquad (5.5.14)$$

The expression of the velocity field can be written as

$$v(r,t)=V(r)+\pi\sum_{n=1}^{\infty}\frac{J_0^2(R_2s_n)\phi_1(s_n,r)}{\left[J_0^2(R_1s_n)-J_0^2(R_2s_n)\right]}\left[\left\{-\frac{A}{s_n^2\upsilon}\left(\frac{J_0(R_1s_n)}{J_0(R_2s_n)}-1\right)\right\}\right.$$
$$\times\left\{1-\sum_{m=0}^{\infty}(-1)^m\left(\frac{\upsilon s_n^2}{\lambda}\right)^{m+1}\sum_{k=0}^{m}\binom{m}{k}\lambda_r^k G_{\alpha,\beta k-m-2,m+1}(-\lambda^{-1},t)\right\}$$
$$-f\sum_{m=0}^{\infty}(-1)^m\left(\frac{\upsilon s_n^2}{\lambda}\right)^{m+1}\sum_{k=0}^{m}\binom{m}{k}\lambda_r^k G_{\alpha,\beta k-m-2,m+1}(-\lambda^{-1},t)$$
$$-\lambda_r f\sum_{m=0}^{\infty}(-1)^m\left(\frac{\upsilon s_n^2}{\lambda}\right)^{m+1}\sum_{k=0}^{m}\binom{m}{k}\lambda_r^k G_{\alpha,\beta k-m+\beta-2,m+1}(-\lambda^{-1},t)$$
$$+\frac{\lambda Ag(s_n)}{\upsilon s_n^2}\sum_{m=0}^{\infty}(-1)^m\left(\frac{\upsilon s_n^2}{\lambda}\right)^{m+1}\sum_{k=0}^{m}\binom{m}{k}\lambda_r^k G_{\alpha,\beta k-m+\alpha-2,m+1}(-\lambda^{-1},t)$$
$$\left.-\frac{\lambda_r Ag(s_n)}{\upsilon s_n^2}\sum_{m=0}^{\infty}(-1)^m\left(\frac{\upsilon s_n^2}{\lambda}\right)^{m+1}\sum_{k=0}^{m}\binom{m}{k}\lambda_r^k G_{\alpha,\beta k-m+\beta-2,m+1}(-\lambda^{-1},t)\right].$$
$$(5.5.15)$$

5.6 Results

As shown in below diagrams, the velocity $v(r,t)$ given by Eq. (5.5.15) has been drawn against r for different values of the time t, f and some other relevant parameters. The motion of the fluid is relatively lower in the neighborhood of the inner cylinder for given boundary conditions. Figure 5.12 is showing the time dependency on the fluid motion. It can be seen that the velocity is the increasing function of time *t*. Figure 5.13 is showing the dependency of the kinematic viscosity υ on the fluid motion. It can be clearly seen that the velocity is the decreasing function of kinematic viscosity υ. Figures 5.14 and 5.15 are showing the effect of the relaxation time λ and retardation time λ_r on the fluid motion. Both parameters have opposite effect on the fluid motion. The velocity is decreasing function of λ and increasing function of λ_r.The influence of fractional parameters α and β on the fluid motion is shown in figures 5.16and 5.17.Both parameters have opposite effect on the fluid motion. The velocity is increasing function of α and decreasing function of β. Figure 5.18 is showing the dependency of *f* on the fluid motion. It can be seen that the velocity is decreasing function of *f*. Figure 5.19 is showing the dependency of A on the fluid motion. It can be seen that the velocity is increasing function of A.

Figure 5.12

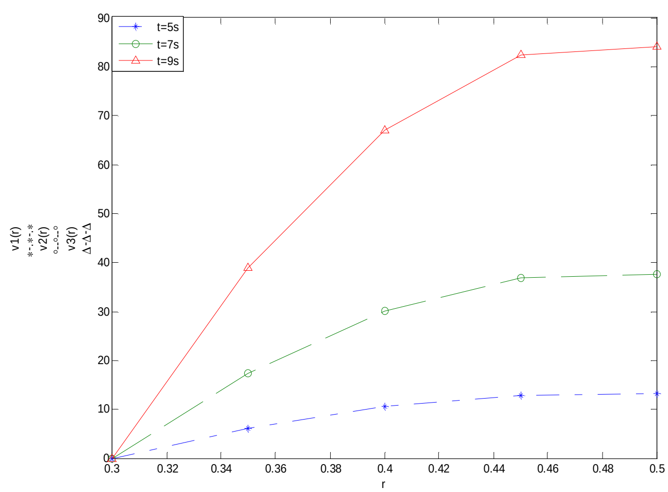

Figure 5.12 Profiles of the velocity *v(r,t)* given by Eq. (5.5.15) for $R_1 = 0.3$, $R_2 = 0.5$, $f = -3$, $\nu = 0.035$, $\lambda = 12$, $\lambda_r = 2.2$, $\alpha = 0.9$, $\beta = 0.6$, $A = 4$ and different values of *t*.

Figure 5.13

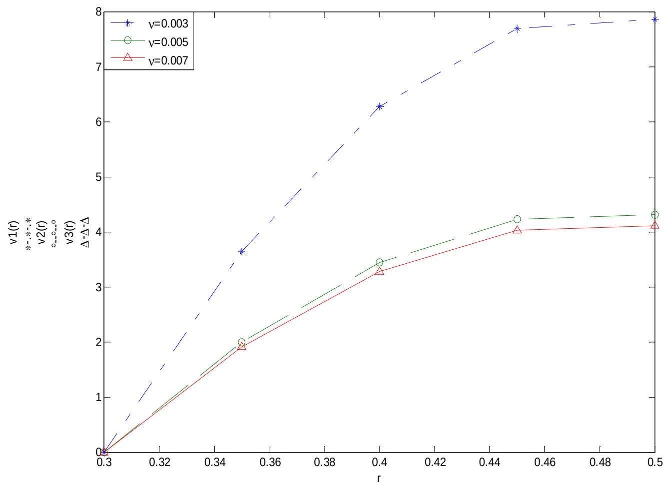

Figure 5.13 Profiles of the velocity $v(r,t)$ given by Eq. (5.5.15) for $R_1=0.3$, $R_2=0.5$, $f=-3$, $t=6s$, $\lambda=9$, $\lambda_r=4$, $\alpha=0.3$, $\beta=0.3$, $A=4$ and different values of ν.

Figure 5.14

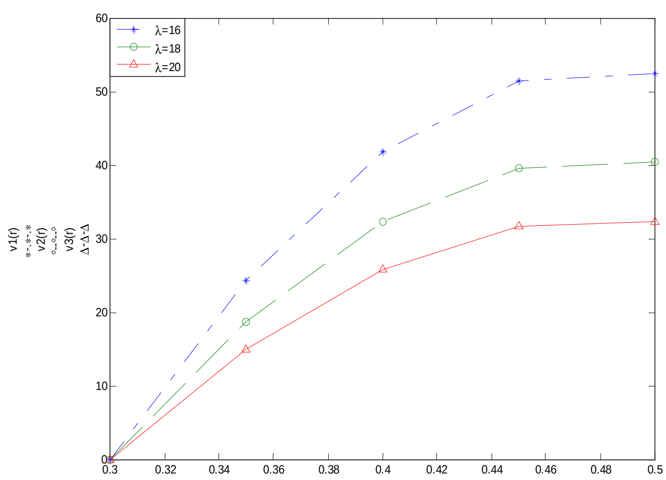

Figure 5.14 Profiles of the velocity $v(r,t)$ given by Eq. (5.5.15) for $R_1=0.3$, $R_2=0.5$, $f=-3$, $t=5s$, $\nu=0.04$, $\lambda_r=7$, $\alpha=0.3$, $\beta=0.3$, $A=4$ and different values of λ.

Figure 5.15

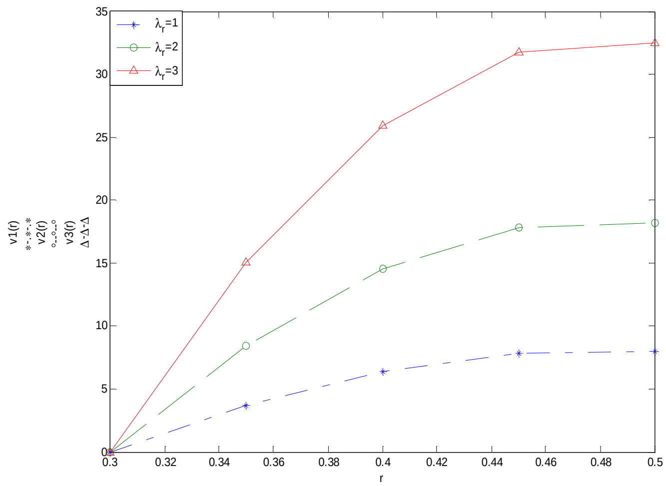

Figure 5.15 Profiles of the velocity $v(r,t)$ given by Eq. (5.5.15) for $R_1=0.3$, $R_2=0.5$, $f=-3$, $t=5s$, $\nu=0.04$, $\lambda=8$, $\alpha=0.3$, $\beta=0.9$, $A=4$ and different values of λ_r.

Figure 5.16

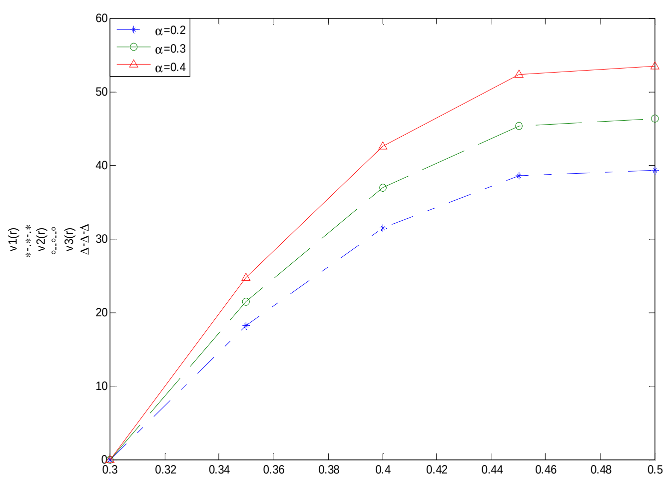

Figure 5.16 Profiles of the velocity $v(r,t)$ given by Eq. (5.5.15) for $R_1=0.3$, $R_2=0.5$, $f=-3$, $t=6s$, $\nu=0.045$, $\lambda=25$, $\lambda_r=8$, $\beta=0.5$, $A=4$ and different values of α.

Figure 5.17

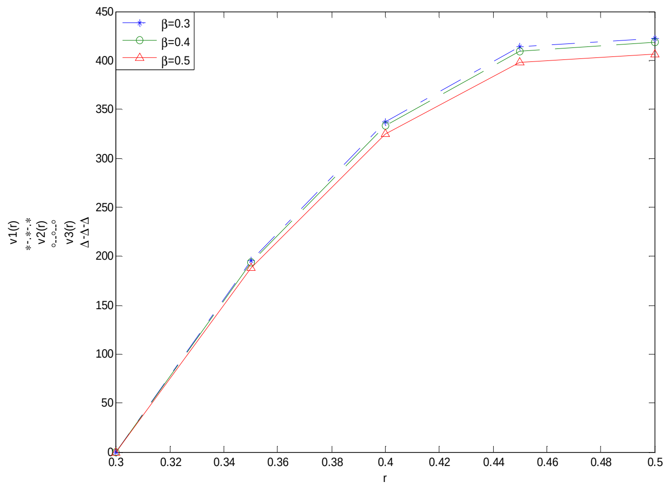

Figure 5.17 Profiles of the velocity *v(r,t)* given by Eq. (5.5.15) for $R_1=0.3$, $R_2=0.5$, $f=-3$, $t=6s$, $v=0.04$, $\lambda=8$, $\lambda_r=5.5$, $\alpha=1$, $A=4$ and different values of β.

Figure 5.18

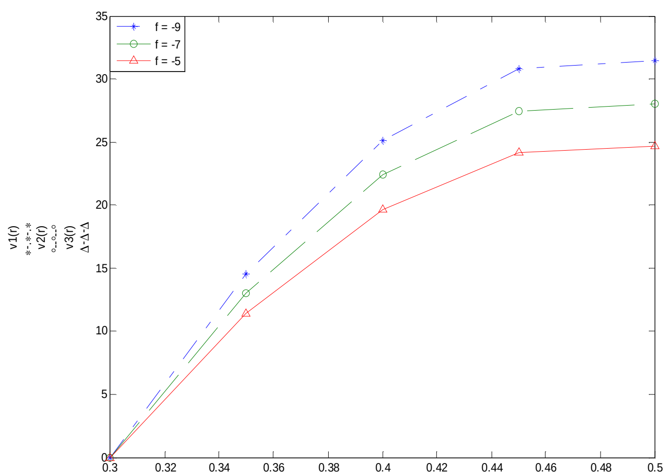

Figure 5.18 Profiles of the velocity *v(r,t)* given by Eq. (5.5.15) for $R_1=0.3$, $R_2=0.5$, $t=5s$, $v=0.045$, $\lambda=14$, $\lambda_r=2.8$, $\alpha=0.8$, β=0.5, $A=4$ and different values of *f*.

Figure 5.19

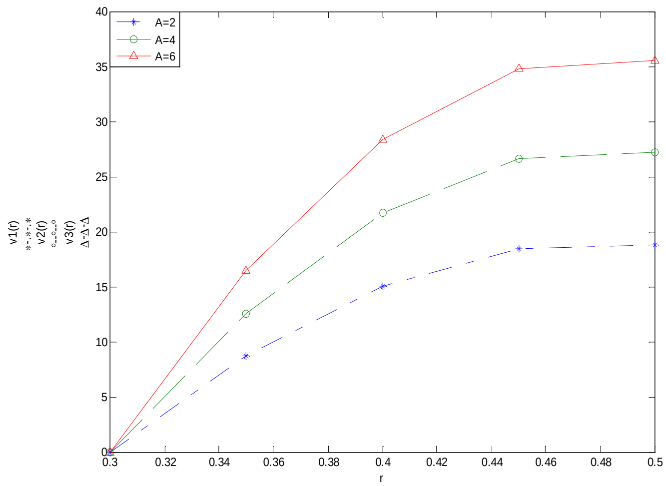

Figure 5.19 Profiles of the velocity $v(r,t)$ given by Eq. (5.5.15) for $R_1=0.3$, $R_2=0.5$, $f=-3$, $t=5s$, $\nu=0.04$, $\lambda=11$, $\lambda_r=2.5$, $\alpha=0.9$, $\beta=0.6$ and different values of A.

Part C

5.7 Flow through the annular region

Consider an Oldroyd-B fluid at rest between two infinitely long coaxial cylinders. Also, consider that radius of inner and outer cylinders are R_1 and $R_2(>R_1)$ respectively. The inner cylinder pulled with constant shear and outer cylinder is moving with time dependent velocity. We have to solve the next initial and boundary problem, in the absence of a pressure gradient in the z-direction.

$$(1+\lambda D_t^{\alpha})\frac{\partial v}{\partial t}=\upsilon(1+\lambda_r D_t^{\beta})\left(\partial_r^2+\frac{1}{r}\partial_r\right)v(r,t), \quad t>0. \tag{5.7.1}$$

The initial and boundary conditions are expressed by

$$v(r,0)=0, \quad \partial_t v(r,0)=0, \quad \mathrm{R}_1\le r\le \mathrm{R}_2, \tag{5.7.2}$$

$$\mu(1+\lambda_r D_t^{\beta})\partial_r v(r,t)|_{r=R_1}=f_1, \quad v(R_2,t)=f_2 t^p, \quad \mathrm{t}>0, \quad \mathrm{p}\ge 0, \tag{5.7.3}$$

where f_1, f_2 are constant.

Making the change to unknown function

$$v(r,t) = V(r) + u(r,t), \tag{5.7.4}$$

where

$$V(r) = \frac{R_1 f_1}{\mu} \ln(r / R_2). \tag{5.7.5}$$

Substitute Eq. (5.7.4) into Eq. (5.7.1), we get

$$(1+\lambda D_t^{\alpha})\frac{\partial u(r,t)}{\partial t} = \upsilon(1+\lambda_r D_t^{\beta})\left(\partial_r^2 + \frac{1}{r}\partial_r\right)u(r,t). \tag{5.7.6}$$

Substitute Eq. (5.7.4) into Eqs. (5.7.2) and (5.7.3), we get

$$u(r,0) = -V(r), \qquad \partial_t u(r,0) = 0, \tag{5.7.7}$$

$$\mu(1+\lambda_r D_t^{\beta})\partial_r u(R_1,t) = -f_1\lambda_r \frac{t^{-\beta}}{\Gamma(1-\beta)}, \qquad u(R_2,t) = f_2 t^p, \quad \mathrm{t}>0, \ \ \mathrm{p}\ge 0. \tag{5.7.8}$$

The Hankel Transform method with respect to r is used and is defined as follows [11]

$$\bar{u} = \int_{R_1}^{R_2} r u(r,s)\phi_1(s_n, r)dr. \tag{5.7.9}$$

The inverse Hankel Transform as defined by

$$u(r,s) = \frac{\pi^2}{2}\sum_{n=1}^{\infty}\frac{s_n^2 J_0^2(R_2 s_n)\bar{u}(s_n,s)\phi_1(s_n,r)}{J_1^2(R_1 s_n) - J_0^2(R_2 s_n)}, \tag{5.7.10}$$

where $\phi_1(s_n,r) = J_1(R_1 s_n)Y_0(s_n r) - Y_1(R_1 s_n)J_0(s_n r)$, $\mathrm{s_n}$ is the positive root of $\phi_1(s_n, R_2) = 0$.

Applying the Hankel transform to Eq. (5.7.6), we obtain

$$(1+\lambda D_t^{\alpha})\frac{\partial\bar{u}(s_n,t)}{\partial t}=-\upsilon s_n^2(1+\lambda_r D_t^{\beta})\bar{u}(s_n,t)+\frac{2\upsilon f_1\lambda_r}{\pi s_n\mu}\frac{t^{-\beta}}{\Gamma(1-\beta)}-\frac{2\upsilon f_2 t^{p}}{\pi}\frac{J_1(R_1s_n)}{J_0(R_2s_n)}$$
$$-\frac{2\upsilon f_2\lambda_r}{\pi}\frac{J_1(R_1s_n)}{J_0(R_2s_n)}\frac{\Gamma(p+1)}{\Gamma(p-\beta+1)}t^{p-\beta}. \qquad (5.7.11)$$

Applying the Hankel transform to Eq. (5.7.7), we obtain

$$\bar{u}(s_n,0)=\frac{2f_1}{\pi\mu s_n^3}\ , \qquad \partial_t\bar{u}(s_n,0)=0. \qquad (5.7.12)$$

Applying Laplace transform to Eq. (5.7.11), we obtain

$$\bar{\bar{u}}(s_n,s)=\bar{u}(s_n,0)\frac{(1+\lambda s^{\alpha}+\upsilon s_n^2\lambda_r s^{\beta-1})}{(s+\lambda s^{\alpha+1}+\upsilon s_n^2+\upsilon s_n^2\lambda_r s^{\beta})}$$
$$+\frac{2\upsilon\lambda_r f_1}{\pi\mu s_n}\frac{1}{s^{1-\beta}(s+\lambda s^{\alpha+1}+\upsilon s_n^2+\upsilon s_n^2\lambda_r s^{\beta})}$$
$$-\frac{2\upsilon f_2\Gamma(p+1)}{\pi}\frac{J_1(R_1s_n)}{J_0(R_2s_n)}\frac{1}{s^{p+1}(s+\lambda s^{\alpha+1}+\upsilon s_n^2+\upsilon s_n^2\lambda_r s^{\beta})}$$
$$-\frac{2\upsilon\lambda_r f_2\Gamma(p+1)}{\pi}\frac{J_1(R_1s_n)}{J_0(R_2s_n)}\frac{1}{s^{p-\beta+1}(s+\lambda s^{\alpha+1}+\upsilon s_n^2+\upsilon s_n^2\lambda_r s^{\beta})}\ . \qquad (5.7.13)$$

Substitute Eq. (5.7.12) into Eq. (5.7.13), we obtain

$$\bar{\bar{u}}(s_n,s)=\frac{2f_1}{\pi\mu s_n}\frac{(1+\lambda s^{\alpha}+\upsilon s_n^2\lambda_r s^{\beta-1})}{s_n^2(s+\lambda s^{\alpha+1}+\upsilon s_n^2+\upsilon s_n^2\lambda_r s^{\beta})}$$
$$+\frac{2\upsilon\lambda_r f_1}{\pi\mu s_n}\frac{1}{s^{1-\beta}(s+\lambda s^{\alpha+1}+\upsilon s_n^2+\upsilon s_n^2\lambda_r s^{\beta})}$$
$$-\frac{2\upsilon f_2\Gamma(p+1)}{\pi}\frac{J_1(R_1s_n)}{J_0(R_2s_n)}\frac{1}{s^{p+1}(s+\lambda s^{\alpha+1}+\upsilon s_n^2+\upsilon s_n^2\lambda_r s^{\beta})}$$
$$-\frac{2\upsilon\lambda_r f_2\Gamma(p+1)}{\pi}\frac{J_1(R_1s_n)}{J_0(R_2s_n)}\frac{1}{s^{p-\beta+1}(s+\lambda s^{\alpha+1}+\upsilon s_n^2+\upsilon s_n^2\lambda_r s^{\beta})}\ . \qquad (5.7.14)$$

Applying Inverse-Laplace transform to Eq. (5.7.14) and taking into account the following result [117]

$$G_{a,b,c}(d,t) = L^{-1}\left\{\frac{q^b}{(q^a-d)^c}\right\}$$
$$= \sum_{j=0}^{\infty} \frac{\mathrm{d}^{\mathrm{j}}\Gamma(c+j)}{\Gamma(c)\Gamma(j+1)} \frac{t^{(c+j)a-b-1}}{\Gamma[(c+j)a-b]};$$

$$\mathrm{Re}(ac-b)>0,\ \left|\frac{\mathrm{d}}{\mathrm{q}^{\mathrm{a}}}\right|<1, \tag{5.7.15}$$

we obtain

$$\bar{u}(s_n,t) = \frac{2f_1}{\pi\mu s_n}\left\{\frac{1}{s_n^2} - \frac{1}{s_n^2}\sum_{m=0}^{\infty}(-1)^m\left(\frac{\upsilon s_n^2}{\lambda}\right)^{m+1}\sum_{k=0}^{m}\binom{m}{k}\lambda_r^k G_{\alpha,\beta k-m-2,m+1}(-\lambda^{-1},t)\right\}$$
$$+\frac{2\lambda_r f_1}{\pi\mu s_n}\frac{1}{s_n^2}\sum_{m=0}^{\infty}(-1)^m\left(\frac{\upsilon s_n^2}{\lambda}\right)^{m+1}\sum_{k=0}^{m}\binom{m}{k}\lambda_r^k G_{\alpha,\beta k-m+\beta-2,m+1}(-\lambda^{-1},t)$$
$$-\frac{2f_2\Gamma(p+1)}{\pi}\frac{J_1(R_1s_n)}{J_0(R_2s_n)}\frac{1}{s_n^2}\sum_{m=0}^{\infty}(-1)^m\left(\frac{\upsilon s_n^2}{\lambda}\right)^{m+1}\sum_{k=0}^{m}\binom{m}{k}\lambda_r^k G_{\alpha,\beta k-m-p-2,m+1}(-\lambda^{-1},t)$$
$$-\frac{2\lambda_r f_2\Gamma(p+1)}{\pi}\frac{J_1(R_1s_n)}{J_0(R_2s_n)}\frac{1}{s_n^2}\sum_{m=0}^{\infty}(-1)^m\left(\frac{\upsilon s_n^2}{\lambda}\right)^{m+1}\sum_{k=0}^{m}\binom{m}{k}\lambda_r^k G_{\alpha,\beta k-m-p+\beta-2,m+1}(-\lambda^{-1},t). \tag{5.7.16}$$

The expression of the velocity field can be written as

$$v(r,t) = V(r) + \pi\sum_{n=1}^{\infty}\frac{J_0^2(R_2s_n)\phi_1(s_n,r)}{J_1^2(R_1s_n)-J_0^2(R_2s_n)}\left[\frac{f_1}{\mu s_n}\left\{1-\sum_{m=0}^{\infty}(-1)^m\left(\frac{\upsilon s_n^2}{\lambda}\right)^{m+1}\sum_{k=0}^{m}\binom{m}{k}\lambda_r^k G_{\alpha,\beta k-m-2,m+1}(-\lambda^{-1},t)\right\}\right.$$
$$+\frac{\lambda_r f_1}{\mu s_n}\sum_{m=0}^{\infty}(-1)^m\left(\frac{\upsilon s_n^2}{\lambda}\right)^{m+1}\sum_{k=0}^{m}\binom{m}{k}\lambda_r^k G_{\alpha,\beta k-m+\beta-2,m+1}(-\lambda^{-1},t)$$
$$-f_2\Gamma(p+1)\frac{J_1(R_1s_n)}{J_0(R_2s_n)}\sum_{m=0}^{\infty}(-1)^m\left(\frac{\upsilon s_n^2}{\lambda}\right)^{m+1}\sum_{k=0}^{m}\binom{m}{k}\lambda_r^k G_{\alpha,\beta k-m-p-2,m+1}(-\lambda^{-1},t)$$
$$\left.-\lambda_r f_2\Gamma(p+1)\frac{J_1(R_1s_n)}{J_0(R_2s_n)}\sum_{m=0}^{\infty}(-1)^m\left(\frac{\upsilon s_n^2}{\lambda}\right)^{m+1}\sum_{k=0}^{m}\binom{m}{k}\lambda_r^k G_{\alpha,\beta k-m-p+\beta-2,m+1}(-\lambda^{-1},t)\right]. \tag{5.7.17}$$

5.8 Results

As shown in below diagrams, the velocity $v(r,t)$ given by Eq. (5.7.17) has been drawn against r for different values of the time t, constants and other relevant parameters. The velocity component v is decreasing function of r. Figure 5.20 shows the influence of the time on the fluid motion. As expected, the velocity is increasing function with respect to *t*. The kinematic viscosity υ , as result from Fig. 5.21, has a strong influence on the velocity. The result indicates that the velocity is increasing function of υ. The influences of the relaxation and retardation times on the fluid motion are shown in the figures 5.22 and 5.23.It indicates that the velocity is decreasing function of λ and λ_r. Figure 5.24 show the influence of the fractional parameter α on the fluid motion. It is clearly seen from the figure that the velocity is increasing function of α. In figure 5.25, it is shown the influence of the fractional parameter β on the fluid motion. It is clearly seen from the figure that the velocity is decreasing function β. Figure 5.26 show the influences of *p* on the fluid motion. It is clearly seen from the figure that the velocity is increasing function of *p*. figures 5.27 and 5.28 show the influences of f_1 and f_2 on the fluid motion. Figure 5.29 show the influence of μ on the fluid motion. It is clearly seen from the figure that the velocity is increasing function of μ.

Figure 5.20

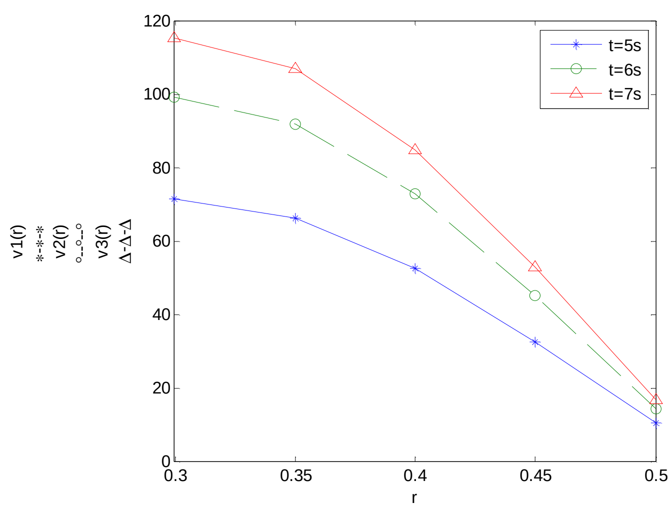

Fig. 5.20 Profiles of the velocity v(r, t) given by Eq. (5.7.17) for $R_1 = 0.3$, $R_2 = 0.5$, $f_1 = 3$, $f_2 = 4$, $\upsilon = 0.035$, $\lambda = 12$, $\lambda_r = 2.2$, $\alpha = 0.9$, $\beta = 0.6$, $p = 2$, $\mu = 30$ and different values of t.

Figure 5.21

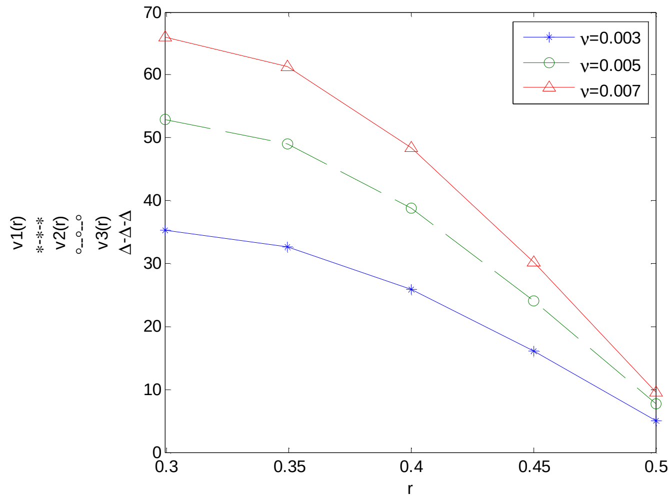

Fig.5.21 Profiles of the velocity v(r,t) given by Eq. (5.7.17) for $R_1 = 0.3$, $R_2 = 0.5$, $f_1 = 3$, $f_2 = 4$, $\mathrm{t} = 6\mathrm{s}$, $\lambda = 9$, $\lambda_r = 4$, $\alpha = 0.3$, $\beta = 0.3$, $\mathrm{p} = 2$, $\mu = 30$ and different values of υ.

Figure 5.22

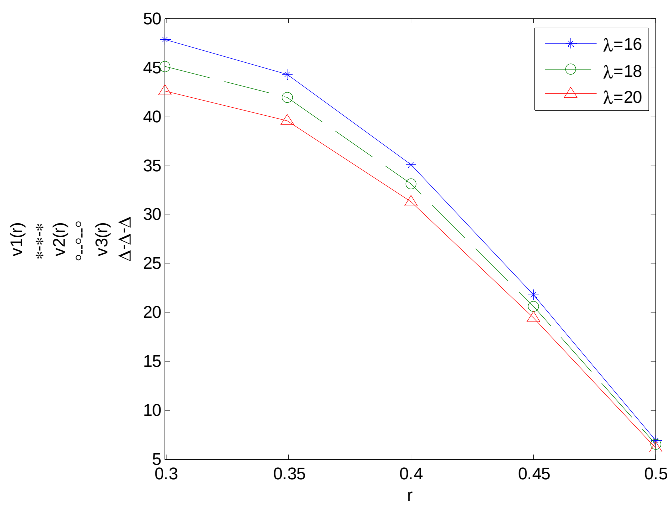

Fig.5.22 Profiles of the velocity v(r,t) given by Eq. (5.7.17) for $R_1 = 0.3$, $R_2 = 0.5$, $f_1 = 3$, $f_2 = 4$, $\mathrm{t} = 5\mathrm{s}$, $\upsilon = 0.01$, $\lambda_r = 7$, $\alpha = 0.3$, $\beta = 0.3$, $\mathrm{p} = 2$, $\mu = 30$ and different values of λ.

Figure 5.23

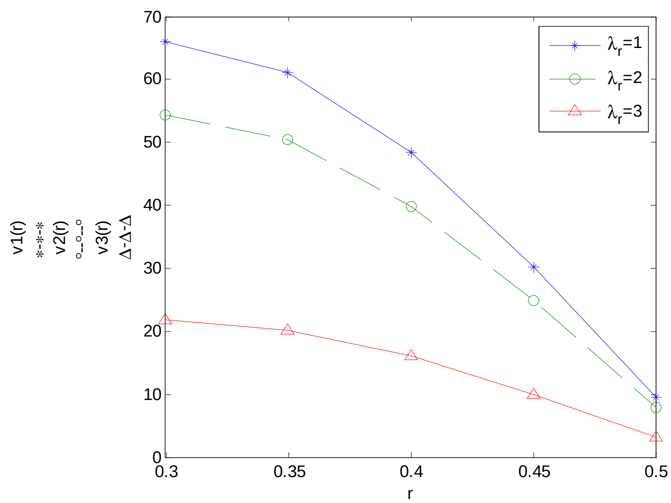

Fig. 5.23 Profiles of the velocity v(r, t) given by Eq. (5.7.17) for $R_1 = 0.3$, $R_2 = 0.5$, $f_1 = 3$, $f_2 = 4$, $\mathrm{t} = 5\mathrm{s}$, $\upsilon = 0.04$, $\lambda = 8$, $\alpha = 0.3$, $\beta = 0.9$, $\mathrm{p} = 2$, $\mu = 30$ and different values of λ_r.

Figure 5.24

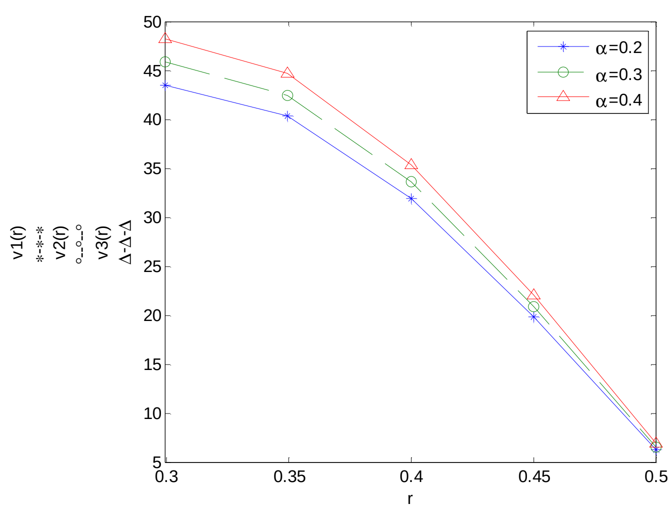

Fig. 5.24 Profiles of the velocity v(r, t) given by Eq. (5.7.17) for $R_1 = 0.3$, $R_2 = 0.5$, $f_1 = 3$, $f_2 = 4$, $\mathrm{t} = 6\mathrm{s}$, $\upsilon = 0.01$, $\lambda = 25$, $\lambda_r = 5$, $\beta = 0.5$, $\mathrm{p} = 2$, $\mu = 30$ and different values of α.

Figure 5.25

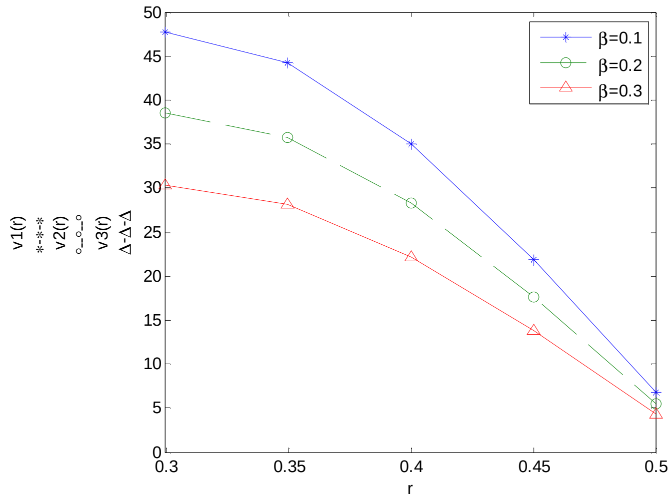

Fig. 5.25 Profiles of the velocity v(r,t) given by Eq. (5.7.17) for $R_1 = 0.3$, $R_2 = 0.5$, $f_1 = 3$, $f_2 = 4$, t = 6s, $\upsilon = 0.04$, $\lambda = 8$, $\lambda_r = 1.5$, $\alpha = 1$, p = 2, $\mu = 30$ and different values of β.

Figure 5.26

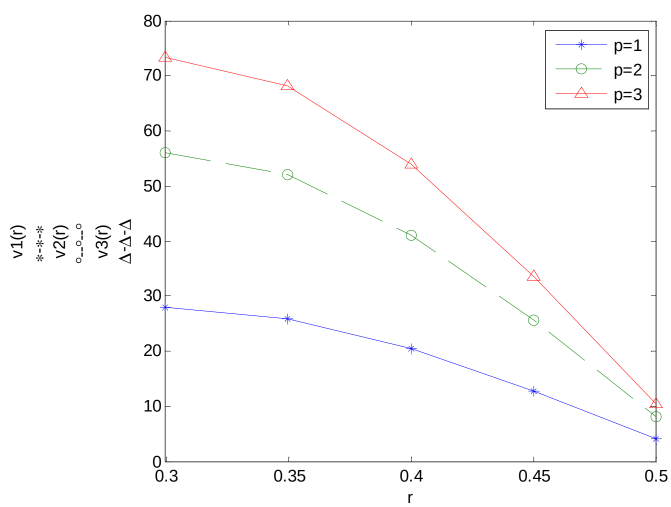

Fig. 5.26 Profiles of the velocity v(r,t) given by Eq. (5.7.17) for $R_1 = 0.3$, $R_2 = 0.5$, $f_1 = 3$, $f_2 = 4$, t = 5s, $\upsilon = 0.04$, $\lambda = 10$, $\lambda_r = 2$, $\alpha = 0.3$, $\beta = 0.9$, $\mu = 30$ and different values of p.

Figure 5.27

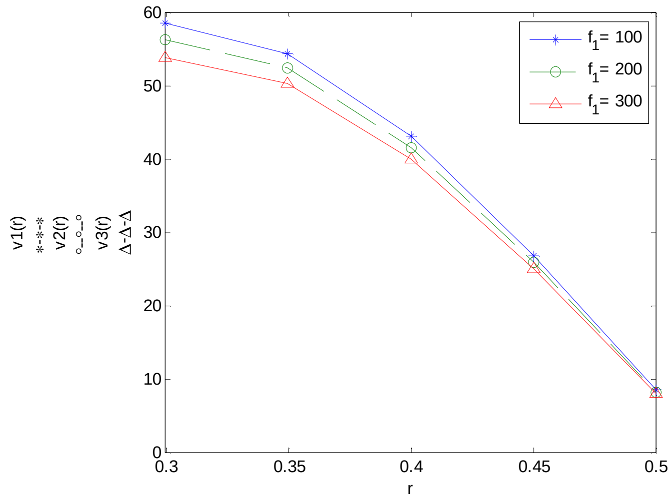

Fig.5.27 Profiles of the velocity v(r,t) given by Eq.(5.7.17) for $R_1 = 0.3,\ R_2 = 0.5,$ $f_2 = 4, t = 5s, \upsilon = 0.045, \lambda = 14, \lambda_r = 2.8,\ \alpha = 0.8, \beta = 0.5, \mathrm{p} = 2, \mu = 30$ and different values of f_1.

Figure 5.28

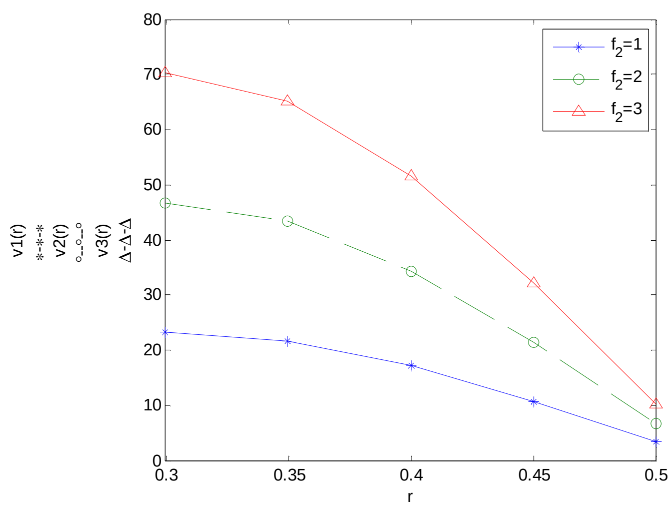

Fig.5.28 Profiles of the velocity v(r,t) given by Eq.(5.7.17) for $R_1 = 0.3,\ R_2 = 0.5,$ $f_1 = 3, t = 6s,\ \upsilon = 0.035, \lambda = 10,\ \lambda_r = 2,\ \alpha = 0.7,\ \beta = 0.4,\ \mathrm{p} = 2, \mu = 30$ and different values of f_2.

Figure 5.29

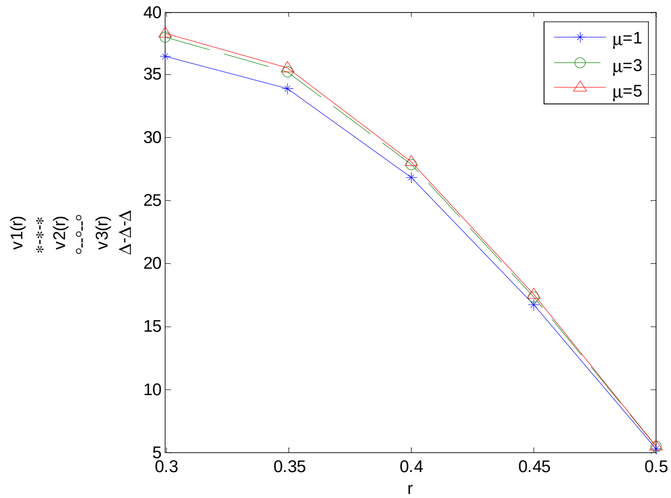

Fig. 5.29 Profiles of the velocity v(r,t) given by Eq.(5.7.17) for $R_1 = 0.3,\ R_2 = 0.5,$ $f_1 = 3,\ f_2 = 4, t = 5s, \upsilon = 0.04,\ \lambda = 11,\ \lambda_r = 2.5,\ \alpha = 0.9,\ \beta = 0.6,\ \mathrm{p} = 2$ and different values of μ.

5.9 Conclusions

The purpose of this chapter is to establish exact solutions for the velocity field corresponding to the flow of Oldroyd-B fluid in the annular region between two infinitely long coaxial cylinders. In part-A, the motion is produced by a constant pressure gradient and the inner cylinder pulled with constant shear and outer cylinder is moving with time dependent velocity. In part-B, the motion is produced by a constant pressure gradient and inner cylinder is moving with constant velocity while the outer cylinder is fixed. In part-C, the motion of the fluid is produced by the inner cylinder pulled with a constant shear and outer cylinder is moving with time dependent velocity. This solution is obtained by using Hankel transform and Laplace transform methods and the result is presented in terms of generalized G functions. This solution satisfies the governing equation and all imposed initial and boundary conditions. The velocity field is also analyzed using graphical illustration for various parameters, constants and fractional coefficients.

In all of above figures, the roots s_n has been approximated by $\dfrac{(2n-1)\pi}{2(R_2 - R_1)}$.

Chapter 6. Exact solutions for the helical flow of fractional Oldroyd-B fluid in a circular cylinder

---

The paper submitted on the work described in this chapter:

1. Khandelwal K. and Mathur V., Exact solutions for the helical flow of fractional Oldroyd-B fluid in a circular cylinder, Advances in Applied Mathematics and Mechanics (communicated).

6.1 Introduction

This chapter presents and analyzes the velocity fields and the adequate shear stresses corresponding to the helical flow of fractional Oldroyd-B fluid. The fluid is assumed to be present in a circular cylinder. We use sequential fractional derivatives Laplace transform and finite Hankel transforms to reach to desired results. The results are presented in terms of generalized G function and they are free from convolution products. Subsequently, we impose appropriate limits to derive solutions for ordinary Oldroyd-B fluid, Newtonian fluid, ordinary Maxwell fluid and fractional Maxwell fluid. Further, this chapter demonstrates the influence of various physical parameters on velocity and shear stress and presents the results graphically. Finally, a comparison is drawn and discussed among different models.

6.2 Governing equations

The constitutive equations of an incompressible Oldroyd-B fluid are given by [21, 71,118]

$$T=-pI+S,\quad S+\lambda(\dot{S}-LS-SL^{T})=\mu[A+\lambda_r(\dot{A}-LA-AL^{T})], \tag{6.2.1}$$

where T is the Cauchy stress tensor, $-pI$ denotes the indeterminate spherical stress, S is the extra-stress tensor, λ and λ_r are relaxation and retardation times, $A=L+L^{T}$ is the first Rivlin-Ericksen tensor with L the velocity gradient, μ is the dynamic viscosity, the superscript T indicates the transpose operation and the dot denotes the material time differentiation.

In cylindrical coordinates (r,θ,z) the helical flow velocity field V and extra stress S are defined as

$$V=V(r,t)=w(r,t)e_\theta+v(r,t)e_z,\qquad S=S(r,t), \tag{6.2.2}$$

where e_θ and e_z are the unit vectors in the θ and z directions. The fluid is assumed to be at rest at $t=0$, then

$$V(\mathrm{r},0)=0,\qquad S(r,0)=0. \tag{6.2.3}$$

Eqs. (6.2.1) and (6.2.2) imply $S_{rr} = S_{\theta\theta} = S_{zz} = S_{\theta z} = 0$ and relevant equations

$$(1+\lambda D_t^{\alpha})\tau_1(r,t) = \mu(1+\lambda_r D_t^{\beta})\left(\frac{\partial}{\partial r} - \frac{1}{r}\right)w(r,t), \tag{6.2.4}$$

$$(1+\lambda D_t^{\alpha})\tau_2(r,t) = \mu(1+\lambda_r D_t^{\beta})\frac{\partial v(r,t)}{\partial r}, \tag{6.2.5}$$

where $\tau_1 = S_{r\theta}$ and $\tau_2 = S_{rz}$ are the shear stresses. The equation of motion, in the absence of a pressure gradient in the axial direction and neglecting body forces, leads to the relevant equations

$$\rho\frac{\partial w(r,t)}{\partial t} = \left(\frac{\partial}{\partial r} + \frac{2}{r}\right)\tau_1(r,t), \tag{6.2.6}$$

$$\rho\frac{\partial v(r,t)}{\partial t} = \left(\frac{\partial}{\partial r} + \frac{1}{r}\right)\tau_2(r,t). \tag{6.2.7}$$

Eliminating τ_1 and τ_2 between Eqs. (6.2.6) and (6.2.7), we obtain

$$(1+\lambda D_t^{\alpha})\frac{\partial w(r,t)}{\partial t} = \upsilon(1+\lambda_r D_t^{\beta})\left(\frac{\partial^2}{\partial r^2} + \frac{1}{r}\frac{\partial}{\partial r} - \frac{1}{r^2}\right)w(r,t), \tag{6.2.8}$$

$$(1+\lambda D_t^{\alpha})\frac{\partial v(r,t)}{\partial t} = \upsilon(1+\lambda_r D_t^{\beta})\left(\frac{\partial^2}{\partial r^2} + \frac{1}{r}\frac{\partial}{\partial r}\right)v(r,t), \tag{6.2.9}$$

where $\upsilon = \dfrac{\mu}{\rho}$ is the kinematic viscosity, ρ is the constant density of the fluid and D_t^{β} is the Caputo fractional derivative of order β as defined by [64]

$$D_t^{\beta} f(t) = \begin{cases} \dfrac{1}{\Gamma(1-\beta)}\dfrac{d}{dt}\displaystyle\int_0^t \dfrac{f(\tau)}{(t-\tau)^{\beta}}d\tau, & 0<\beta<1; \\ \dfrac{d}{dt}f(t), & \beta = 1, \end{cases} \tag{6.2.10}$$

where $\Gamma(.)$ is the Gamma function. This model can be reduced to ordinary Oldroyd-B model when $\alpha \to 1$ and $\beta \to 1$.

6.3 Helical flow through an infinite circular cylinder

Let us consider an incompressible fractional Oldroyd-B fluid at rest in an infinite circular cylinder of radius *R*. At time $t=0^+$, the cylinder begins to oscillate around its axis with the velocity $R\sin\omega t$ and to slide along the same axis with the velocity Ut^a, where ω is the angular frequency of velocity, *U* and *a* are constants. The appropriate initial and boundary conditions are

$$w(r,0)=v(r,0)=0, \tag{6.3.1}$$

and

$$w(R,t)=R\sin\omega t, \qquad v(R,t)=Ut^a, \qquad \mathrm{t}\geq 0,\ \ \mathrm{a}\geq 0. \tag{6.3.2}$$

In order to solve this problem, we use fractional derivative Laplace and finite Hankel transforms.

6.3.1 Calculation of the velocity field

Applying Laplace transform to Eqs. (6.2.8) and (6.2.9), in terms of sequential fractional derivative Laplace transform [64] and using the initial conditions as given in Eq. (6.3.1), we obtain

$$\left(q+\lambda q^{\alpha+1}\right)\overline{w}(r,q)=\upsilon\left(1+\lambda_r q^{\beta}\right)\left(\frac{\partial^2}{\partial r^2}+\frac{1}{r}\frac{\partial}{\partial r}-\frac{1}{r^2}\right)\overline{w}(r,q), \tag{6.3.3}$$

$$\left(q+\lambda q^{\alpha+1}\right)\overline{v}(r,q)=\upsilon\left(1+\lambda_r q^{\beta}\right)\left(\frac{\partial^2}{\partial r^2}+\frac{1}{r}\frac{\partial}{\partial r}\right)\overline{v}(r,q). \tag{6.3.4}$$

Applying Laplace transform to Eq. (6.3.2), we obtain

$$\overline{w}(R,q)=\frac{R\omega}{q^2+\omega^2}, \qquad \overline{v}(R,q)=\frac{U\Gamma(a+1)}{q^{a+1}}. \tag{6.3.5}$$

Multiplying both sides of Eqs. (6.3.3) and (6.3.4) by $rJ_1(rr_{1n})$ and $rJ_0(rr_{0n})$, respectively, integrating them with respect to r from *0* to R and taking into account the following results

$$\int_0^R r\left(\frac{\partial^2 w}{\partial r^2}+\frac{1}{r}\frac{\partial w}{\partial r}-\frac{w}{r^2}\right)J_1(rr_{1n})dr = Rr_{1n}J_2(Rr_{1n})w(R,t)\text{-}r_{1n}^2 w_H(r_{1n},t), \qquad (6.3.6)$$

$$\int_0^R r\left(\frac{\partial^2 v}{\partial r^2}+\frac{1}{r}\frac{\partial v}{\partial r}\right)J_0(rr_{0n})dr = Rr_{0n}J_1(Rr_{0n})v(R,t)\text{-}r_{0n}^2 v_H(r_{0n},t), \qquad (6.3.7)$$

we obtain

$$\overline{w}_H(r_{1n},q) = \upsilon R^2\omega r_{1n}J_2(Rr_{1n})\frac{\left(1+\lambda_r q^{\beta}\right)}{(q^2+\omega^2)(q+\lambda q^{\alpha+1}+\upsilon r_{1n}^2+\upsilon\lambda_r r_{1n}^2 q^{\beta})}, \qquad (6.3.8)$$

and

$$\overline{v}_H(r_{0n},q) = \upsilon Rr_{0n}J_1(Rr_{0n})U\Gamma(a+1)\frac{\left(1+\lambda_r q^{\beta}\right)}{q^{a+1}(q+\lambda q^{\alpha+1}+\upsilon r_{0n}^2+\upsilon\lambda_r r_{0n}^2 q^{\beta})}, \qquad (6.3.9)$$

where

$$\overline{w}_H(r_{1n},q) = \int_0^R r\overline{w}(r,q)J_1(rr_{1n})dr, \qquad \overline{v}_H(r_{0n},q) = \int_0^R r\overline{v}(r,q)J_0(rr_{0n})dr, \quad (6.3.10)$$

are the Hankel transform of $\overline{w}(r,q)$ and $\overline{v}(r,q)$, while r_{1n} and r_{0n} are the positive roots of the transcendental equations $J_1(Rr)=0$ and $J_0(Rr)=0$ respectively. The inverse Hankel transform, as defined by [116], can be given as

$$\overline{w}(r,q) = \frac{2}{R^2}\sum_{n=1}^{\infty}\frac{J_1(rr_{1n})}{J_2^2(Rr_{1n})}\overline{w}_H(r_{1n},q), \qquad (6.3.11)$$

and

$$\overline{v}(r,q) = \frac{2}{R^2}\sum_{n=1}^{\infty}\frac{J_0(rr_{0n})}{J_1^2(Rr_{0n})}\overline{v}_H(r_{0n},q). \qquad (6.3.12)$$

Applying inverse Hankel transform to Eqs. (6.3.8) and (6.3.9), we obtain

$$\overline{w}(r,q)=2\upsilon\omega\sum_{n=1}^{\infty}r_{1n}\,\frac{J_1(rr_{1n})}{J_2(Rr_{1n})}\,\frac{\left(1+\lambda_r q^{\beta}\right)}{(q^2+\omega^2)(q+\lambda q^{\alpha+1}+\upsilon r_{1n}^2+\upsilon\lambda_r r_{1n}^2 q^{\beta})}, \tag{6.3.13}$$

and

$$\bar{v}(r,q)=\frac{2}{R}\,\upsilon U\Gamma(a+1)\sum_{n=1}^{\infty}r_{0n}\,\frac{J_0(rr_{0n})}{J_1(Rr_{0n})}\,\frac{\left(1+\lambda_r q^{\beta}\right)}{q^{a+1}(q+\lambda q^{\alpha+1}+\upsilon r_{0n}^2+\upsilon\lambda_r r_{0n}^2 q^{\beta})}, \tag{6.3.14}$$

Applying Inverse-Laplace transform to Eqs. (6.3.13) and (6.3.14), taking into account the following results [117]

$$\frac{1}{q+\lambda q^{\alpha+1}+\upsilon r_n^2+\upsilon\lambda_r r_n^2 q^{\beta}}=\frac{1}{\lambda}\sum_{m=0}^{\infty}\sum_{k=0}^{m}\frac{m!}{k!(m-k)!}\left(\frac{-\upsilon r_n^2}{\lambda}\right)^m\lambda_r^k\,\frac{q^{\beta k-m-1}}{(q^{\alpha}+\lambda^{-1})^{m+1}}, \tag{6.3.15}$$

and

$$G_{a,b,c}(d,t)=L^{-1}\left\{\frac{q^b}{(q^a-d)^c}\right\}$$
$$=\sum_{j=0}^{\infty}\frac{d^j\Gamma(c+j)}{\Gamma(c)\Gamma(j+1)}\frac{t^{(c+j)a-b-1}}{\Gamma[(c+j)a-b]};$$

$$\mathrm{Re}(ac-b)>0,\quad \mathrm{Re}(q)>0,\quad \left|\frac{d}{q^a}\right|<1, \tag{6.3.16}$$

we obtain

$$w(r,t)=\frac{2\upsilon\omega}{\lambda}\sum_{n=1}^{\infty}r_{1n}\,\frac{J_1(rr_{1n})}{J_2(Rr_{1n})}\sum_{j=0}^{\infty}(-\omega^2)^j\sum_{m=0}^{\infty}\left(\frac{-\upsilon r_{1n}^2}{\lambda}\right)^m\sum_{k=0}^{m}\frac{m!}{k!(m-k)!}\lambda_r^k$$
$$\times\left\{G_{\alpha,\beta k-m-2j-3,m+1}(-\lambda^{-1},t)+\lambda_r G_{\alpha,\beta(k+1)-m-2j-3,m+1}(-\lambda^{-1},t)\right\}, \tag{6.3.17}$$

and

$$v(r,t)=\frac{2}{R}\,\frac{\upsilon U\Gamma(a+1)}{\lambda}\sum_{n=1}^{\infty}r_{0n}\,\frac{J_0(rr_{0n})}{J_1(Rr_{0n})}\sum_{m=0}^{\infty}\left(\frac{-\upsilon r_{0n}^2}{\lambda}\right)^m\sum_{k=0}^{m}\frac{m!}{k!(m-k)!}\lambda_r^k$$
$$\times\left\{G_{\alpha,\beta k-m-a-2,m+1}(-\lambda^{-1},t)+\lambda_r G_{\alpha,\beta(k+1)-m-a-2,m+1}(-\lambda^{-1},t)\right\}. \tag{6.3.18}$$

6.3.2 Calculation of the shear stress

Applying Laplace transform to Eqs. (6.2.4) and (6.2.5), we obtain

$$\bar{\tau}_1(r,q)=\mu\frac{(1+\lambda_r q^{\beta})}{(1+\lambda q^{\alpha})}\left(\frac{\partial}{\partial r}-\frac{1}{r}\right)\overline{w}(r,q), \tag{6.3.19}$$

and

$$\bar{\tau}_2(r,q)=\mu\frac{(1+\lambda_r q^{\beta})}{(1+\lambda q^{\alpha})}\frac{\partial\bar{v}(r,q)}{\partial r}. \tag{6.3.20}$$

Substitute Eqs. (6.3.13) and (6.3.14) into Eqs. (6.3.19) and (6.3.20), we obtain

$$\bar{\tau}_1(r,q)=-2\mu\upsilon\omega\sum_{n=1}^{\infty}r_{1n}^2\frac{J_2(rr_{1n})}{J_2(Rr_{1n})}\frac{\left(1+\lambda_r q^{\beta}\right)^2}{(q^2+\omega^2)(1+\lambda q^{\alpha})(q+\lambda q^{\alpha+1}+\upsilon r_{1n}^2+\upsilon\lambda_r r_{1n}^2 q^{\beta})}, \tag{6.3.21}$$

and

$$\bar{\tau}_2(r,q)=-\frac{2}{R}\mu\upsilon U\Gamma(a+1)\sum_{n=1}^{\infty}r_{0n}^2\frac{J_1(rr_{0n})}{J_1(Rr_{0n})}\frac{\left(1+\lambda_r q^{\beta}\right)^2}{q^{a+1}(1+\lambda q^{\alpha})(q+\lambda q^{\alpha+1}+\upsilon r_{0n}^2+\upsilon\lambda_r r_{0n}^2 q^{\beta})}. \tag{6.3.22}$$

Applying inverse Laplace transform to Eqs. (6.3.21) and (6.3.22), then using Eqs. (6.3.15) and (6.3.16), we obtain

$$\begin{aligned}\tau_1(r,t)=&-\frac{2\mu\upsilon\omega}{\lambda^2}\sum_{n=1}^{\infty}r_{1n}^2\frac{J_2(rr_{1n})}{J_2(Rr_{1n})}\sum_{j=0}^{\infty}(-\omega^2)^j\sum_{m=0}^{\infty}\left(\frac{-\upsilon r_{1n}^2}{\lambda}\right)^m\sum_{k=0}^{m}\frac{m!}{k!(m-k)!}\lambda_r^k\\&\times\left\{G_{\alpha,\beta k-m-2j-3,m+2}(-\lambda^{-1},t)+\lambda_r^2 G_{\alpha,\beta(k+2)-m-2j-3,m+2}(-\lambda^{-1},t)\right.\\&\left.+2\lambda_r G_{\alpha,\beta(k+1)-m-2j-3,m+2}(-\lambda^{-1},t)\right\},\end{aligned} \tag{6.3.23}$$

and

$$\begin{aligned}\tau_2(r,t)=&-\frac{2}{R}\frac{\mu\upsilon U\Gamma(a+1)}{\lambda^2}\sum_{n=1}^{\infty}r_{0n}^2\frac{J_1(rr_{0n})}{J_1(Rr_{0n})}\sum_{m=0}^{\infty}\left(\frac{-\upsilon r_{0n}^2}{\lambda}\right)^m\sum_{k=0}^{m}\frac{m!}{k!(m-k)!}\lambda_r^k\\&\times\left\{G_{\alpha,\beta k-m-a-2,m+2}(-\lambda^{-1},t)+\lambda_r^2 G_{\alpha,\beta(k+2)-m-a-2,m+2}(-\lambda^{-1},t)+2\lambda_r G_{\alpha,\beta(k+1)-m-a-2,m+2}(-\lambda^{-1},t)\right\}.\end{aligned} \tag{6.3.24}$$

6.4 Limiting Cases

6.4.1 Ordinary Oldroyd-B fluid

Applying $\alpha \to 1$ and $\beta \to 1$ into Eqs. (6.3.17), (6.3.18), (6.3.23) and (6.3.24), we obtain the velocity field

$$w_{OB}(r,t) = \frac{2\upsilon\omega}{\lambda}\sum_{n=1}^{\infty} r_{1n}\frac{J_1(rr_{1n})}{J_2(Rr_{1n})}\sum_{j=0}^{\infty}(-\omega^2)^j\sum_{m=0}^{\infty}\left(\frac{-\upsilon r_{1n}^2}{\lambda}\right)^m\sum_{k=0}^{m}\frac{m!}{k!(m-k)!}\lambda_r^k \times\left\{G_{1,k-m-2j-3,m+1}(-\lambda^{-1},t)+\lambda_r G_{1,k-m-2j-2,m+1}(-\lambda^{-1},t)\right\}, \quad (6.4.1)$$

$$v_{OB}(r,t) = \frac{2}{R}\frac{\upsilon U\Gamma(a+1)}{\lambda}\sum_{n=1}^{\infty} r_{0n}\frac{J_0(rr_{0n})}{J_1(Rr_{0n})}\sum_{m=0}^{\infty}\left(\frac{-\upsilon r_{0n}^2}{\lambda}\right)^m\sum_{k=0}^{m}\frac{m!}{k!(m-k)!}\lambda_r^k \times\left\{G_{1,k-m-a-2,m+1}(-\lambda^{-1},t)+\lambda_r G_{1,k-m-a-1,m+1}(-\lambda^{-1},t)\right\}, \quad (6.4.2)$$

and the tangential stress corresponding to ordinary Oldroyd-B fluid performing the same motion.

$$\tau_{1OB}(r,t) = -\frac{2\mu\upsilon\omega}{\lambda^2}\sum_{n=1}^{\infty} r_{1n}^2\frac{J_2(rr_{1n})}{J_2(Rr_{1n})}\sum_{j=0}^{\infty}(-\omega^2)^j\sum_{m=0}^{\infty}\left(\frac{-\upsilon r_{1n}^2}{\lambda}\right)^m\sum_{k=0}^{m}\frac{m!}{k!(m-k)!}\lambda_r^k \times\left\{G_{1,k-m-2j-3,m+2}(-\lambda^{-1},t)+\lambda_r^2 G_{1,k-m-2j-1,m+2}(-\lambda^{-1},t)+2\lambda_r G_{1,k-m-2j-2,m+2}(-\lambda^{-1},t)\right\}, \quad (6.4.3)$$

$$\tau_{2OB}(r,t) = -\frac{2}{R}\frac{\mu\upsilon U\Gamma(a+1)}{\lambda^2}\sum_{n=1}^{\infty} r_{0n}^2\frac{J_1(rr_{0n})}{J_1(Rr_{0n})}\sum_{m=0}^{\infty}\left(\frac{-\upsilon r_{0n}^2}{\lambda}\right)^m\sum_{k=0}^{m}\frac{m!}{k!(m-k)!}\lambda_r^k \times\left\{G_{1,k-m-a-2,m+2}(-\lambda^{-1},t)+\lambda_r^2 G_{1,k-m-a,m+2}(-\lambda^{-1},t)+2\lambda_r G_{1,k-m-a-1,m+2}(-\lambda^{-1},t)\right\}. \quad (6.4.4)$$

6.4.2 Fractional Maxwell fluid

Applying $\lambda_r \to 0$ into Eqs. (6.3.17), (6.3.18), (6.3.23) and (6.3.24), we obtain the velocity field

$$w_{FM}(r,t) = \frac{2\upsilon\omega}{\lambda}\sum_{n=1}^{\infty} r_{1n}\frac{J_1(rr_{1n})}{J_2(Rr_{1n})}\sum_{j=0}^{\infty}(-\omega^2)^j\sum_{m=0}^{\infty}\left(\frac{-\upsilon r_{1n}^2}{\lambda}\right)^m G_{\alpha,-m-2j-3,m+1}(-\lambda^{-1},t), \quad (6.4.5)$$

$$v_{FM}(r,t)=\frac{2}{R}\frac{\upsilon U\Gamma(a+1)}{\lambda}\sum_{n=1}^{\infty} r_{0n}\frac{J_0(rr_{0n})}{J_1(Rr_{0n})}\sum_{m=0}^{\infty}\left(\frac{-\upsilon r_{0n}^2}{\lambda}\right)^m G_{\alpha,-m-a-2,m+1}(-\lambda^{-1},t), \tag{6.4.6}$$

and the shear stress corresponding to the fractional Maxwell fluid performing the same motion.

$$\tau_{1FM}(r,t)=-\frac{2\mu\upsilon\omega}{\lambda^2}\sum_{n=1}^{\infty} r_{1n}^2\frac{J_2(rr_{1n})}{J_2(Rr_{1n})}\sum_{j=0}^{\infty}(-\omega^2)^j\sum_{m=0}^{\infty}\left(\frac{-\upsilon r_{1n}^2}{\lambda}\right)^m G_{\alpha,-m-2j-3,m+2}(-\lambda^{-1},t), \tag{6.4.7}$$

$$\tau_{2FM}(r,t)=-\frac{2}{R}\frac{\mu\upsilon U\Gamma(a+1)}{\lambda^2}\sum_{n=1}^{\infty} r_{0n}^2\frac{J_1(rr_{0n})}{J_1(Rr_{0n})}\sum_{m=0}^{\infty}\left(\frac{-\upsilon r_{0n}^2}{\lambda}\right)^m G_{\alpha,-m-a-2,m+2}(-\lambda^{-1},t). \tag{6.4.8}$$

6.4.3 Ordinary Maxwell fluid

Applying $\lambda_r \to 0$ and $\alpha \to 1$ into Eqs. (6.3.17), (6.3.18), (6.3.23) and (6.3.24), we obtain the velocity field

$$w_M(r,t)=\frac{2\upsilon\omega}{\lambda}\sum_{n=1}^{\infty} r_{1n}\frac{J_1(rr_{1n})}{J_2(Rr_{1n})}\sum_{j=0}^{\infty}(-\omega^2)^j\sum_{m=0}^{\infty}\left(\frac{-\upsilon r_{1n}^2}{\lambda}\right)^m G_{1,-m-2j-3,m+1}(-\lambda^{-1},t), \tag{6.4.9}$$

$$v_M(r,t)=\frac{2}{R}\frac{\upsilon U\Gamma(a+1)}{\lambda}\sum_{n=1}^{\infty} r_{0n}\frac{J_0(rr_{0n})}{J_1(Rr_{0n})}\sum_{m=0}^{\infty}\left(\frac{-\upsilon r_{0n}^2}{\lambda}\right)^m G_{1,-m-a-2,m+1}(-\lambda^{-1},t), \tag{6.4.10}$$

and its associated tangential stress corresponding to ordinary Maxwell fluid performing the same motion.

$$\tau_{1M}(r,t)=-\frac{2\mu\upsilon\omega}{\lambda^2}\sum_{n=1}^{\infty} r_{1n}^2\frac{J_2(rr_{1n})}{J_2(Rr_{1n})}\sum_{j=0}^{\infty}(-\omega^2)^j\sum_{m=0}^{\infty}\left(\frac{-\upsilon r_{1n}^2}{\lambda}\right)^m G_{1,-m-2j-3,m+2}(-\lambda^{-1},t), \tag{6.4.11}$$

$$\tau_{2M}(r,t) = -\frac{2}{R}\frac{\mu\upsilon U\Gamma(a+1)}{\lambda^2}\sum_{n=1}^{\infty} r_{0n}^2 \frac{J_1(rr_{0n})}{J_1(Rr_{0n})}\sum_{m=0}^{\infty}\left(\frac{-\upsilon r_{0n}^2}{\lambda}\right)^m G_{1,-m-a-2,m+2}(-\lambda^{-1},t). \tag{6.4.12}$$

6.4.4 Newtonian Fluid

Applying $\lambda \to 0$ into Eqs. (6.4.9), (6.4.10), (6.4.11) and (6.4.12) and taking into account the following result [22]

$$\lim_{\lambda\to 0}\frac{1}{\lambda^m}G_{1,b,m}(-\lambda^{-1},t) = \frac{t^{-b-1}}{\Gamma(-b)},$$

we obtain the corresponding solutions for the Newtonian fluid as follows

$$w_N(r,t) = 2\upsilon\omega\sum_{n=1}^{\infty} r_{1n}\frac{J_1(rr_{1n})}{J_2(Rr_{1n})}\sum_{j=0}^{\infty}(-\omega^2)^j\sum_{m=0}^{\infty}(-\upsilon r_{1n}^2)^m\frac{t^{m+2j+2}}{\Gamma(m+2j+3)}, \tag{6.4.13}$$

$$v_N(r,t) = \frac{2}{R}\upsilon U\Gamma(a+1)\sum_{n=1}^{\infty} r_{0n}\frac{J_0(rr_{0n})}{J_1(Rr_{0n})}\sum_{m=0}^{\infty}(-\upsilon r_{0n}^2)^m\frac{t^{m+a+1}}{\Gamma(m+a+2)}, \tag{6.4.14}$$

$$\tau_{1N}(r,t) = -2\mu\upsilon\omega\sum_{n=1}^{\infty} r_{1n}^2\frac{J_2(rr_{1n})}{J_2(Rr_{1n})}\sum_{j=0}^{\infty}(-\omega^2)^j\sum_{m=0}^{\infty}(-\upsilon r_{1n}^2)^m\frac{t^{m+2j+2}}{\Gamma(m+2j+3)}, \tag{6.4.15}$$

$$\tau_{2N}(r,t) = -\frac{2}{R}\mu\upsilon U\Gamma(a+1)\sum_{n=1}^{\infty} r_{0n}^2\frac{J_1(rr_{0n})}{J_1(Rr_{0n})}\sum_{m=0}^{\infty}(-\upsilon r_{0n}^2)^m\frac{t^{m+a+1}}{\Gamma(m+a+2)}. \tag{6.4.16}$$

6.5 Conclusions and Numerical results

In this chapter, we obtained and presented a solution for the helical flow of an incompressible fractional Oldroyd-B fluid. The motion is created as cylinder begins to oscillate around its axis and slides along the same axis with prescribed velocity. The expressions for the velocity fields and the shear stresses have been determined using

Laplace transform of sequential fractional derivatives and finite Hankel transforms in terms of generalized G function and they satisfy all the initial and boundary conditions. Furthermore, our solutions can be simplified for Newtonian fluids and some non-Newtonian fluids such as ordinary Oldroyd-B fluid, fractional Maxwell fluid, ordinary Maxwell fluid. Thus, the technique and the fractional Oldroyd-B model will be useful in the theory of non-Newtonian fluids.

In order to demonstrate impact of physical parameters, the obtained results are presented in the form of diagrams for both components of the velocity and shear stresses. They are given by Eqs. (6.3.17), (6.3.18), (6.3.23) and (6.3.24) and have been drawn against r for different values of the time t and other relevant parameters as shown in diagrams. It can be observed from figures that the velocity component $v(r,t)$ decreases with the radius *r*. Figure 6.1 shows the fluid motion at different times. It is observed that the velocities are increasing while the shear stresses area decreasing function of time *t*. Figure 6.2 shows the effect of different values of kinematic viscosity on the fluid motion. It indicates that the velocity profiles increase while the shear stresses decrease, when kinematic viscosity increases. The dependencies of the relaxation and retardation times on the fluid motion are shown in the figures 6.3 & 6.4. The figures indicate that both components of velocity are decreasing and the shear stresses are increasing function of λ. As well as the velocities are increasing and the shear stresses are decreasing function of retardation time λ_r. Fig. 6.5 demonstrates the velocities and the shear stresses changes with the fractional parameter α. It can be observed that the two components of the velocity increases while the shear stresses decreases with increasing value of α. The influence of the fractional parameter β on the fluid motion is shown in figure 6.6. It indicates that the velocity profiles are decreasing and the shear stresses are increasing function of β.

Figure 6.7 exhibits a comparative diagram of both components of velocity and the shear stresses corresponding to the motions of a fractional Oldroyd-B fluid, ordinary Oldroyd-B fluid, fractional Maxwell fluid, ordinary Maxwell fluid and Newtonian fluid in a circular cylinder, for same values of the common material constants and time *t*. In all cases, the velocities of the Newtonian fluid are the swiftest while they are slowest for the fractional Maxwell fluid on the whole flow domain. Similarly, shear stresses on the whole flow domains are highest for fractional Maxwell fluid while it is slowest for the Newtonian fluid. In all of the figures 6.1-6.7, the units of the material constants are in SI units and the roots r_{0n} and r_{1n} have been approximated by $\dfrac{(4n-1)\pi}{4R}$ and $\dfrac{(4n+1)\pi}{4R}$ respectively.

Figure 6.1

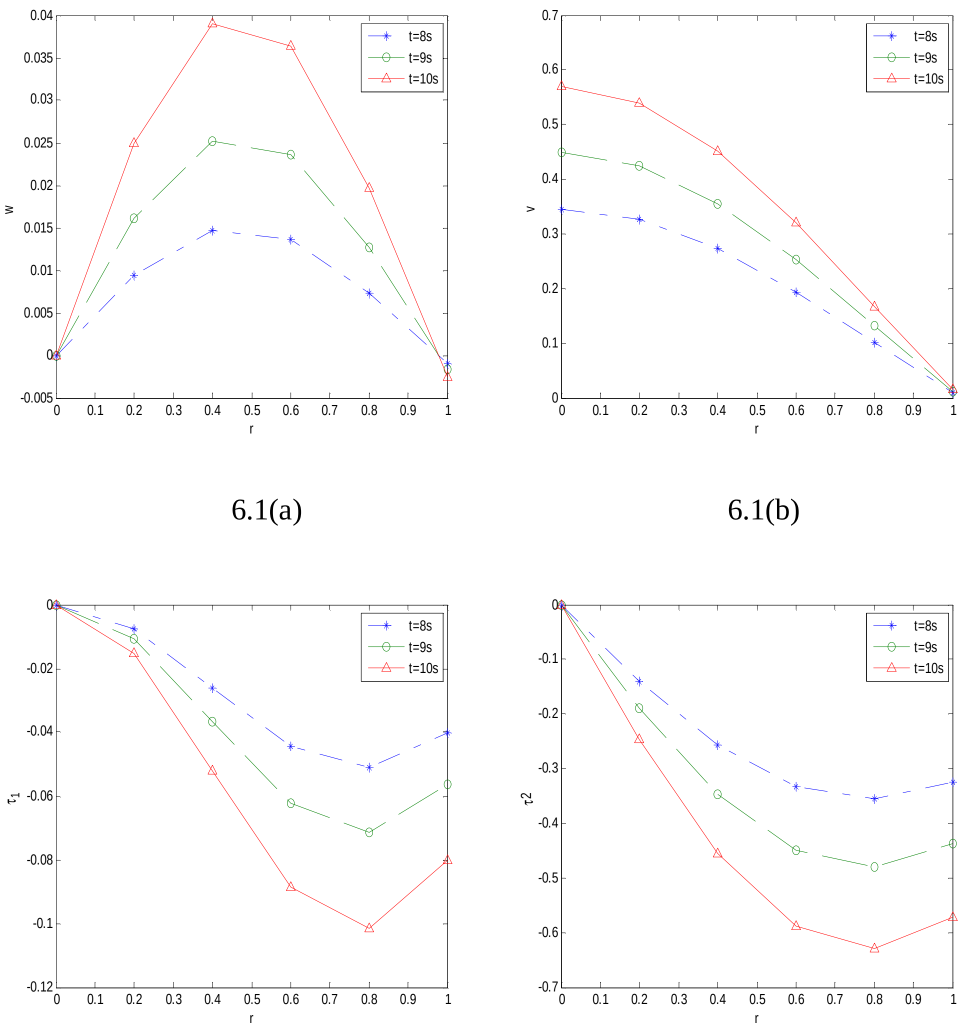

6.1(a) 6.1(b)

6.1(c) 6.1(d)

Fig. 6.1 Profiles of the velocities w(r, t), v(r, t) and shear stresses τ_1(r, t), τ_2(r, t) given by Eqs. (6.3.17), (6.3.18), (6.3.23) and (6.3.24) for $R=1$, $\omega=1$, U = 1, a = 1, $\upsilon=0.0016$, $\mu=1.01$, $\lambda=10$, $\lambda_r=5$, $\alpha=0.9$, $\beta=0.6$ and different values of t.

Figure 6.2

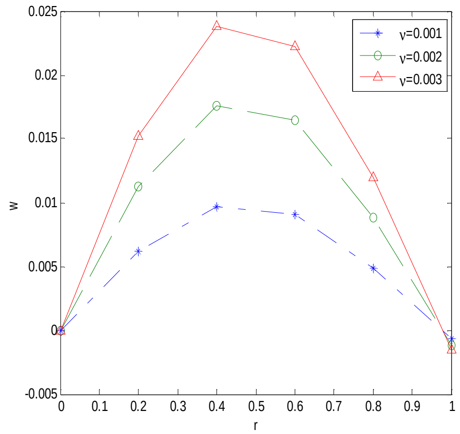

6.2(a)

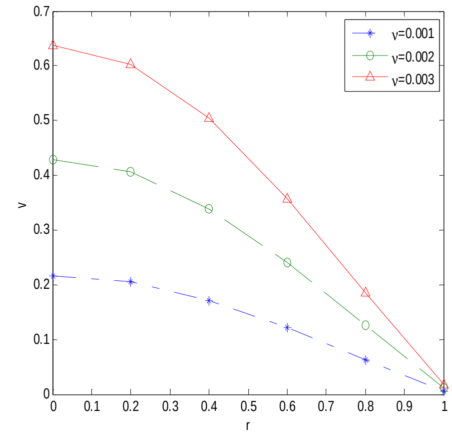

6.2(b)

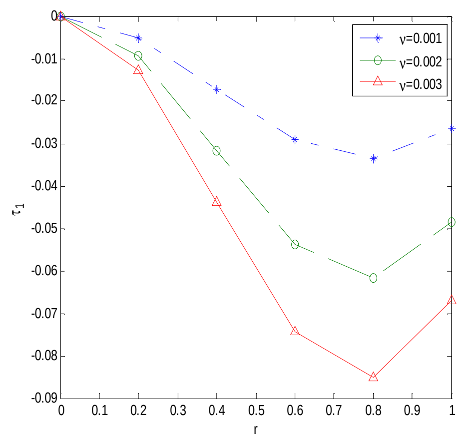

6.2(c)

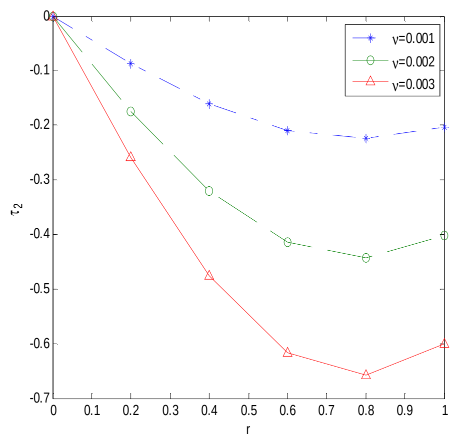

6.2(d)

Fig.6.2 Profiles of the velocities $w(r,t)$, $v(r,t)$ and shear stresses $\tau_1(r,t)$, $\tau_2(r,t)$ given by Eqs.(6.3.17), (6.3.18), (6.3.23) and (6.3.24) for $R=1, \omega=1, U=1, a=1, t=8, \mu=1.01, \lambda=10, \lambda_r=5, \alpha=0.9, \beta=0.6$ and different values of υ.

Figure 6.3

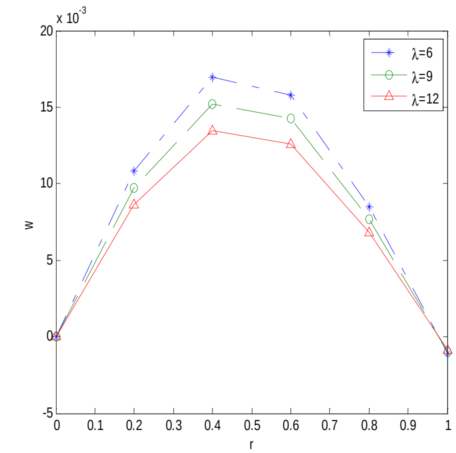

6.3(a)

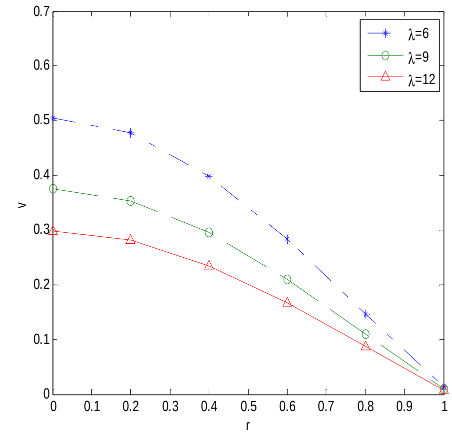

6.3(b)

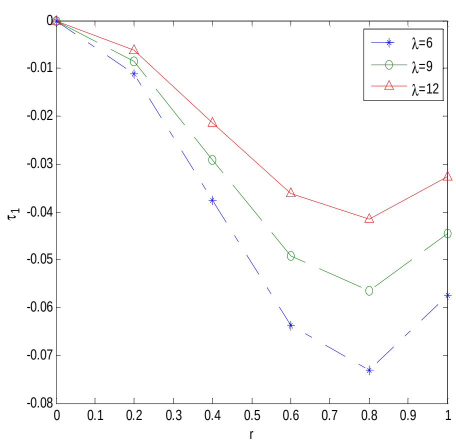

6.3(c)

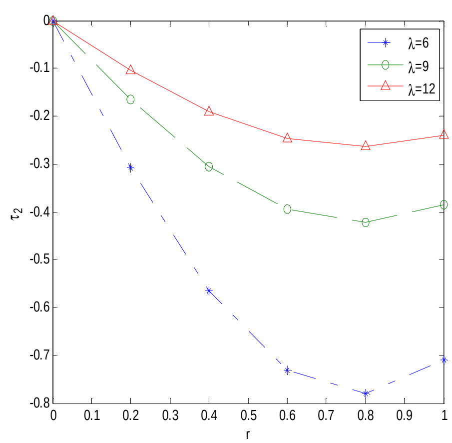

6.3(d)

Fig. 6.3 Profiles of the velocities $w(r,t)$, $v(r,t)$ and shear stresses $\tau_1(r,t)$, $\tau_2(r,t)$ given by Eqs. (6.3.17), (6.3.18), (6.3.23) and (6.3.24) for $R=1$, $\omega=1$, $U=1$, $a=1$, $t=8$, $\upsilon=0.0016$, $\mu=1.01$, $\lambda_r=5$, $\alpha=0.9$, $\beta=0.6$ and different values of λ.

Figure 6.4

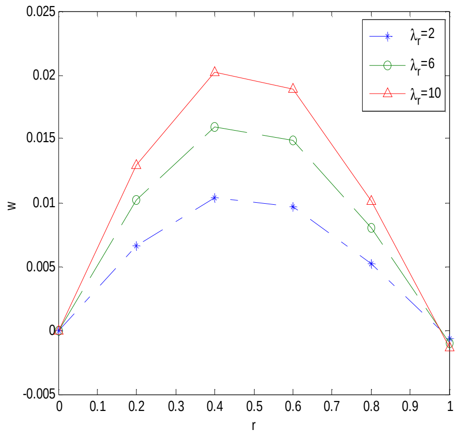

6.4(a)

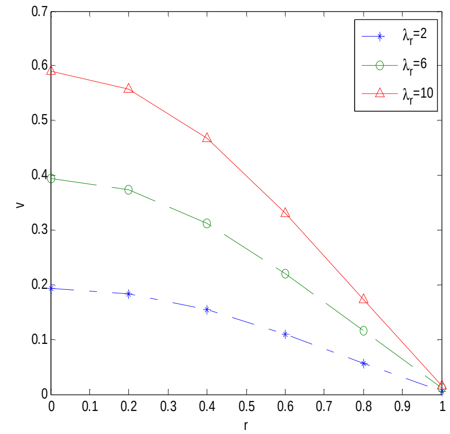

6.4(b)

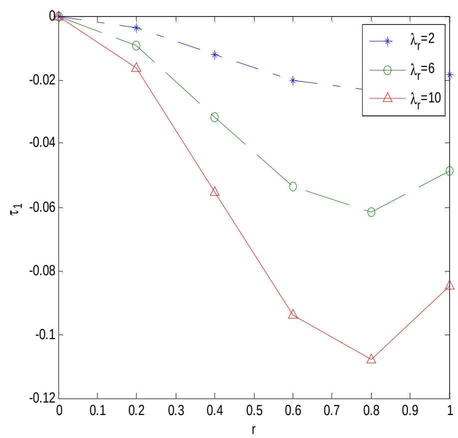

6.4(c)

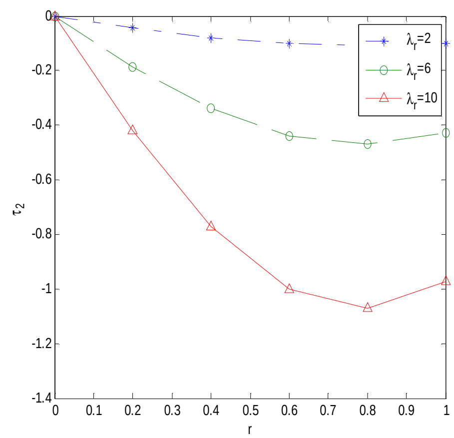

6.4(d)

Fig. 6.4 Profiles of the velocities $w(r,t)$, $v(r,t)$ and shear stresses $\tau_1(r,t)$, $\tau_2(r,t)$ given by Eqs. (6.3.17), (6.3.18), (6.3.23) and (6.3.24) for $R=1$, $\omega=1$, $U=1$, $a=1$, $t=8$, $\upsilon=0.0016$, $\mu=1.01$, $\lambda=10$, $\alpha=0.9$, $\beta=0.6$ and different values of λ_r.

Figure 6.5

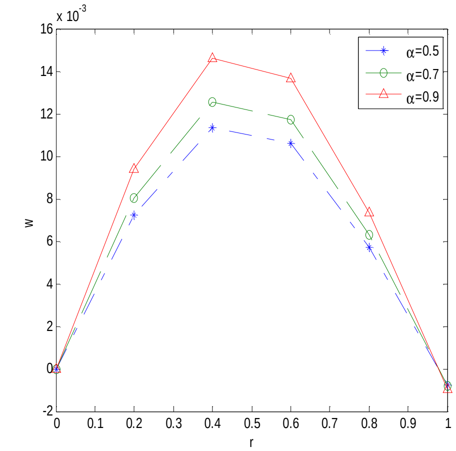

6.5(a)

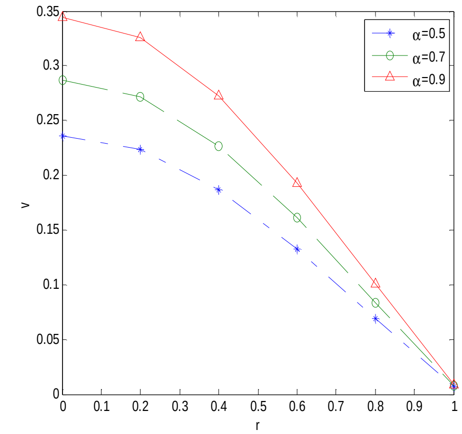

6.5(b)

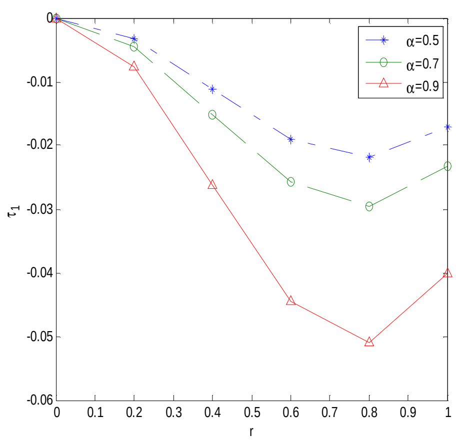

6.5(c)

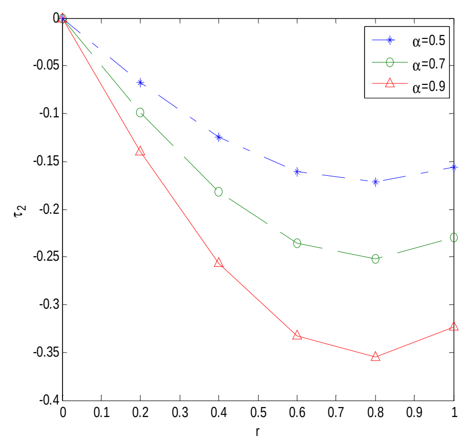

6.5(d)

Fig.6.5 Profiles of the velocities $w(r,t)$, $v(r,t)$ and shear stresses $\tau_1(r,t)$, $\tau_2(r,t)$ given by Eqs.(6.3.17),(6.3.18),(6.3.23)and (6.3.24) for $R=1, \omega=1$, $U=1$, $a=1$, $t=8$, $\upsilon=0.0016$, $\mu=1.01$, $\lambda=10, \lambda_r=5$, $\beta=0.6$ and different values of α.

Figure 6.6

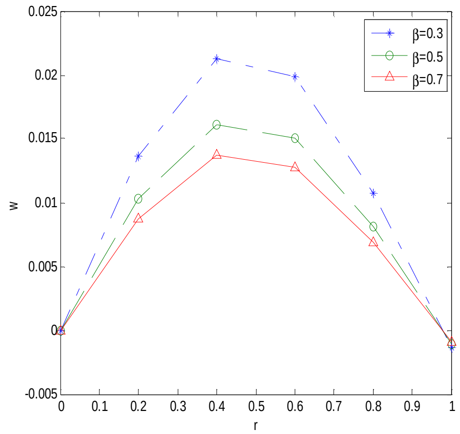

6.6(a)

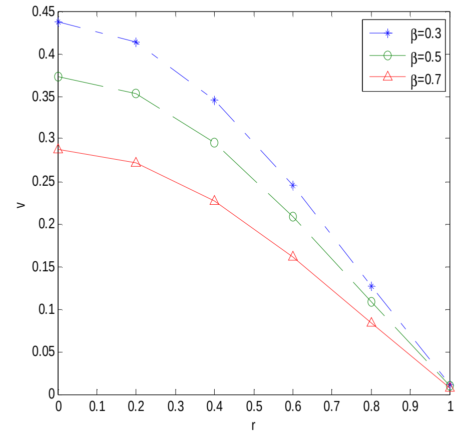

6.6(b)

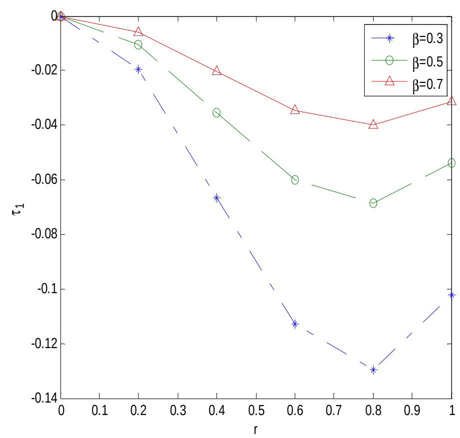

6.6(c)

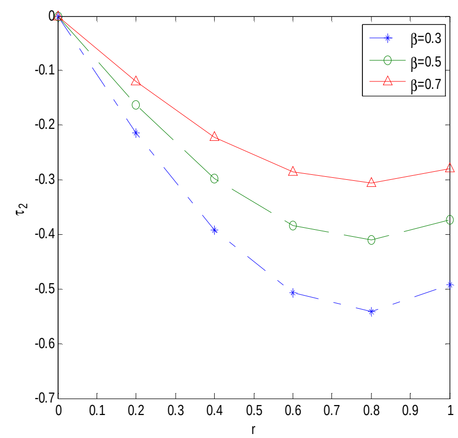

6.6(d)

Fig.6.6 Profiles of the velocities $w(r,t)$, $v(r,t)$ and shear stresses $\tau_1(r,t)$, $\tau_2(r,t)$ given by Eqs.(6.3.17),(6.3.18), (6.3.23) and (6.3.24) for $R=1$, $\omega=1$, $U=1$, $a=1$, $t=8$, $\upsilon=0.0016$, $\mu=1.01$, $\lambda=10$, $\lambda_r=5$, $\alpha=0.9$ and different values of β.

Figure 6.7

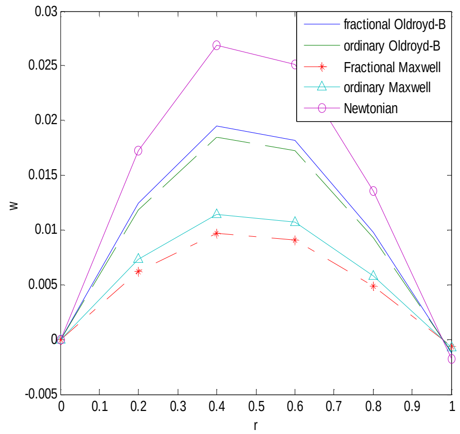

6.7(a)

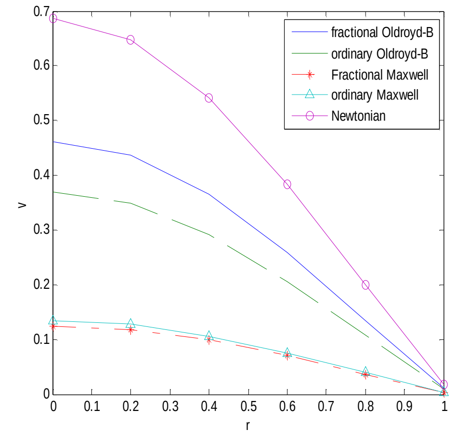

6.7(b)

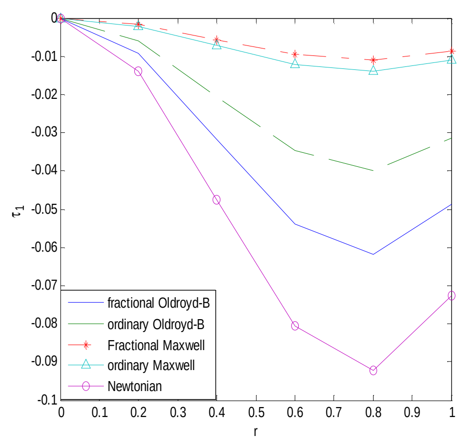

6.7(c)

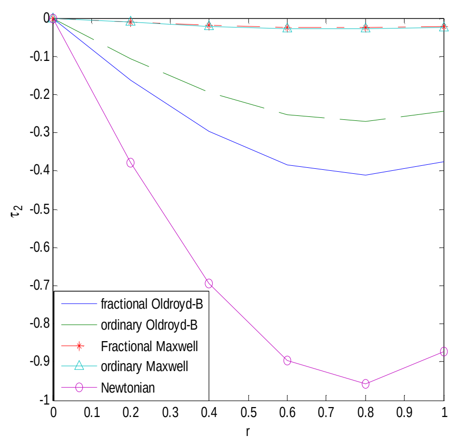

6.7(d)

Fig. 6.7 Profiles of the velocities $w(r,t)$, $v(r,t)$ and shear stresses $\tau_1(r,t)$, $\tau_2(r,t)$ corresponding to the fractional Oldroyd - B, ordinary Oldroyd - B, fractional Maxwell, ordinary Maxwell and Newtonian fluids, for $R=1$, $\omega=1$, $U=1$, $a=1$, $t=8$, $\upsilon=0.0025$, $\mu=1.02$, $\lambda=12$, $\lambda_r=5$, $\alpha=0.9$ and $\beta=0.6$.

Chapter 7. Exact solutions for fractional Oldroyd-B fluid filled between moving outer and rotating inner coaxial circular cylinders

The paper submitted on the work described in this chapter:

1. Khandelwal K. and Mathur V., Exact solutions for fractional Oldroyd-B fluid filled between moving outer and rotating inner coaxial circular cylinders, Arnold Mathematical Journal (communicated).

7.1 Introduction

The constitutive equations of an incompressible Oldroyd-B fluid, as it is given by Eq. (6.2.1), are

$$T = -pI + S, \quad S + \lambda(\dot{S} - LS - SL^T) = \mu[A + \lambda_r(\dot{A} - LA - AL^T)], \tag{7.1.1}$$

where T, $-pI$, S, λ, λ_r, A, L, μ, the superscript T and $\dot{S}$ have the same significance as before.

The intent of this chapter is to propose the exact solution for the velocity field and shear stress of rotational flow for fractional Oldroyd-B fluid filled between two coaxial circular cylinders. At time t=0^+, the inner cylinder begins to rotate about its axis with a time dependent shear stress while outer cylinder is moving at a constant velocity. We use Hankel and Laplace transforms to reach the exact solution. The obtained solutions are presented in terms of generalized G functions and satisfy all the initial and boundary conditions. The solution of ordinary Oldroyd-B fluid, fractional Maxwell fluid, ordinary Maxwell fluid and Newtonian fluid are obtained by limiting cases of $\gamma, \beta \to 1$; $\lambda_r \to 0$; $\lambda_r \to 0$, $\gamma \to 1$ and $\lambda \to 0$ respectively. The expression for the velocity field and shear stress are in the most simplified form and are free from convolution product.

7.2 Governing equations

Consider an incompressible fractional Oldroyd-B fluid that has a velocity v and extra stress S as given by

$$v = v(r,t) = w(r,t)e_\theta, \qquad S = S(r,t), \tag{7.2.1}$$

where e_θ is the unit vector in the θ direction of the cylindrical coordinates.

At time t=0, the fluid is at rest in an annular region between two infinite coaxial circular cylinders. At time t=0^+, the inner cylinder begins to rotate about its axis with a time dependent shear stress and the outer cylinder moving at a constant velocity. For these flows, the constraint of incompressibility is automatically satisfied. Initially the fluid is at rest, hence

$$V(\mathrm{r},0)=0, \qquad S(r,0)=0. \tag{7.2.2}$$

The governing equations corresponding to an incompressible fractional Oldroyd-B fluid are [22]

$$\left(1+\lambda D_t^{\gamma}\right)\frac{\partial w(r,t)}{\partial t}=\upsilon\left(1+\lambda_r D_t^{\beta}\right)\left(\frac{\partial^2}{\partial r^2}+\frac{1}{r}\frac{\partial}{\partial r}-\frac{1}{r^2}\right)w(r,t); \tag{7.2.3}$$

$$\left(1+\lambda D_t^{\gamma}\right)\tau(r,t)=\mu\left(1+\lambda_r D_t^{\beta}\right)\left(\frac{\partial}{\partial r}-\frac{1}{r}\right)w(r,t). \tag{7.2.4}$$

where $\tau(r,t)=S_{r\theta}(r,t)$ is the non-trivial shear stress, λ and λ_r are relaxation and retardation times respectively, $\upsilon=\dfrac{\mu}{\rho}$ is the kinematic viscosity, ρ is the constant density of the fluid and D_t^{β} is the Caputo fractional derivative of order β as defined by [64]

$$D_t^{\beta} f(t)=\begin{cases}\dfrac{1}{\Gamma(1-\beta)}\dfrac{d}{dt}\displaystyle\int_0^t \frac{f(\tau)}{(t-\tau)^{\beta}}d\tau, & 0<\beta<1;\\[2ex] \dfrac{d}{dt}f(t), & \beta=1,\end{cases} \tag{7.2.5}$$

where $\Gamma(.)$ is the Gamma function.

7.3 Flow through the annular region between moving outer and rotating inner cylinders

Let us consider an incompressible fractional Oldroyd-B fluid at rest in infinite coaxial circular cylinders. At time $t=0^+$, the inner cylinder begins to rotate about its axis with a time dependent shear stress and outer cylinder moving at a constant velocity. Also, consider that radius of inner and outer cylinders are R_1 and $R_2(>R_1)$ respectively. At time $t=0^+$, a time dependent shear stress [22]

$$\tau(R_1,t)=\frac{f_1}{\lambda}R_{\gamma,-1}\left(-\frac{1}{\lambda},t\right); \qquad 0\le\gamma<1, \tag{7.3.1}$$

is applied at the boundary of the inner cylinder, where f_1 is a constant and generalized function R is define by [117]

$$R_{a,b}(d,t) = L^{-1}\left\{\frac{q^b}{q^a - d}\right\} = \sum_{n=0}^{\infty}\frac{d^n t^{(n+1)a-b-1}}{\Gamma[(n+1)a-b]};$$
$$\mathrm{Re}(a-b) > 0, \quad \mathrm{Re}(q) > 0, \quad \left|\frac{\mathrm{d}}{\mathrm{q}^{\mathrm{a}}}\right| < 1. \tag{7.3.2}$$

The governing equations are given by Eqs. (7.2.3) and (7.2.4), while appropriate initial and boundary conditions are

$$w(r,0) = 0, \quad \tau(\mathrm{r},0) = 0, \tag{7.3.3}$$

and

$$\left(1+\lambda D_t^{\gamma}\right)\tau(r,t)\Big|_{r=R_1} = \mu\left(1+\lambda_r D_t^{\beta}\right)\left(\frac{\partial}{\partial r} - \frac{1}{r}\right)w(r,t)\Big|_{r=R_1} = f_1,$$
$$w(R_2,t) = f_2; \quad t > 0, \tag{7.3.4}$$

where f_2 is the constant velocity of outer cylinder. Eq. (7.3.1) is the solution of first equation of (7.3.4). To solve this problem we use Laplace and Hankel transforms.

7.3.1 Calculation of the velocity field

By applying Laplace transform to Eq. (7.2.3) and using the initial conditions as given in Eq. (7.3.3), we obtain

$$\left(q+\lambda q^{\gamma+1}\right)\overline{w}(r,q) = \upsilon\left(1+\lambda_r q^{\beta}\right)\left(\frac{\partial^2}{\partial r^2} + \frac{1}{r}\frac{\partial}{\partial r} - \frac{1}{r^2}\right)\overline{w}(r,q). \tag{7.3.5}$$

Applying Laplace transform to Eq. (7.3.4), we obtain

$$\left(\frac{\partial}{\partial r} - \frac{1}{r}\right)\overline{w}(r,q)\Big|_{r=R_1} = \frac{f_1}{\mu q(1+\lambda_r q^{\beta})};$$
$$\overline{w}(R_2,q) = \frac{f_2}{q}. \tag{7.3.6}$$

The Hankel transform method with respect to r is used and defined as follows [17]

$$\overline{w}_H(r_n,q)=\int_{R_1}^{R_2} r\,\overline{w}(r,q)B(r,r_n)dr, \tag{7.3.7}$$

where

$$B(r,r_n)=J_1(rr_n)Y_2(R_1r_n)-J_2(R_1r_n)Y_1(rr_n), \tag{7.3.8}$$

r_n being the positive roots of the transcendental equation $B(R_2,r)=0$. The inverse Hankel transform, as defined by [17], is given by

$$\overline{w}(r,q)=\frac{\pi^2}{2}\sum_{n=1}^{\infty}\frac{r_n^2J_1^2(R_2r_n)B(r,r_n)}{J_2^2(R_1r_n)-J_1^2(R_2r_n)}\overline{w}_H(r_n,q). \tag{7.3.9}$$

Multiplying both sides of Eq. (7.3.5) by $rB(r, r_n)$ and integrating with respect to r from R_1 to R_2, Taking into account the Eq. (7.3.6) and the equality

$$\int_{R_1}^{R_2} r\left(\frac{\partial^2}{\partial r^2}+\frac{1}{r}\frac{\partial}{\partial r}-\frac{1}{r^2}\right)\overline{w}(r,q)B(r,r_n)dr$$

$$=-r_n^2\overline{w}_H(r_n,q)+\frac{2}{\pi r_n}\left(\frac{\partial}{\partial r}-\frac{1}{r}\right)\overline{w}(r,q)\Big|_{r=R_1}+R_2r_n\overline{w}(R_2,q)[Y_2(R_1r_n)J_2(R_2r_n)-J_2(R_1r_n)Y_2(R_2r_n)]$$

$$=-r_n^2\overline{w}_H(r_n,q)+\frac{2}{\pi r_n}\frac{f_1}{\mu q(1+\lambda_r q^{\beta})}+\frac{R_2r_nf_2}{q}[Y_2(R_1r_n)J_2(R_2r_n)-J_2(R_1r_n)Y_2(R_2r_n)], \tag{7.3.10}$$

we obtain

$$\overline{w}_H(r_n,q)$$
$$=\frac{2f_1\upsilon}{\pi\mu r_n}\frac{1}{q(q+\lambda q^{\gamma+1}+\upsilon r_n^2+\upsilon\lambda_r r_n^2q^{\beta})}$$
$$+\upsilon R_2r_nf_2[Y_2(R_1r_n)J_2(R_2r_n)-J_2(R_1r_n)Y_2(R_2r_n)]\frac{(1+\lambda_r q^{\beta})}{q(q+\lambda q^{\gamma+1}+\upsilon r_n^2+\upsilon\lambda_r r_n^2q^{\beta})}. \tag{7.3.11}$$

Rewriting Eq. (7.3.11) into a suitable equivalent form, we obtain below

$$\overline{w}_H(r_n, q)$$
$$= \frac{2f_1}{\pi\mu r_n^3}\frac{1}{q} - \frac{2f_1(1+\lambda q^{\gamma} + \upsilon\lambda_r r_n^2 q^{\beta-1})}{\pi\mu r_n^3(q+\lambda q^{\gamma+1} + \upsilon r_n^2 + \upsilon\lambda_r r_n^2 q^{\beta})}$$
$$+\upsilon R_2 r_n f_2[Y_2(R_1 r_n)J_2(R_2 r_n) - J_2(R_1 r_n)Y_2(R_2 r_n)]\frac{(1+\lambda_r q^{\beta})}{q(q+\lambda q^{\gamma+1} + \upsilon r_n^2 + \upsilon\lambda_r r_n^2 q^{\beta})}. \tag{7.3.12}$$

Applying inverse Hankel transform to Eq. (7.3.12) and taking into account the following result

$$\int_{R_1}^{R_2}\left(r^2 - R_2^2\right)B(r, r_n)dr = \frac{4}{\pi r_n^3}\left(\frac{R_2}{R_1}\right)^2, \tag{7.3.13}$$

we obtain

$$\overline{w}(r, q)$$
$$= \frac{f_1}{2\mu}\left(\frac{R_1}{R_2}\right)^2\left(r - \frac{R_2^2}{r}\right)\frac{1}{q} - \frac{\pi f_1}{\mu}\sum_{n=1}^{\infty}\frac{J_1^2(R_2 r_n)B(r, r_n)}{r_n[J_2^2(R_1 r_n) - J_1^2(R_2 r_n)]}\frac{(1+\lambda q^{\gamma} + \upsilon\lambda_r r_n^2 q^{\beta-1})}{(q+\lambda q^{\gamma+1} + \upsilon r_n^2 + \upsilon\lambda_r r_n^2 q^{\beta})}$$
$$+\frac{\pi^2}{2}\upsilon R_2 f_2\sum_{n=1}^{\infty}\frac{r_n^3 J_1^2(R_2 r_n)B(r, r_n)}{[J_2^2(R_1 r_n) - J_1^2(R_2 r_n)]}[Y_2(R_1 r_n)J_2(R_2 r_n) - J_2(R_1 r_n)Y_2(R_2 r_n)]$$
$$\times\frac{(1+\lambda_r q^{\beta})}{q(q+\lambda q^{\gamma+1} + \upsilon r_n^2 + \upsilon\lambda_r r_n^2 q^{\beta})}. \tag{7.3.14}$$

Taking into account the following result

$$\frac{1}{q+\lambda q^{\gamma+1} + \upsilon r_n^2 + \upsilon\lambda_r r_n^2 q^{\beta}} = \frac{1}{\lambda}\sum_{m=0}^{\infty}\sum_{k=0}^{m}\frac{m!}{k!(m-k)!}\left(\frac{-\upsilon r_n^2}{\lambda}\right)^m \lambda_r^{\,k}\frac{q^{\beta k-m-1}}{(q^{\gamma} + \lambda^{-1})^{m+1}}, \tag{7.3.15}$$

we find Eq. (7.3.14) as

$$\bar{w}(r,q)$$

$$= \frac{f_1}{2\mu}\left(\frac{R_1}{R_2}\right)^2\left(r - \frac{R_2^2}{r}\right)\frac{1}{q} - \frac{\pi f_1}{\mu\lambda}\sum_{n=1}^{\infty}\frac{J_1^2(R_2 r_n)B(r,r_n)}{r_n[J_2^2(R_1 r_n) - J_1^2(R_2 r_n)]}\sum_{m=0}^{\infty}\sum_{k=0}^{m}\left(\frac{-\upsilon r_n^2}{\lambda}\right)^m \frac{m!}{k!(m-k)!}\lambda_r^k$$

$$\times\frac{(\mathrm{q}^{\beta\mathrm{k-m-1}} + \lambda\mathrm{q}^{\gamma+\beta\mathrm{k-m-1}} + \upsilon\lambda_r r_n^2 \mathrm{q}^{\beta(\mathrm{k+1})\mathrm{-m-2}})}{(\mathrm{q}^{\gamma} + \lambda^{-1})^{\mathrm{m+1}}}$$

$$+\frac{\pi^2}{2}\frac{\upsilon R_2 f_2}{\lambda}\sum_{n=1}^{\infty}\frac{r_n^3 J_1^2(R_2 r_n)B(r,r_n)}{[J_2^2(R_1 r_n) - J_1^2(R_2 r_n)]}[Y_2(R_1 r_n)J_2(R_2 r_n) - J_2(R_1 r_n)Y_2(R_2 r_n)]$$

$$\times\sum_{m=0}^{\infty}\sum_{k=0}^{m}\left(\frac{-\upsilon r_n^2}{\lambda}\right)^m \frac{m!}{k!(m-k)!}\lambda_r^k\frac{(\mathrm{q}^{\beta\mathrm{k-m-2}} + \lambda_r \mathrm{q}^{\beta(\mathrm{k+1})\mathrm{-m-2}})}{(\mathrm{q}^{\gamma} + \lambda^{-1})^{\mathrm{m+1}}}. \qquad (7.3.16)$$

Applying Inverse-Laplace transform of Eq. (7.3.16) and taking into account the following result [117]

$$G_{a,b,c}(d,t) = L^{-1}\left\{\frac{q^b}{(q^a - d)^c}\right\}$$

$$= \sum_{\mathrm{j=0}}^{\infty}\frac{\mathrm{d}^{\mathrm{j}}\Gamma(c+j)}{\Gamma(c)\Gamma(j+1)}\frac{t^{(c+j)a-b-1}}{\Gamma[(c+j)a-b]};$$

$$\mathrm{Re}(ac-b) > 0,\ \left|\frac{\mathrm{d}}{\mathrm{q}^{\mathrm{a}}}\right| < 1, \qquad (7.3.17)$$

we obtain

$$w(r,t)$$

$$= \frac{f_1}{2\mu}\left(\frac{R_1}{R_2}\right)^2\left(r - \frac{R_2^2}{r}\right) - \frac{\pi f_1}{\mu\lambda}\sum_{n=1}^{\infty}\frac{J_1^2(R_2 r_n)B(r,r_n)}{r_n[J_2^2(R_1 r_n) - J_1^2(R_2 r_n)]}\sum_{m=0}^{\infty}\sum_{k=0}^{m}\left(\frac{-\upsilon r_n^2}{\lambda}\right)^m \frac{m!}{k!(m-k)!}\lambda_r^k$$

$$\times\left[G_{\gamma,\beta k-m-1,m+1}(-\lambda^{-1},t) + \lambda G_{\gamma,\gamma+\beta k-m-1,m+1}(-\lambda^{-1},t) + \upsilon\lambda_r r_n^2 G_{\gamma,\beta(k+1)-m-2,m+1}(-\lambda^{-1},t)\right]$$

$$+\frac{\pi^2}{2}\frac{\upsilon R_2 f_2}{\lambda}\sum_{n=1}^{\infty}\frac{r_n^3 J_1^2(R_2 r_n)B(r,r_n)}{[J_2^2(R_1 r_n) - J_1^2(R_2 r_n)]}[Y_2(R_1 r_n)J_2(R_2 r_n) - J_2(R_1 r_n)Y_2(R_2 r_n)]$$

$$\times\sum_{m=0}^{\infty}\sum_{k=0}^{m}\left(\frac{-\upsilon r_n^2}{\lambda}\right)^m \frac{m!}{k!(m-k)!}\lambda_r^k\left[G_{\gamma,\beta k-m-2,m+1}(-\lambda^{-1},t) + \lambda_r G_{\gamma,\beta(k+1)-m-2,m+1}(-\lambda^{-1},t)\right].$$

(7.3.18)

7.3.2 Calculation of the shear stress

Applying Laplace transform to Eq. (7.2.4), we obtain

$$\bar{\tau}(r,q) = \mu \frac{(1+\lambda_r q^{\beta})}{(1+\lambda q^{\gamma})} \left(\frac{\partial}{\partial r} - \frac{1}{r} \right) \bar{w}(r,q). \tag{7.3.19}$$

Now, we rewrite Eq. (7.3.11) in a more suitable equivalent form for the shear stress $\tau(r,t)$

$$\begin{aligned} &\bar{w}_H(r_n, q) \\ &= \frac{2 f_1}{\pi \mu r_n^3 (1+\lambda_r q^{\beta})} \frac{1}{q} - \frac{2 f_1 (1+\lambda q^{\gamma})}{\pi \mu r_n^3 (1+\lambda_r q^{\beta})(q + \lambda q^{\gamma+1} + \upsilon r_n^2 + \upsilon \lambda_r r_n^2 q^{\beta})} \\ &\quad + \upsilon R_2 r_n f_2 [Y_2(R_1 r_n) J_2(R_2 r_n) - J_2(R_1 r_n) Y_2(R_2 r_n)] \frac{(1+\lambda_r q^{\beta})}{q(q + \lambda q^{\gamma+1} + \upsilon r_n^2 + \upsilon \lambda_r r_n^2 q^{\beta})}. \end{aligned} \tag{7.3.20}$$

Applying inverse Hankel transform to Eq. (7.3.20), we obtain

$$\begin{aligned} &\bar{w}(r,q) \\ &= \frac{f_1}{2} \left(\frac{R_1}{R_2} \right)^2 \left(r - \frac{R_2^2}{r} \right) \frac{1}{\mu (1+\lambda_r q^{\beta})} \frac{1}{q} - \pi f_1 \sum_{n=1}^{\infty} \frac{J_1^2(R_2 r_n) B(r, r_n)}{r_n [J_2^2(R_1 r_n) - J_1^2(R_2 r_n)]} \\ &\quad \times \frac{(1+\lambda q^{\gamma})}{\mu (1+\lambda_r q^{\beta})(q + \lambda q^{\gamma+1} + \upsilon r_n^2 + \upsilon \lambda_r r_n^2 q^{\beta})} \\ &\quad + \frac{\pi^2}{2} \sum_{n=1}^{\infty} \frac{r_n^3 J_1^2(R_2 r_n) B(r, r_n)}{[J_2^2(R_1 r_n) - J_1^2(R_2 r_n)]} \upsilon R_2 f_2 [Y_2(R_1 r_n) J_2(R_2 r_n) - J_2(R_1 r_n) Y_2(R_2 r_n)] \\ &\quad \times \frac{(1+\lambda_r q^{\beta})}{q(q + \lambda q^{\gamma+1} + \upsilon r_n^2 + \upsilon \lambda_r r_n^2 q^{\beta})}, \end{aligned} \tag{7.3.21}$$

where

$$
\begin{aligned}
&\left(\frac{\partial}{\partial r}-\frac{1}{r}\right)\overline{w}(r,q)\\
&= f_1\left(\frac{R_1}{r}\right)^2\frac{1}{\mu(1+\lambda_r q^{\beta})}\frac{1}{q}+\pi f_1\sum_{n=1}^{\infty}\frac{J_1^2(R_2r_n)\overline{B}(r,r_n)}{[J_2^2(R_1r_n)-J_1^2(R_2r_n)]}\\
&\quad\times\frac{(1+\lambda q^{\gamma})}{\mu(1+\lambda_r q^{\beta})(q+\lambda q^{\gamma+1}+\upsilon r_n^2+\upsilon\lambda_r r_n^2 q^{\beta})}\\
&\quad-\frac{\pi^2}{2}\upsilon R_2 f_2\sum_{n=1}^{\infty}\frac{r_n^4 J_1^2(R_2r_n)\overline{B}(r,r_n)}{[J_2^2(R_1r_n)-J_1^2(R_2r_n)]}[Y_2(R_1r_n)J_2(R_2r_n)-J_2(R_1r_n)Y_2(R_2r_n)]\\
&\quad\times\frac{(1+\lambda_r q^{\beta})}{q(q+\lambda q^{\gamma+1}+\upsilon r_n^2+\upsilon\lambda_r r_n^2 q^{\beta})}. \qquad (7.3.22)
\end{aligned}
$$

Substitute Eq. (7.3.22) into Eq. (7.3.19), we obtain

$$
\begin{aligned}
\overline{\tau}(r,q)&= f_1\left(\frac{R_1}{r}\right)^2\frac{1}{q(1+\lambda q^{\gamma})}+\pi f_1\sum_{n=1}^{\infty}\frac{J_1^2(R_2r_n)\overline{B}(r,r_n)}{[J_2^2(R_1r_n)-J_1^2(R_2r_n)]}\frac{1}{(q+\lambda q^{\gamma+1}+\upsilon r_n^2+\upsilon\lambda_r r_n^2 q^{\beta})}\\
&-\frac{\pi^2}{2}\mu R_2 f_2\sum_{n=1}^{\infty}\frac{r_n^2 J_1^2(R_2r_n)\overline{B}(r,r_n)}{[J_2^2(R_1r_n)-J_1^2(R_2r_n)]}[Y_2(R_1r_n)J_2(R_2r_n)-J_2(R_1r_n)Y_2(R_2r_n)]\\
&\times(1+\lambda_r q^{\beta})\left[\frac{1}{q(1+\lambda q^{\gamma})}-\frac{1}{(q+\lambda q^{\gamma+1}+\upsilon r_n^2+\upsilon\lambda_r r_n^2 q^{\beta})}\right], \qquad (7.3.23)
\end{aligned}
$$

where

$$
\overline{B}(r,r_n)=J_2(rr_n)Y_2(R_1r_n)-J_2(R_1r_n)Y_2(rr_n). \qquad (7.3.24)
$$

Substitute Eq. (7.3.15) into Eq. (7.3.23), we obtain

$$
\begin{aligned}
\overline{\tau}(r,q)&= f_1\left(\frac{R_1}{r}\right)^2\frac{1}{q(1+\lambda q^{\gamma})}+\frac{\pi f_1}{\lambda}\sum_{n=1}^{\infty}\frac{J_1^2(R_2r_n)\overline{B}(r,r_n)}{[J_2^2(R_1r_n)-J_1^2(R_2r_n)]}\sum_{m=0}^{\infty}\sum_{k=0}^{m}\left(\frac{-\upsilon r_n^2}{\lambda}\right)^m\frac{m!}{k!(m-k)!}\lambda_r^k\frac{q^{\beta k-m-1}}{(q^{\gamma}+\lambda^{-1})^{m+1}}\\
&-\frac{\pi^2}{2}\mu R_2 f_2\sum_{n=1}^{\infty}\frac{r_n^2 J_1^2(R_2r_n)\overline{B}(r,r_n)}{[J_2^2(R_1r_n)-J_1^2(R_2r_n)]}[Y_2(R_1r_n)J_2(R_2r_n)-J_2(R_1r_n)Y_2(R_2r_n)]\\
&\times\left[\frac{1}{q(1+\lambda q^{\gamma})}+\lambda_r\frac{1}{q^{1-\beta}(1+\lambda q^{\gamma})}-\frac{1}{\lambda}\sum_{m=0}^{\infty}\sum_{k=0}^{m}\left(\frac{-\upsilon r_n^2}{\lambda}\right)^m\frac{m!}{k!(m-k)!}\lambda_r^k\frac{q^{\beta k-m-1}}{(q^{\gamma}+\lambda^{-1})^{m+1}}\right.\\
&\left.-\frac{\lambda_r}{\lambda}\sum_{m=0}^{\infty}\sum_{k=0}^{m}\left(\frac{-\upsilon r_n^2}{\lambda}\right)^m\frac{m!}{k!(m-k)!}\lambda_r^k\frac{q^{\beta(k+1)-m-1}}{(q^{\gamma}+\lambda^{-1})^{m+1}}\right]. \qquad (7.3.25)
\end{aligned}
$$

Applying inverse Laplace transform to Eq. (7.3.25) and using Eq. (7.3.17), we obtain

$$\tau(r,t)=f_1\left(\frac{R_1}{r}\right)^2\frac{1}{\lambda}R_{\gamma,-1}(-\lambda^{-1},t)$$
$$+\frac{\pi f_1}{\lambda}\sum_{n=1}^{\infty}\frac{J_1^2(R_2r_n)\overline{B}(r,r_n)}{[J_2^2(R_1r_n)-J_1^2(R_2r_n)]}\sum_{m=0}^{\infty}\sum_{k=0}^{m}\left(\frac{-\upsilon r_n^2}{\lambda}\right)^m\frac{m!}{k!(m-k)!}\lambda_r^kG_{\gamma,\beta k-m-1,m+1}(-\lambda^{-1},t)$$
$$-\frac{\pi^2}{2}\mu R_2f_2\sum_{n=1}^{\infty}\frac{r_n^2J_1^2(R_2r_n)\overline{B}(r,r_n)}{[J_2^2(R_1r_n)-J_1^2(R_2r_n)]}[Y_2(R_1r_n)J_2(R_2r_n)-J_2(R_1r_n)Y_2(R_2r_n)]$$
$$\times\left[\frac{1}{\lambda}R_{\gamma,-1}(-\lambda^{-1},t)+\frac{\lambda_r}{\lambda}R_{\gamma,\beta-1}(-\lambda^{-1},t)-\frac{1}{\lambda}\sum_{m=0}^{\infty}\sum_{k=0}^{m}\left(\frac{-\upsilon r_n^2}{\lambda}\right)^m\frac{m!}{k!(m-k)!}\lambda_r^kG_{\gamma,\beta k-m-1,m+1}(-\lambda^{-1},t)\right.$$
$$\left.-\frac{\lambda_r}{\lambda}\sum_{m=0}^{\infty}\sum_{k=0}^{m}\left(\frac{-\upsilon r_n^2}{\lambda}\right)^m\frac{m!}{k!(m-k)!}\lambda_r^kG_{\gamma,\beta(k+1)-m-1,m+1}(-\lambda^{-1},t)\right].\qquad(7.3.26)$$

7.4 Limiting cases

7.4.1 Ordinary Oldroyd-B fluid

Applying $\gamma\to 1$ and $\beta\to 1$ into Eqs. (7.3.18) and (7.3.26), we obtain the velocity field

$$w_{OB}(r,t)$$
$$=\frac{f_1}{2\mu}\left(\frac{R_1}{R_2}\right)^2\left(r-\frac{R_2^2}{r}\right)-\frac{\pi f_1}{\mu\lambda}\sum_{n=1}^{\infty}\frac{J_1^2(R_2r_n)B(r,r_n)}{r_n[J_2^2(R_1r_n)-J_1^2(R_2r_n)]}\sum_{m=0}^{\infty}\sum_{k=0}^{m}\left(\frac{-\upsilon r_n^2}{\lambda}\right)^m\frac{m!}{k!(m-k)!}\lambda_r^k$$
$$\times\left[\lambda G_{1,k-m,m+1}(-\lambda^{-1},t)+(1+\upsilon\lambda_rr_n^2)G_{1,k-m-1,m+1}(-\lambda^{-1},t)\right]$$
$$+\frac{\pi^2}{2}\frac{\upsilon R_2f_2}{\lambda}\sum_{n=1}^{\infty}\frac{r_n^3J_1^2(R_2r_n)B(r,r_n)}{[J_2^2(R_1r_n)-J_1^2(R_2r_n)]}[Y_2(R_1r_n)J_2(R_2r_n)-J_2(R_1r_n)Y_2(R_2r_n)]$$
$$\times\sum_{m=0}^{\infty}\sum_{k=0}^{m}\left(\frac{-\upsilon r_n^2}{\lambda}\right)^m\frac{m!}{k!(m-k)!}\lambda_r^k\left[G_{1,k-m-2,m+1}(-\lambda^{-1},t)+\lambda_rG_{1,k-m-1,m+1}(-\lambda^{-1},t)\right],\quad(7.4.1)$$

and the tangential stress corresponding to ordinary Oldroyd-B fluid performing the same motion.

$$\tau_{OB}(r,t)=f_1\left(\frac{R_1}{r}\right)^2\left\{1-\exp\left(-\frac{t}{\lambda}\right)\right\}$$
$$+\frac{\pi f_1}{\lambda}\sum_{n=1}^{\infty}\frac{J_1^2(R_2r_n)\overline{B}(r,r_n)}{[J_2^2(R_1r_n)-J_1^2(R_2r_n)]}\sum_{m=0}^{\infty}\sum_{k=0}^{m}\left(\frac{-\upsilon r_n^2}{\lambda}\right)^m\frac{m!}{k!(m-k)!}\lambda_r^k G_{1,k-m-1,m+1}(-\lambda^{-1},t)$$
$$-\frac{\pi^2}{2}\mu R_2 f_2\sum_{n=1}^{\infty}\frac{r_n^2J_1^2(R_2r_n)\overline{B}(r,r_n)}{[J_2^2(R_1r_n)-J_1^2(R_2r_n)]}[Y_2(R_1r_n)J_2(R_2r_n)-J_2(R_1r_n)Y_2(R_2r_n)]$$
$$\times\left[1-\exp\left(-\frac{t}{\lambda}\right)+\frac{\lambda_r}{\lambda}\exp\left(-\frac{t}{\lambda}\right)-\frac{1}{\lambda}\sum_{m=0}^{\infty}\sum_{k=0}^{m}\left(\frac{-\upsilon r_n^2}{\lambda}\right)^m\frac{m!}{k!(m-k)!}\lambda_r^k G_{1,k-m-1,m+1}(-\lambda^{-1},t)\right.$$
$$\left.-\frac{\lambda_r}{\lambda}\sum_{m=0}^{\infty}\sum_{k=0}^{m}\left(\frac{-\upsilon r_n^2}{\lambda}\right)^m\frac{m!}{k!(m-k)!}\lambda_r^k G_{1,k-m,m+1}(-\lambda^{-1},t)\right]. \tag{7.4.2}$$

7.4.2 Fractional Maxwell fluid

Applying $\lambda_r\to 0$ into Eqs. (7.3.18) and (7.3.26), we obtain the velocity field

$$w_{FM}(r,t)$$
$$=\frac{f_1}{2\mu}\left(\frac{R_1}{R_2}\right)^2\left(r-\frac{R_2^2}{r}\right)-\frac{\pi f_1}{\mu\lambda}\sum_{n=1}^{\infty}\frac{J_1^2(R_2r_n)B(r,r_n)}{r_n[J_2^2(R_1r_n)-J_1^2(R_2r_n)]}\sum_{m=0}^{\infty}\left(\frac{-\upsilon r_n^2}{\lambda}\right)^m$$
$$\times\left[G_{\gamma,-m-1,m+1}(-\lambda^{-1},t)+\lambda G_{\gamma,\gamma-m-1,m+1}(-\lambda^{-1},t)\right]$$
$$+\frac{\pi^2}{2}\frac{\upsilon R_2 f_2}{\lambda}\sum_{n=1}^{\infty}\frac{r_n^3J_1^2(R_2r_n)B(r,r_n)}{[J_2^2(R_1r_n)-J_1^2(R_2r_n)]}[Y_2(R_1r_n)J_2(R_2r_n)-J_2(R_1r_n)Y_2(R_2r_n)]$$
$$\times\sum_{m=0}^{\infty}\left(\frac{-\upsilon r_n^2}{\lambda}\right)^m\left[G_{\gamma,-m-2,m+1}(-\lambda^{-1},t)\right], \tag{7.4.3}$$

and the shear stress corresponding to the fractional Maxwell fluid performing the same

$$\tau_{FM}(r,t)=f_1\left(\frac{R_1}{r}\right)^2\frac{1}{\lambda}R_{\gamma,-1}(-\lambda^{-1},t)+\frac{\pi f_1}{\lambda}\sum_{n=1}^{\infty}\frac{J_1^2(R_2r_n)\overline{B}(r,r_n)}{[J_2^2(R_1r_n)-J_1^2(R_2r_n)]}\sum_{m=0}^{\infty}\left(\frac{-\upsilon r_n^2}{\lambda}\right)^m G_{\gamma,-m-1,m+1}(-\lambda^{-1},t)$$
$$-\frac{\pi^2}{2}\mu R_2 f_2\sum_{n=1}^{\infty}\frac{r_n^2J_1^2(R_2r_n)\overline{B}(r,r_n)}{[J_2^2(R_1r_n)-J_1^2(R_2r_n)]}[Y_2(R_1r_n)J_2(R_2r_n)-J_2(R_1r_n)Y_2(R_2r_n)]$$
$$\times\left[\frac{1}{\lambda}R_{\gamma,-1}(-\lambda^{-1},t)-\frac{1}{\lambda}\sum_{m=0}^{\infty}\left(\frac{-\upsilon r_n^2}{\lambda}\right)^m G_{\gamma,-m-1,m+1}(-\lambda^{-1},t)\right]. \qquad (7.4.4)$$

7.4.3 Ordinary Maxwell fluid

Applying $\lambda_r \to 0$ and $\gamma \to 1$ into Eqs. (7.3.18) and (7.3.26), we obtain the velocity field

$$w_M(r,t)$$
$$=\frac{f_1}{2\mu}\left(\frac{R_1}{R_2}\right)^2\left(r-\frac{R_2^2}{r}\right)-\frac{\pi f_1}{\mu}\sum_{n=1}^{\infty}\frac{J_1^2(R_2r_n)B(r,r_n)}{r_n[J_2^2(R_1r_n)-J_1^2(R_2r_n)]}\sum_{m=0}^{\infty}\left(\frac{-\upsilon r_n^2}{\lambda}\right)^m$$
$$\times\left[\lambda^{-1}G_{1,-m-1,m+1}(-\lambda^{-1},t)+G_{1,-m,m+1}(-\lambda^{-1},t)\right]$$
$$+\frac{\pi^2}{2}\frac{\upsilon R_2 f_2}{\lambda}\sum_{n=1}^{\infty}\frac{r_n^3J_1^2(R_2r_n)B(r,r_n)}{[J_2^2(R_1r_n)-J_1^2(R_2r_n)]}[Y_2(R_1r_n)J_2(R_2r_n)-J_2(R_1r_n)Y_2(R_2r_n)]$$
$$\times\sum_{m=0}^{\infty}\left(\frac{-\upsilon r_n^2}{\lambda}\right)^m\left[G_{1,-m-2,m+1}(-\lambda^{-1},t)\right], \qquad (7.4.5)$$

and its associated tangential stress corresponding to ordinary Maxwell fluid performing the same motion.

$$\tau_M(r,t)=f_1\left(\frac{R_1}{r}\right)^2\left\{1-\exp\left(-\frac{t}{\lambda}\right)\right\}$$
$$+\frac{\pi f_1}{\lambda}\sum_{n=1}^{\infty}\frac{J_1^2(R_2r_n)\overline{B}(r,r_n)}{[J_2^2(R_1r_n)-J_1^2(R_2r_n)]}\sum_{m=0}^{\infty}\left(\frac{-\upsilon r_n^2}{\lambda}\right)^m G_{1,-m-1,m+1}(-\lambda^{-1},t)$$
$$-\frac{\pi^2}{2}\mu R_2 f_2\sum_{n=1}^{\infty}\frac{r_n^2J_1^2(R_2r_n)\overline{B}(r,r_n)}{[J_2^2(R_1r_n)-J_1^2(R_2r_n)]}[Y_2(R_1r_n)J_2(R_2r_n)-J_2(R_1r_n)Y_2(R_2r_n)]$$
$$\times\left[1-\exp\left(-\frac{t}{\lambda}\right)-\frac{1}{\lambda}\sum_{m=0}^{\infty}\left(\frac{-\upsilon r_n^2}{\lambda}\right)^m G_{1,-m-1,m+1}(-\lambda^{-1},t)\right]. \qquad (7.4.6)$$

7.4.4 Newtonian Fluid

Applying $\lambda \to 0$ into Eqs. (7.4.5) and (7.4.6) and taking into account the following result [17]

$$\lim_{\lambda\to 0}\frac{1}{\lambda^m}G_{1,b,m}(-\lambda^{-1},t)=\frac{t^{-b-1}}{\Gamma(-b)}, \tag{7.4.7}$$

we obtain the corresponding solutions for the Newtonian fluid as follows

$$\begin{aligned} w_N(r,t) &= \frac{f_1}{2\mu}\left(\frac{R_1}{R_2}\right)^2\left(r-\frac{R_2^2}{r}\right)-\frac{\pi f_1}{\mu}\sum_{n=1}^{\infty}\frac{J_1^2(R_2r_n)B(r,r_n)}{r_n[J_2^2(R_1r_n)-J_1^2(R_2r_n)]}\sum_{m=0}^{\infty}(-\upsilon r_n^2)^m\frac{t^m}{m!} \\ &+\frac{\pi^2}{2}\upsilon R_2 f_2\sum_{n=1}^{\infty}\frac{r_n^3J_1^2(R_2r_n)B(r,r_n)}{[J_2^2(R_1r_n)-J_1^2(R_2r_n)]}[Y_2(R_1r_n)J_2(R_2r_n)-J_2(R_1r_n)Y_2(R_2r_n)] \\ &\times\sum_{m=0}^{\infty}(-\upsilon r_n^2)^m\frac{t^{m+1}}{(m+1)!}, \end{aligned} \tag{7.4.8}$$

and

$$\begin{aligned} \tau_N(r,t) &= f_1\left(\frac{R_1}{r}\right)^2+\pi f_1\sum_{n=1}^{\infty}\frac{J_1^2(R_2r_n)\overline{B}(r,r_n)}{[J_2^2(R_1r_n)-J_1^2(R_2r_n)]}\sum_{m=0}^{\infty}(-\upsilon r_n^2)^m\frac{t^m}{m!} \\ &-\frac{\pi^2}{2}\mu R_2 f_2\sum_{n=1}^{\infty}\frac{r_n^2J_1^2(R_2r_n)\overline{B}(r,r_n)}{[J_2^2(R_1r_n)-J_1^2(R_2r_n)]}[Y_2(R_1r_n)J_2(R_2r_n)-J_2(R_1r_n)Y_2(R_2r_n)] \\ &\times\left[1-\sum_{m=0}^{\infty}(-\upsilon r_n^2)^m\frac{t^m}{m!}\right]. \end{aligned} \tag{7.4.9}$$

These solutions can also be written in a simpler form as

$$\begin{aligned} w_N(r,t) &= \frac{f_1}{2\mu}\left(\frac{R_1}{R_2}\right)^2\left(r-\frac{R_2^2}{r}\right)-\frac{\pi f_1}{\mu}\sum_{n=1}^{\infty}\frac{J_1^2(R_2r_n)B(r,r_n)}{r_n[J_2^2(R_1r_n)-J_1^2(R_2r_n)]}\exp(-\upsilon r_n^2t) \\ &+\frac{\pi^2}{2}\upsilon R_2 f_2\sum_{n=1}^{\infty}\frac{r_n^3J_1^2(R_2r_n)B(r,r_n)}{[J_2^2(R_1r_n)-J_1^2(R_2r_n)]}[Y_2(R_1r_n)J_2(R_2r_n)-J_2(R_1r_n)Y_2(R_2r_n)] \\ &\times\frac{1}{(-\upsilon r_n^2)}\left\{\exp(-\upsilon r_n^2t)-1\right\}, \end{aligned} \tag{7.4.10}$$

$$\tau_N(r,t) = f_1\left(\frac{R_1}{r}\right)^2 + \pi f_1 \sum_{n=1}^{\infty} \frac{J_1^2(R_2 r_n)\overline{B}(r,r_n)}{[J_2^2(R_1 r_n) - J_1^2(R_2 r_n)]} \exp(-\upsilon r_n^2 t)$$

$$-\frac{\pi^2}{2}\mu R_2 f_2 \sum_{n=1}^{\infty} \frac{r_n^2 J_1^2(R_2 r_n)\overline{B}(r,r_n)}{[J_2^2(R_1 r_n) - J_1^2(R_2 r_n)]}[Y_2(R_1 r_n)J_2(R_2 r_n) - J_2(R_1 r_n)Y_2(R_2 r_n)]$$

$$\times\left[1 - \exp(-\upsilon r_n^2 t)\right]. \quad (7.4.11)$$

7.5 Conclusions and Numerical results

The main objective of this chapter is to provide exact solution for the velocity field and shear stress of rotational flow for fractional Oldroyd-B fluid between two coaxial circular cylinders where inner cylinder is rotating with a time dependent shear stress and outer circle is moving at a constant velocity. This solution is obtained by using Hankel transform and Laplace transform methods and the result is presented in terms of generalized G function. The similar solutions for ordinary Oldroyd-B fluid, Fractional Maxwell fluid, ordinary Maxwell fluid, Newtonian fluid are also obtained as limiting cases of the solution for fractional Oldroyd-B fluid.

As shown in below diagrams, the velocity $w(r,t)$ and the shear stress $\tau(r,t)$ given by Eqs. (7.3.18) and (7.3.26) have been drawn against *r* for different values of the time *t*, f_1, f_2 and other relevant parameters. The velocity component *w* and the shear stress component τ are decreasing function of *r*. The fluid motion and the shear stress are relatively higher at the neighborhood of the inner cylinder for given boundary conditions and f_1<0, f_2>0. The influence of time *t* on the fluid motion is shown in figure 7.1. It can be seen that the velocity and the shear stress are decreasing function of time *t*. Figures 7.2(a) and 7.2(b) are showing the effect of different values of kinematic viscosity on the fluid motion. The result indicates that the velocity decreases while the shear stress increases when kinematic viscosity decreases. The dependencies of the relaxation and retardation times on the fluid motion are shown in the figures 7.3 and 7.4. It indicates that the velocity is decreasing and the shear stress is increasing function of λ. Also, the velocity and the shear stress are decreasing function of retardation time λ_r. Figures 7.5(a) and 7.5(b) indicate that the velocity and the shear stress are decreasing function of γ. Figures 7.6(a) and 7.6(b) are showing the effect of different values of fractional parameter β on the fluid motion. It can be seen that the velocity is decreasing while the shear stress is increasing function of β. Figures 7.7 and 7.8 are showing the behavior of f_1 and f_2 on the fluid motion for their different values. Figure 7.9 is showing a comparison diagram of the velocity $w(r,t)$ and the shear stress $\tau(r,t)$ among corresponding five models (fractional Oldroyd-B fluid, ordinary Oldroyd-B fluid, Fractional Maxwell fluid, ordinary Maxwell fluid and Newtonian fluid) for same values of the common material constants and time t. In all cases the velocity of the fluid is a decreasing function w.r.t. r and the ordinary Maxwell fluid is the swiftest while the fractional Oldroyd-B fluid has the smallest velocity on the whole flow domain. In all of the figures 1-9, the units of the material constants are in SI units and the root r_n has been approximated by $\frac{(2n-1)\pi}{2(R_2-R_1)}$.

Figure 7.1

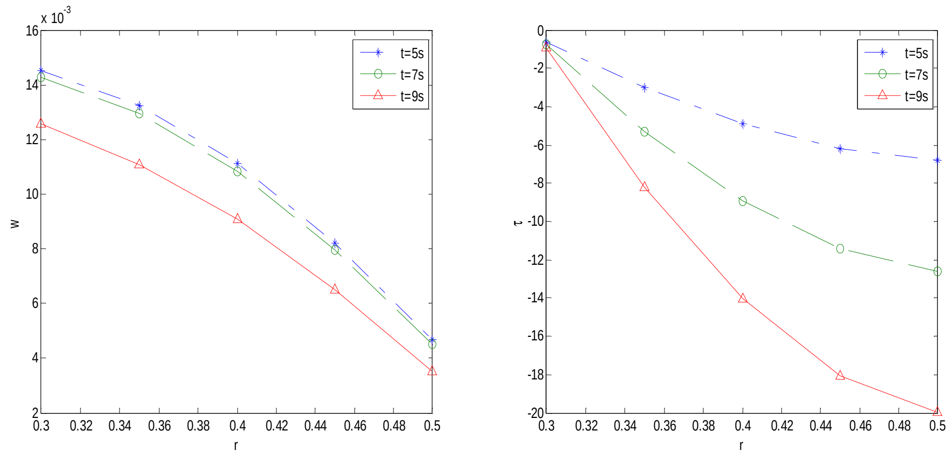

7.1(a) 7.1(b)

Fig. 7.1 Profiles of the velocity w(r, t) and shear stress τ(r, t) given by Eqs. (7.3.18) and (7.3.26) for $R_1 = 0.3$, $R_2 = 0.5$, $f_1 = -2$, $f_2 = 2$, $\upsilon = 0.035$, $\mu = 30$, $\lambda = 12$, $\lambda_r = 2.2$, $\gamma = 0.9$, $\beta = 0.6$ and different values of t.

Figure 7.2

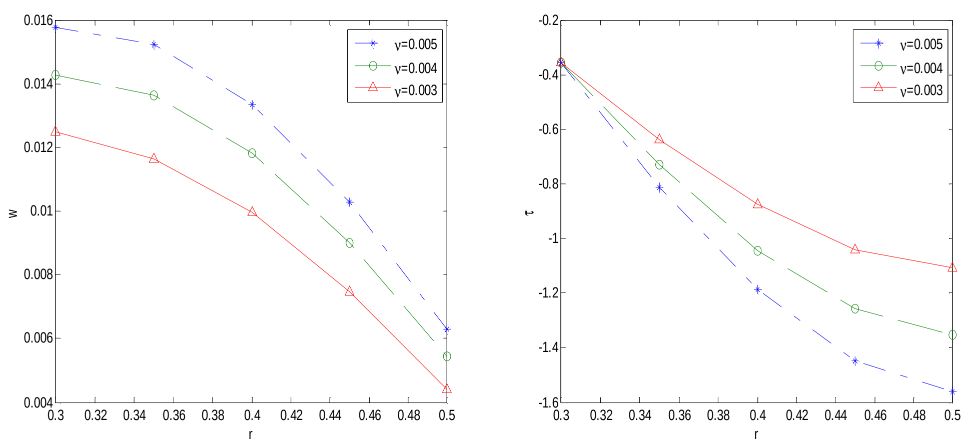

7.2(a) 7.2(b)

Fig. 7.2 Profiles of the velocity w(r, t) and shear stress τ(r, t) given by Eqs. (7.3.18) and (7.3.26) for $R_1 = 0.3$, $R_2 = 0.5$, $f_1 = -2$, $f_2 = 2$, t = 6s, $\mu = 40$, $\lambda = 9$, $\lambda_r = 3$, $\gamma = 0.3$, $\beta = 0.3$ and different values of υ.

Figure 7.3

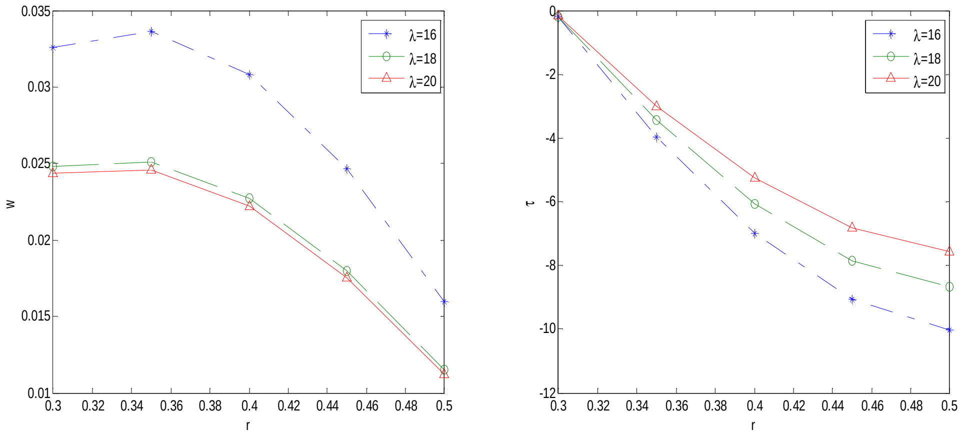

7.3(a) 7.3(b)

Fig. 7.3 Profiles of the velocity w(r, t) and shear stress $\tau(\mathrm{r,t})$ given by Eqs. (7.3.18) and (7.3.26) for $R_1 = 0.3,\ R_2 = 0.5,\ f_1 = -2,\ f_2 = 2,\ \mathrm{t} = 5\mathrm{s},\ \upsilon = 0.04,\ \mu = 40,\ \lambda_{\mathrm{r}} = 7,\ \gamma = 0.3,\ \beta = 0.3$ and different values of λ.

Figure 7.4

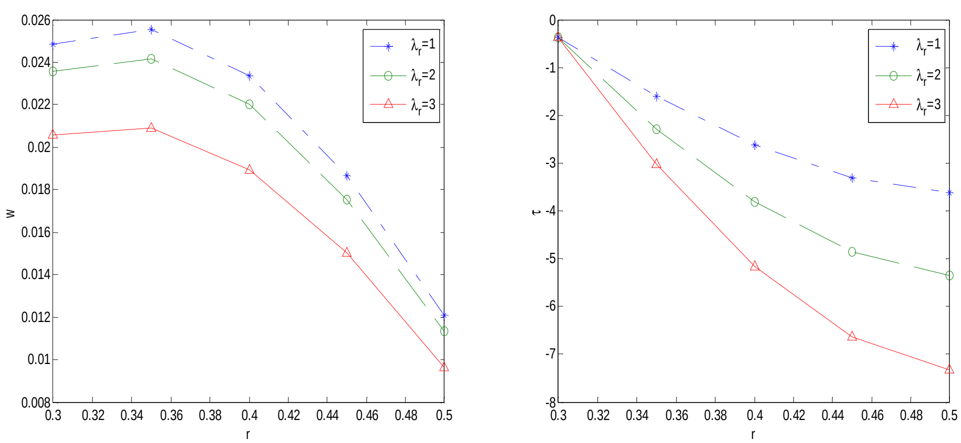

7.4(a) 7.4(b)

Fig. 7.4 Profiles of the velocity w(r, t) and shear stress $\tau(\mathrm{r,t})$ given by Eqs. (7.3.18) and (7.3.26) for $R_1 = 0.3,\ R_2 = 0.5,\ f_1 = -2,\ f_2 = 2,\ \mathrm{t} = 5\mathrm{s},\ \upsilon = 0.04,\ \mu = 50,\ \lambda = 8,\ \gamma = 0.3,\ \beta = 0.9$ and different values of λ_r.

Figure 7.5

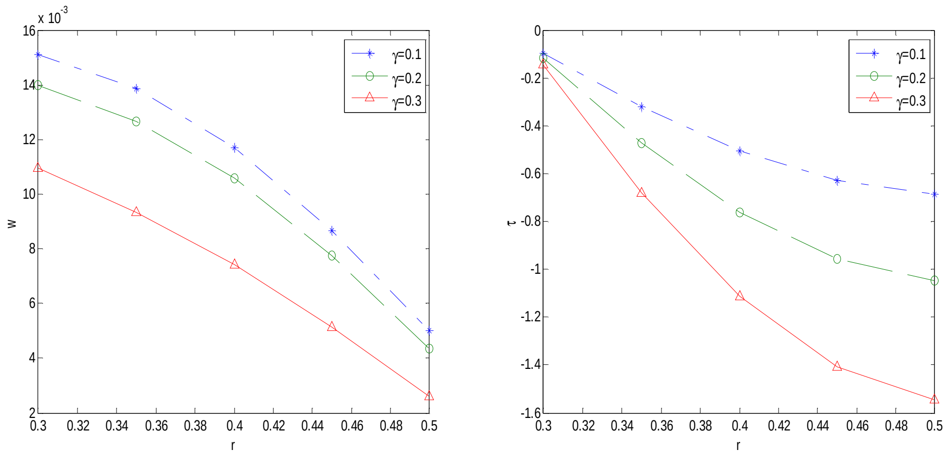

7.5(a) 7.5(b)

Fig. 7.5 Profiles of the velocity w(r, t) and shear stress τ(r, t) given by Eqs. (7.3.18) and (7.3.26) for $R_1 = 0.3$, $R_2 = 0.5$, $f_1 = -2$, $f_2 = 2$, t = 6s, $\upsilon = 0.045$, $\mu = 30$, $\lambda = 25$, $\lambda_r = 8$, $\beta = 1$ and different values of γ.

Figure 7.6

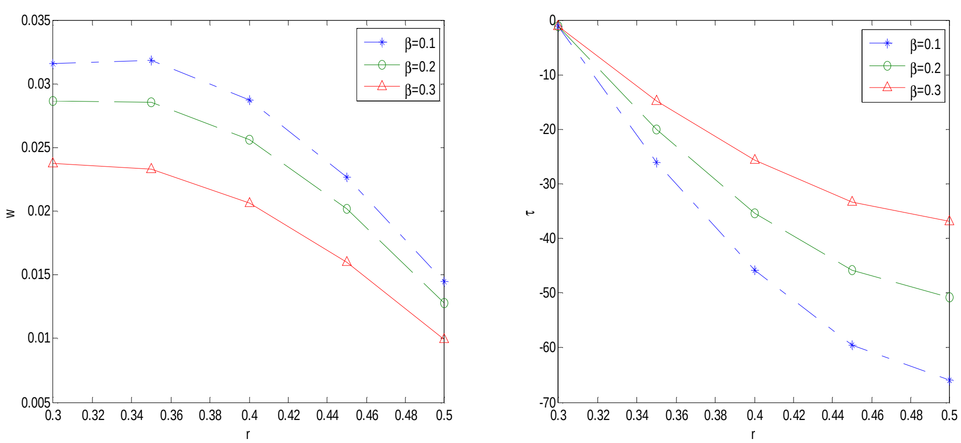

7.6(a) 7.6(b)

Fig.7.6 Profiles of the velocity w(r,t) and shear stress τ(r,t) given by Eqs.(7.3.18) and (7.3.26) for $R_1 = 0.3$, $R_2 = 0.5$, $f_1 = -2$, $f_2 = 2$, t = 6s, $\upsilon = 0.04$, $\mu = 30$, $\lambda = 8$, $\lambda_r = 5.5$, $\gamma = 1$ and different values of β.

Figure 7.7

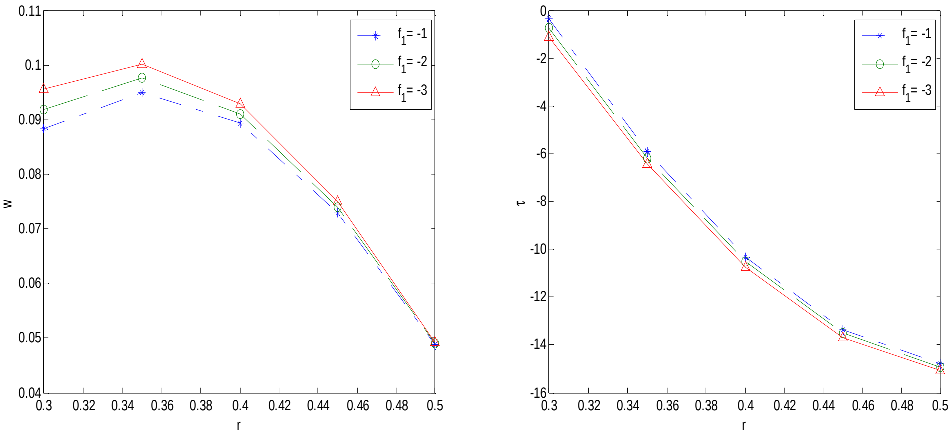

7.7(a) 7.7(b)

Fig.7.7 Profiles of the velocity w(r,t) and shear stress $\tau(r,t)$ given by Eqs.(7.3.18) and (7.3.26) for $R_1 = 0.3$, $R_2 = 0.5$, $f_2 = 2$, $t = 6s$, $\upsilon = 0.045$, $\mu = 30$, $\lambda = 11$, $\lambda_r = 2.1$, $\gamma = 0.9$, $\beta = 0.5$ and different values of f_1.

Figure 7.8

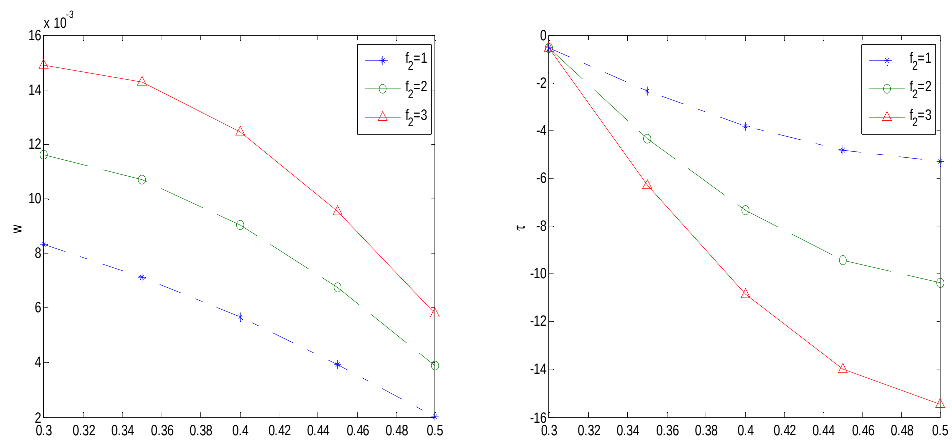

7.8(a) 7.8(b)

Fig.7.8 Profiles of the velocity w(r,t) and shear stress $\tau(r,t)$ given by Eqs.(7.3.18) and (7.3.26) for $R_1 = 0.3$, $R_2 = 0.5$, $f_1 = -2$, $t = 5s$, $\upsilon = 0.04$, $\mu = 40$, $\lambda = 13$, $\lambda_r = 2.5$, $\gamma = 0.9$, $\beta = 0.6$ and different values of f_2.

Figure 7.9

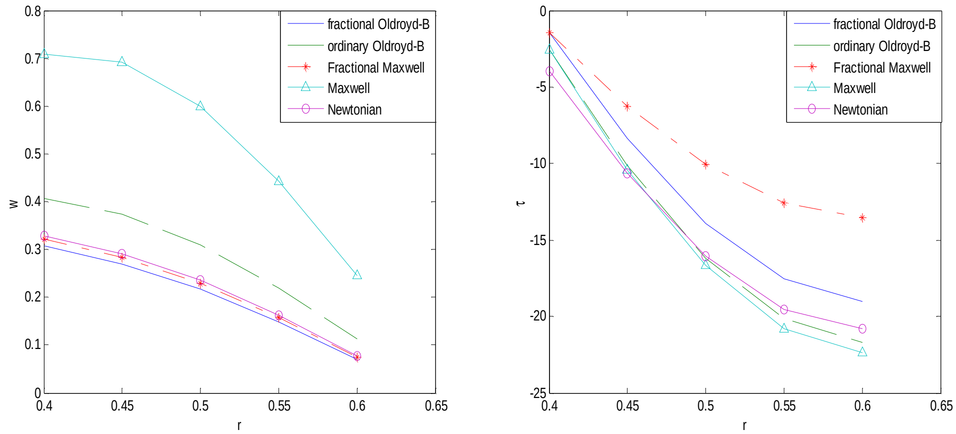

7.9(a) 7.9(b)

Fig. 7.9 Profiles of the velocity $w(r,t)$ and shear stress $\tau(r,t)$ corresponding to the ordinary Oldroyd-B fluid, Fractional Maxwell fluid, ordinary Maxwell fluid, Newtonian fluid, for $R_1 = 0.4$, $R_2 = 0.6$, $f_1 = -4$, $f_2 = 2$, $t = 5$ s, $\upsilon = 0.035$, $\mu = 2.96$, $\lambda = 5$, $\lambda_r = 1$, $\gamma = 0.5$ and $\beta = 0.5$.

References

1. **Fridtjov Irgens**, *Rheology and non-Newtonian fluids,* Springer Cham Heidelberg New York Dordrecht London (2014). ISBN 978-3-319-01053-3 (eBook) DOI 10.1007/978-3-319-01053-3

2. **Rajagopal K.R. and Srinivasa A.R.,** A thermodynamical frame-work for rate type fluid models, *J. Non-Newtonian Fluid Mech.* **88** (2000), 207-227.

3. **Dunn J.E. and Rajagopal K.R.,** Fluids of differential type: critical review and thermodynamic analysis, *International Journal of Engineering Science* **33** (1995), 689-729.

4. **Batchelor G.K.,** *An introduction to fluid dynamics*, Cambridge University Press, Cambridge (1967).

5. **Ting T.W.,** Certain non-steady flows of second-order fluids, *Arch. Rational Mech. Anal.* **14** (1963), 1–23.

6. **Srivastava P.N.,** Non-steady helical flow of a viscoelastic liquid, *Arch. Mech. Stos.***18** (1966), 145–150.

7. **Waters N.D. and King M.J.,** The unsteady flow of an Elastico-viscous liquid in a straight pipe of circular cross section, *J. Phys. D Appl. Phys.***4** (1971), 204–211.

8. **Bandelli R. and Rajagopal K.R.,** Start-up flows of second grade fluids in domains with one finite dimension, *Int. J. Non-Linear Mech.* **30** (1995), 817-839.

9. **Bandelli R., Rajagopal K.R. and Galdi G.P.,** On some unsteady motions of fluids of second grade, *Arch. Mech.***47** (1995), 661–676.

10. **Rubbab Q., Husnine S.M. and Mahmood,** An exact solutions of generalized Oldroyd-B fluid subject to a time-dependent shear stress in a pipe, *Journal of Prime Research in Mathematics* **5** (2009), 139-148.

11. **Tong D., Wang R. and Yang H.,** Exact solutions for the flow of non-Newtonian fluid with fractional derivative in an annular pipe, *Science in China Ser. G Physics, Mechanics & Astronomy* **48** (2005), 485-495.

12. **Athar M., Fetecau C., Kamran M., Sohail A. and Imran M.,** Exact solutions for unsteady axial Couette flow of a fractional Maxwell fluid due to an accelerated shear, *Nonlinear Analysis, Modelling and Control* **16** (2011), 135–151.

13. **Amir M., Fetecau C. and Imran S.,** Exact solutions for some unsteady flows of generalized second grade fluids in cylindrical domains, *Journal of Prime Research in Mathematics* **4** (2008), 171-180.

14. **Shen F., Tan W., Zhao Y. and Masuoka T.,** The Rayleigh–stokes problem for a heated generalized second grade fluid with fractional derivative model, *Nonlinear Analysis: Real World Applications* **7** (2006), 1072 – 1080.

15. **Kamran M., Imran M. and Athar M.,** Exact solutions for the unsteady rotational flow of a generalized second grade fluid through a circular cylinder, *Nonlinear Analysis: Modelling and Control* **15** (2010), 437–444.

16. **Athar M., Awan A.U. and Fetecau C.,** A note on the unsteady flow of a fractional Maxwell fluid through a circular cylinder, *Acta Mech. Sin.* **28** (2012), 308–314.

17. **Jamil M., Fetecau C. and Fetecau C.,** Unsteady flow of viscoelastic fluid between two cylinders using fractional Maxwell model, *Acta Mech. Sin.* **28** (2012), 274–280.

18. **Athar M., Kamran M. and Fetecau M.,** Taylor–Couette flow of a generalized second grade fluid due to a constant couple, *Nonlinear Analysis: Modelling and Control* **15** (2010), 3–13.

19. **Kamran M., Athar M. and Imran M.,** On the unsteady linearly accelerating flow of a fractional second grade fluid through a circular cylinder, *International Journal of Nonlinear Science* **11** (2011), 317-324.

20. **Imran M., Kamran M., Athar M. and Zafar A.A.,** Taylor–Couette flow of a fractional second grade fluid in an annulus due to a time-dependent couple, *Nonlinear Analysis: Modelling and Control* **16** (2011), 47–58.

21. **Fetecau C.,** Analytical solutions for non-Newtonian fluid flows in pipe-like domains, *Int. J. Non-Linear Mechanics* **39** (2004), 225-231.

22. **Kamran M., Imran M., Athar M. and Imran M.A.,** On the unsteady rotational flow of fractional Oldroyd-B fluid in cylindrical domains, *Meccanica* **47** (2012), 573–584.

23. **Qi H. and Jin H.,** Unsteady rotating flows of a viscoelastic fluid with the fractional Maxwell model between coaxial cylinders, *Acta Mechanica Sinica* **22** (2006), 301–305.

24. **Tong D.K. and Liu Y.S.,** Exact solutions for the unsteady rotational flow of non-Newtonian fluid in an annular pipe, *Int. J. Eng. Sci*.**43** (2005), 281-289.

25. **Hayat T., Nadeem S. and Asghar S.,** Periodic unidirectional flows of a viscoelastic fluid with the fractional Maxwell model, *Applied Mathematics and Computation* **151** (2004), 153–161.

26. **Tan W.C and Xu M.Y.,** Plane surface suddenly set in motion in a viscoelastic fluid with fractional Maxwell model, *Acta Mech. Sinica* **18** (2002), 342-349.

27. **Stokes G.G.,** *On the effect of the rotation of cylinders and spheres about their axis in increasing the logarithmic decrement of the arc of vibration*, Cambridge University Press, Cambridge (1886).

28. **Casarella M.J. and Laura P.A.,** Drag on oscillating rod with longitudinal and torsional motion, *Journal of Hydronautics* **3** (1969), 180-183.

29. **Rajagopal K.R.,** Longitudinal and torsional oscillations of a rod in a non-Newtonian fluid, *Acta Mechanica* **49** (1983), 281-285.

30. **Rajagopal K.R. and Bhatnagar R.K.,** Exact solutions for some simple flows of an Oldroyd-B fluid, *Acta Mechanica* **113** (1995), 233-239.

31. **Khan M., Asghar S. and Hayat T.,** *Oscillating flow of a Burgers' fluid in a pipe*, The Abdus Salam International Center for Theoretical Physics, Trieste, Italy (2005).

32. **Hayat T., Khan M., Siddiqui A.M. and Asghar S.,** Transient flows of a Second grade fluid, *International Journal of Non-Linear Mechanics* **39** (2004), 1621-1633.

33. **Fetecau C. and Fetecau Corina,** Starting solutions for the motion of a Second grade fluid due to longitudinal and torsional oscillations of a circular cylinder, *International Journal of Engineering Science* **44** (2006), 788–796.

34. **Vieru D., Akhtar W., Fetecau Corina and Fetecau C.,** Starting solutions for the oscillating motion of a Maxwell fluid in cylindrical domains, *Meccanica* **42** (2007), 573–583.

35. **Fetecau Corina, Hayat T. and Fetecau C.,** Starting solutions for oscillating motions of Oldroyd-B fluids in cylindrical domains, *Journal of Non-Newtonian Fluid Mechanics* **153** (2008), 191–201.

36. **Mahmood A., Parveen S., Ara A. and Khan N.A.,** Exact analytic solutions for the unsteady flow of a non-Newtonian fluid between two cylinders with fractional derivative model, *Communications in Nonlinear Science and Numerical Simulation* **14** (2009), 3309–3319.

37. **Khan M., Ali S.H. and Qi H.,** On accelerated flows of a viscoelastic fluid with the fractional Burgers' model, *Nonlinear Analysis: Real World Applications* **10** (2009), 2286–2296.

38. **Fetecau Corina, Akhtar W., Imran M.A. and Vieru D.,** On the oscillating motion of an Oldroyd-B fluid between two infinite circular cylinders, *Computers and Mathematics with Applications* **59** (2010), 2836–2845.

39. **Tong D.,** Starting solutions for oscillating motions of a generalized Burgers' fluid in cylindrical domains, *Acta Mechanica* **214** (2010), 395–407.

40. **Liu Y., Zheng L., Zhang X. and Zong F.,** Some oscillation flows of a generalized Oldroyd-B fluid in uniform magnetic field, *In Proceedings of the World Congress on Engineering (WCE '10)* **3** (2010), 1971–1974.

41. **Fetecau C. and Fetecau Corina,** On the unsteady of some helical flows of a second grade fluid, *Acta Mech.***57** (1985), 247-252.

42. **Fetecau C., Mahmood A., Fetecau Corina and Vieru D.,** Some exact solutions for the helical flow of a generalized Oldroyd-B fluid in a circular cylinder, *Computers and Mathematics with Applications* **56** (2008), 3096-3108.

43. **Wood W.P.,** Transient viscoelastic helical flows in pipes of circular and annular cross-section, *J. Non-Newtonian Fluid Mech.* **100** (2001), 115-126.

44. **Haitao Qi and Hui Jin,** Unsteady helical flows of a generalized Oldroyd-B fluid with fractional derivative, *Nonlinear Anal. RWA* **10** (2009), 2700–2708.

45. **Fetecau C. and Fetecau Corina,** Unsteady helical flows of a Oldroyd-B fluid, *Proc. Roy Acad. Ser. A* **5** (2004), 13–19.

46. **Fetecau C**., Starting flow of an Oldroyd-B fluid between rotating co-axial cylinders, *Proc. Roy Acad. Ser. A* **6** (2005), 1–8.

47. **Fetecau C, Fetecau Corina and Vieru D.,** On some helical flows of Oldroyd-B fluids, *Acta Mech.* **189** (2007), 53-63.

48. **Jamil M. and Fetecau C.,** Helical flows of Maxwell fluid between coaxial cylinders with given shear stresses on the boundary, *Nonlinear Analysis: Real World Applications* **11** (2010), 4302-4311.

49. **Jamil M., Fetecau C. and Imran M.,** Unsteady helical flows of Oldroyd-B fluids, *Commun. Nonlinear Sci. Numer. Simulat.* **16** (2011), 1378-1386.

50. **Jamil M., Rauf A., Fetecau C. and Khan N.A.,** Helical flows of second grade fluid due to constantly accelerated shear stresses, *Communications in Nonlinear Science and Numerical Simulation* **16**(4) (2011), 1959–1969.

51. **Jamil M., Zafar A.A., Rauf A. and Khan N.A.,** Some new exact analytical solutions for helical flows of second grade fluids, *Communications in Nonlinear Science and Numerical Simulation* **17**(1) (2012), 141–153.

52. **Shah S.H.A.M.,** Some helical flows of a Burgers' fluid with fractional derivative, *Meccanica* **45** (2010), 143-151.

53. **Bagley R.L.,** A theoretical basis for the application of fractional calculus to viscoelasticity, *Journal of Rheology* **27** (1983), 201-210.

54. **Friedrich C.H.R.,** Relaxation and retardation functions of the Maxwell model with fractional derivatives, *Rheologica Acta* **30** (1991), 151-158.

55. **Makris N. and Constantinou M.C.,** Fractional-derivative Maxwell model for viscous dampers, *Journal of Structural Engineering* **117** (1991), 2708-2724.

56. **Glockle W.G. and Nonnenmacher T.F.,** Fractional relaxation and the time-temperature superposition principle, *Rheologica Acta* **33** (1994), 337-343.

57. **Mainardi F.,** Fractional relaxation oscillation and fractional diffusion-wave phenomena, *Chaos, Solitons & Fractals* **7** (1996), 1461-1477.

58. **Rossikhin Y.A. and Shitikova M.V.,** A new method for solving dynamic problems of fractional derivative viscoelasticity, *International Journal of Engineering Science* **39** (2000), 149-176.

59. **Rossikhin Y.A. and Shitikova M.V.,** Analysis of dynamic behaviour of viscoelastic rods whose rheological models contain fractional derivatives of two different orders, *Zeitschrift Für Angewandte Mathematik und Mechanik (ZAMM)* **81** (2001), 363-376.

60. **Mainardi F. and Gorenflo R.,** On Mittag-Lefler type functions in fractional evolution processes, *Journal of Computational and Applied Mathematics* **118** (2000), 283-299.

61. **Hilfer R.,** *Applications of fractional calculus in physics*, World Scientific Press, Singapore (2000).

62. **Huang J.Q. and Liu C.Q.,** Analysis of general second-grade fluid flow in double cylinder rheometer, *Science in China*, *Ser. A.* **26** (1996), 912-920.

63. **Tan W.C., Xian F. and Wei L.,** Exact solution for the unsteady Couette flow of the generalized second grade fluid, *Chinese Science Bulletin* **47** (2002), 1226-1228.

64. **Podlubny I.,** *Fractional differential equations*, Academic Press, San Diego (1999).

65. **Fetecau C., Awan A.U. and Fetecau C.,** Taylor-Couette flow of an Oldroyd-B fluid in a circular cylinder subject to a time-dependent rotation, *Bull. Math. Soc. Sci. Math. Roumanie* **52** (2009), 117-128.

66. **Fetecau C., Fetecau C. and Imran M.,** Axial Couette flow of an Oldroyd-B fluid due to a time dependent shear stress, *Math. Reports* **11** (2009), 145-154.

67. **Nazar M., Fetecau C. and Awan A.U.,** A note on the unsteady flow of a generalized second-grade fluid through a circular cylinder subject to a time dependent shear stress, *Nonlinear Analysis: Real World Applications* **11** (2010), 2207-2214.

68. **Siddique I. and Vieru D.,** Exact solution for the longitudinal flow of a generalized second grade fluid in a circular cylinder, *Acta Mech. Sin.* **25** (2009), 777-785.

69. **Wang S. and Xu M.,** Axial Couette flow of two kinds of fractional viscoelastic fluids in an annulus, *Nonlinear Analysis: Real World Applications* **10** (2009), 1087-1096.

70. **Coleman B.D., Markovitz H. and Noll W.,** *Viscometric flows of non-Newtonian fluids: theory and experiment*, Springer Tracts in Natural Philosophy, Volume 5, Springer, Berlin New York (1966).

71. **Akhtar W.,** Exact solutions for some unsteady flows of non-Newtonian fluids of rate type, Ph.D Thesis, Abdus Salam School of Mathematical Sciences GC University Lahore, Pakistan (2008).

72. **Caputo M.,** Linear model of Dissipation whose Q is almost frequency independent-II, *Geophysics J.R. Astr. Soc.* **13** (1967), 529-539.

73. **Oldham K.B. and Spanier J.,** *The fractional calculus*, Academic Press, New York and London (1974).

74. **Mc Bride A.C. and Roach G.F.,** *Fractional Calculus*, University of Strathclyde, Glasgow, Pitman Advanced Publishing Program (1985).

75. **Gorenflo R. and Vessella S.,** *Abel integral equations: Analysis and applications*, Lecture Notes in Mathematics, Vol. 1461, Springer-Verlag Berlin (1991).

76. **Samko S.G., Kilbas A.A. and Marichev O.I.,** *Fractional integrals and Derivatives: Theory and applications*, Gordon and Breach, New York (1993).

77. **Miller K.S and Ross B.,** *An Introduction to Fractional Calculus and Fractional Differential equations*, John Wiley and Sons, New York (1993).

78. **Kiryakova V.S.,** *Generalized fractional calculus and applications*, Longman pitman Res Notes in Math. Ser. 301, Harlow (1994).

79. **Nishimoto K.,** *Fractional Calculus Vols. I-V*, Descartes Press, Koriyama, Japan (1984, 87, 89, 91, 96).

80. **Davis H. D.,** *The theory of linear operators*, Principia Press, Bloomington, Indiana (1936).

81. **Ross B.,** Fractional calculus: an historical apologia for the development of a calculus using differentiation and anti differentiation of non integral orders, *Mathematics Magazine* **50** (3) (1977), 115-122.

82. **Kober H.,** On fractional integrals and derivatives, *Quart. J. Math. Oxford Ser.***11** (1940), 193-212.

83. **Erdélyi A.,** On fractional integration and its application to the theory of Hankel transforms, *Quart. J. Math. Oxford Ser.* **2**(2) (1940), 293-303.

84. **Erdélyi A.,** On some functional transformations, *Univ. Politec. Torino. Rend. Sem. Mat.* **10** (1950-51), 217-234.

85. **Manocha H.L.,** Transformation of integral expression for F_4 by means of fractional integration by parts, *Bull. Math. Soc. Sci. Math. R.S. Roumanie (NS)* **9**(57) (1965), 337-341.

86. **Manocha H.L.,** Some expansion by fractional derivatives, *Mathematica (cluj)* **9** (32) (1967), 303-309.

87. **Saxena R.K.,** On fractional integration operators, *Math. Zeitschr.* **96** (1967), 288-291.

88. **Kalla S.L. and Saxena R.K.,** Integral operators involving hypergeometric functions, *Math. Zeitschr.* **108** (1969), 231-234.

89. **Kalla S.L.,** *On operators of fractional integration*, Math. Notae, **22** (1970/71), 89-93.

90. **Saigo M.,** A remark on integration operators involving the Gauss hypergeometric function, *Math. Reports of college of Gen.Edu. Kyushu University* **11** (1978), 135-145.

91. **Raina R.K. and Kiryakova V.S.,** On the Weyl fractional calculus, *Proc. Amer. Math. Soc.***73** (1979), 188-192.

92. **Srivastava H.M. and Goyal S.P.,** Fractional derivative of the H-function of several variables, *J. Math. Anal. Appl.* **112** (1985), 641-651.

93. **Sneddon I.N.,** *Mixed boundary value problem in potential theory*, North Holland Publ. Co. Amsterdam (1986).

94. **Kalla S.L. and Kiryakova V.S.,** An H-function generalized fractional calculus based upon compositions of Erdélyi-Kober operators, *Lp. Math. Japonica* **35**(6) (1990), 1151-1171.

95. **Kalla S.L. and Kiryakova V.S.,** A generalized fractional calculus dealing with H-functions (In proceedings of International conference on fractional calculus and its applications, college of engineering, Nihon University, Tokyo) (1990), 62-69.

96. **Srivastava H.M., Goyal S.P. and Jain R.,** Fractional integral operators involving a general class of polynomial, *J. Math. Anal. Appl.* **148** (1990), 87-100.

97. **Gupta K.C. and Jain R.,** A study of Multidimensional fractional integral operators involving a general class of polynomials and a generalized hyper-geometric function, *Ganita Sandesh* **5**(2) (1991), 55-64.

98. **Goyal S.P. and Salim O. Tariq,** Multidimensional fractional integral operators involving generalized polynomial set, *Kyungpook Math. J.* **38** (1998), 301-315.

99. **Gupta K.C. and Soni R.C.,** On basic integral formula involving the product of the $\overline{H}-$function and Fox $\overline{H}-$function, *J. Raj. Acad. Phy. Sci.* **4**(3) (2005), 157-164.

100. **Srivastava H.M. and Saxena R.K.,** Operators of fractional integration and their applications, *Elsevier, Appl. Math. Comput.* **118** (2001), 1-52.

101. **Caputo M.,** *Elasticitâ e Dissipazione, Zanichelli*, Bologna (1969).

102. **Smit and Vries,** Rheological models containing fractional derivatives, *Rheologica Acta* **9** (1970), 525-534.

103. **Mainardi F.,** Fractional relaxation-oscillation and fractional diffusion-wave phenomena, *Chaos, Solitons and Fractals* **7** (1996), 1461-1477.

104. **Luchko Yu. and Srivastava H.M.,** The exact solution of certain differential equations of fractional order by using operational calculus, *computers Math. Applic.* **29**(8) (1995), 73-85.

105. **Hadid S.B. and Luchko Yu.,** An operational method for solving fractional differential equations of an arbitrary real order, *Panam. Math. J.* **6**(1) (1996), 57-73.

106. **Giona M., Gerbelli S. and Roman H.E.,** Fractional diffusion equation and relaxation in complex viscoelastic materials, *Physica A* **191** (1992), 449-453.

107. **Friedrich Ch.,** Mechanical stress relaxation in polymers: fractional integral model versus fractional differential model, *J. Non-Newtonian fluid Mech.* **46** (1993), 307-314.

108. **Fenander Ǻ.,** Modal synthesis when modeling damping by use of fractional derivatives, *AIAA Journal* **34**(5) (1998), 1051-1058.

109. **Enelund M. and Josefson B.L.,** Time domain finite element analysis of viscoelastic structures with fractional derivatives constitutive equations, *AIAA Journal* **35**(10) (1997), 1630-1637.

110. **El-Sayed A.M.A.,** On the fractional differential equations, *Apll. Math. and Comput.* **49** (1992), 2-3.

111. **El-Sayed A.M.A.,** Multivalued fractional differential equations, *Apll. Math. and Comput.* **80**(1994), 1-11.

112. **Beyer H. and Kempfle S.,** Definition of physically consistent damping laws with fractional derivatives, *Z. angew. Math. Mech.* **75**(8) (1995), 623-635.

113. **Bagley R.L. and Torvik P.J.,** On the appearence of the fractional derivative in the behavior of real materials, *J. Appl. Mech.* **51** (1984), 294-298.

114. **Jamil M., Rauf A., Zafar A.A. and Khan N.A.,** New exact analytical solutions for Stokes' first problem of Maxwell fluid with fractional derivative approach, *Computers and Mathematics with Applications* **62** (2011), 1013-1023.

115. **Akhtar W., Nazar M.,** Exact Solutions for the rotational flow of generalized Maxwell fluids in a circular cylinder, *Bull. Math. Soc. Sci. Math. Roumanie Tome* **51** (2008), 93–101.

116. Debnath L., Bhatta D., *Integral Transforms and their Applications*, Chapman and Hall/CRC Press, Boca Raton, Fla, USA (2007).

117. Lorenzo C.F., Hartley T.T., Generalized Functions for the Fractional Calculus, NASA/TP-1999-209424/REV1, (1999).

118. Jamil M., Fetecau C. and Rana M., Some exact solutions for Oldroyd-B fluid due to time dependent prescribed shear stress, Journal of Theoretical and Applied Mechanics **50 (**2012**)**, 549-562.

Brief bio-data

PERSONAL DETAILS

Name: Ms. Kavita Khandelwal

Father's name: Shri Suraj Mal Gupta

Date of Birth: March 21, 1986

Address: 15/236, Adarsh Colony, Dausa (Rajasthan).

Educational Qualifications

Examination	University/Board	Year	Percentage
M.Phil	University of Rajasthan, Jaipur	2009	79.25%
M.Sc.	University of Rajasthan, Jaipur	2008	70.70%
B.Sc.	University of Rajasthan, Jaipur	2006	79.26%
XII	RBSE	2003	78.46%
X	RBSE	2001	73.33%

Work Experience

- Taking tutorial classes of B.Tech and M.Sc. in Malaviya National Institute of technology, Jaipur.
- Worked as Lecturer in Apex Institute of Engineering and Technology since Sep-2009 to December-2011

Awards

- Secured **342th rank in GATE-2011**.
- Awarded with **Dhiru Bhai Ambani scholarship**.
- Participated in **State Level Running Competition** organized under Adarsh Vidya Mandir in year 2000.

Schools, Workshops and Conferences

1. Participated in the **AFS-II** conducted in CEMS, Department of Mathematics, SSJ campus, Kumaun University, Almora during 01st May to 28th May 2014.

2. Participated and presented a paper in the **National Conference on Mathematical Analysis and Computation (NCMAC-2015)** held at Malaviya National Institute of technology, Jaipur during Feburary 20-21, 2015.

3. Attended short term course on **Mathematical Modeling, MATLAB Programming and their Applications in Engineering and Sciences** held at Malaviya National Institute of technology, Jaipur during January 19-23, 2015.

4. Attended short term course on **Analysis and Applications (STCAA 2014)** held at Malaviya National Institute of technology, Jaipur in the collaboration with National Institute of technical Teachers Training and Research Chandigarh during November 10-14, 2014.

5. Participated in the **Workshop on Self Empowerment: Coping with Workplace Harassment** held at Women's Cell, Malaviya National Institute of technology, Jaipur on April 11, 2014.

6. Participated in the **International Conference on Special Functions and their Applications (12th Annual Conference of SSFA) & symposium on Applications in Diverse Fields of Engineering and Technology (ICSFA-2013)** held at Malaviya National Institute of technology, Jaipur during December 13-15, 2013.

7. Participated in the **2nd National Conference on Computational and Mathematical Sciences (COMPUTATIA-II, 2012)** held at VIT Campus, Jaipur during November 30 & December 01, 2012.

8. Attended short term course on **Mathematical Methods and its Applications in Engineering and Sciences** held at Malaviya National Institute of technology, Jaipur during October 29 – November 03, 2012.

List of Research Papers

List of Research Papers

1. Exact solutions for the flow of fractional Maxwell fluid in pipe-like domains, Advances in Applied Mathematics and Mechanics, 8, 1-11 (2016). DOI: 10.4208/aamm.2014.m588
2. Exact solutions for an unsteady flow of viscoelastic fluid in cylindrical domains using the fractional Maxwell model, International Journal of Applied and Computational Mathematics 1, 143-156, (2015).
3. Flow of fractional Maxwell fluid in pipe-like domains, International Journal of Applied and Computational Mathematics, 1-18. DOI: 10.1007/s40819-016-0139-x
4. Exact solution for the flow of Oldroyd-B fluid due to constant shear and time dependent velocity, IOSR Journal of Mathematics 10, 38-45 (2014).
5. Exact solution for the flow of Oldroyd-B fluid between coaxial cylinders, International Journal of Engineering Research & Technology 3, 949-954, (2014).
6. Unsteady unidirectional flow of Oldroyd-B fluid between two infinitely long coaxial cylinders, International Journal of Mathematical Sciences & Applications 4, 1-10, (2014).
7. Exact solutions for the helical flow of fractional Oldroyd-B fluid in a circular cylinder, Advances in Applied Mathematics and Mechanics (communicated).
8. Exact solutions for fractional Oldroyd-B fluid filled between moving outer and rotating inner coaxial circular cylinders, Arnold Mathematical Journal (communicated).